



Stanford ME469: Common low-Mach Discretization Approaches



PRESENTED BY

Stefan P. Domino

Computational Thermal and Fluid Mechanics

Sandia National Laboratories SAND2018-4536 PE



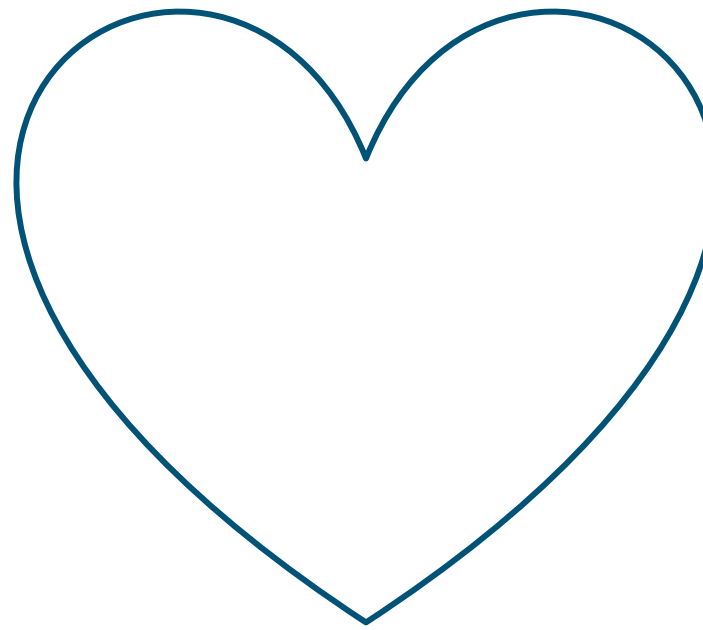
Sandia National Laboratories is a multimission laboratory managed and operated by National Technology & Engineering Solutions of Sandia, LLC, a wholly owned subsidiary of Honeywell International Inc., for the U.S. Department of Energy's National Nuclear Security Administration under contract DE-NA0003525.

2 | Common low-Mach Discretization Approaches: Outline



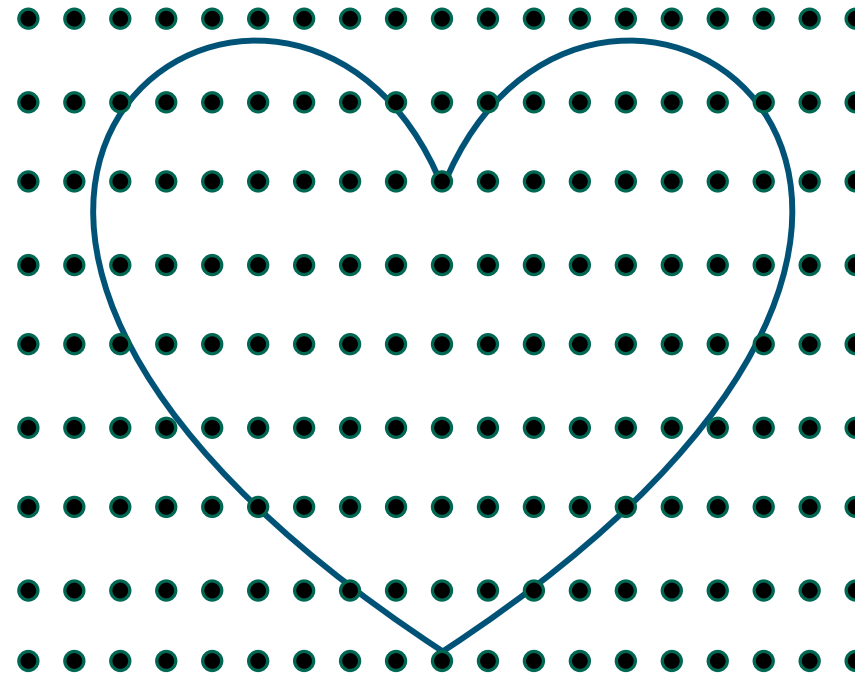
- The Concept of Meshing
- Why Unstructured?
- Unstructured Element Typoes
- Finite Element Method (FEM)
- Control-Volume Finite Element Method (CVFEM)
- Edge-based Vertex-Centered (EBVC)
- Cell-centered Finite Volume (FV)
- Staggered arrangement
- Conclusions

Introducing a Mesh over Heart Domain, Ω



- Notes: Geometry is:
 1. Complex
 2. Curved
 3. Sharp

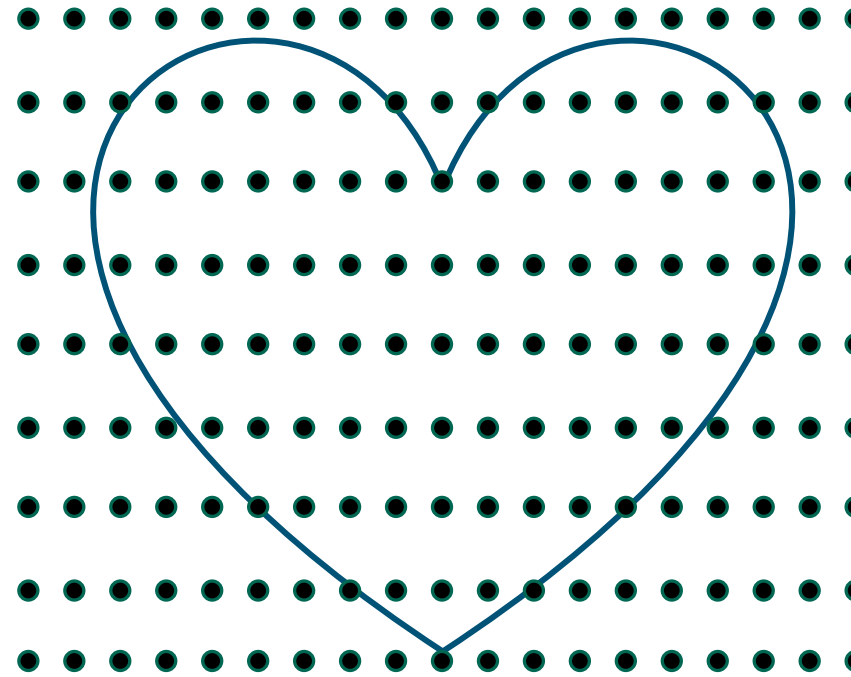
Introducing a [Finite Difference] Mesh over Heart Domain, Ω



? What breaks..

- Notes: Geometry is:
 1. Complex
 2. Curved
 3. Sharp

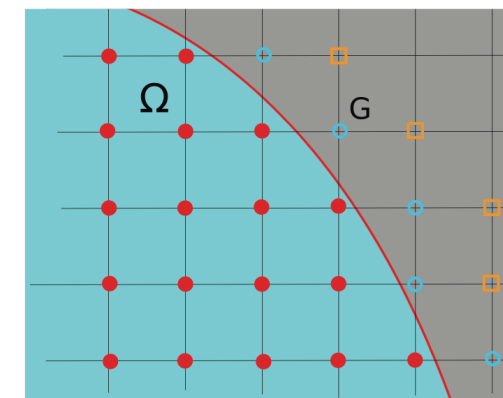
Introducing a [Finite Difference] Mesh over Heart Domain, Ω



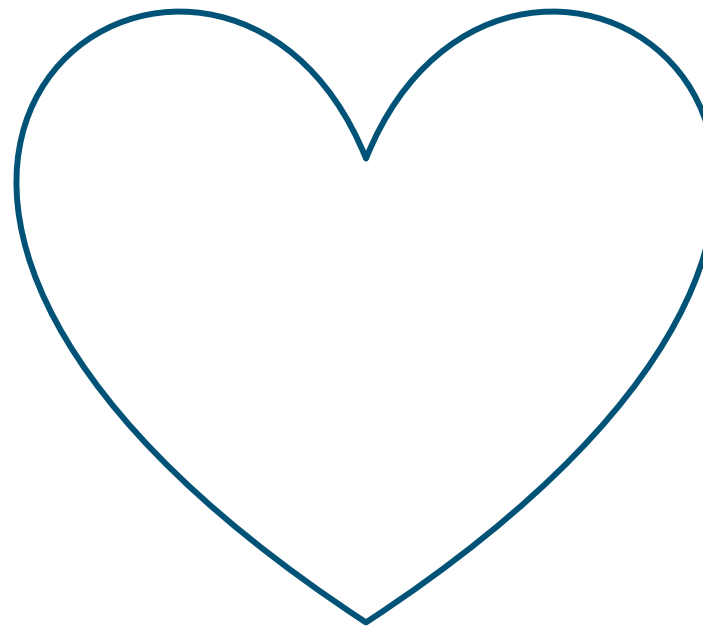
? What breaks..

- Notes: Geometry is:

1. Complex Not impossible: Chertock, et al., “A Second-Order Finite-Difference Method for Compressible Fluids in Domains with Moving Boundaries”, Commun. Comput. Phys., 2018
2. Curved
3. Sharp

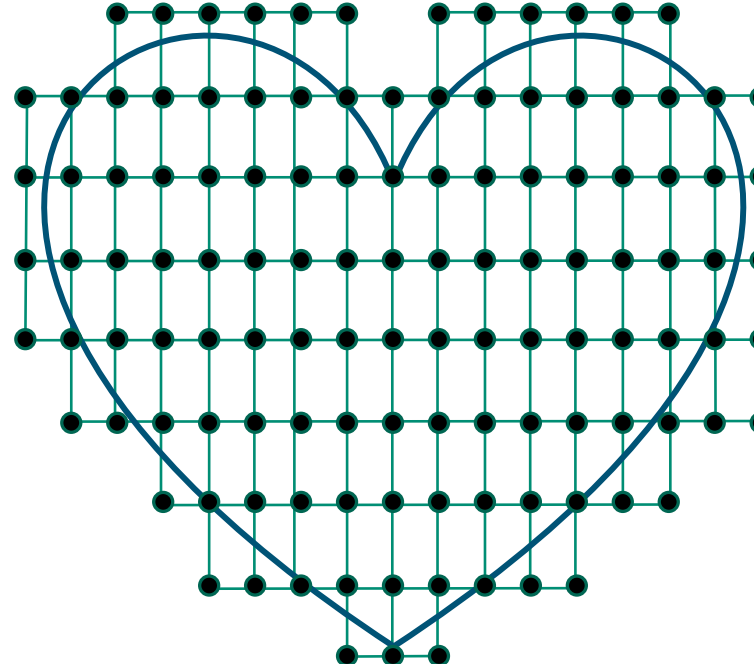


6 | Introducing a [Structured Mesh] over Heart Domain, Ω ;



- Notes: Geometry is:
 1. Complex
 2. Curved
 3. Sharp

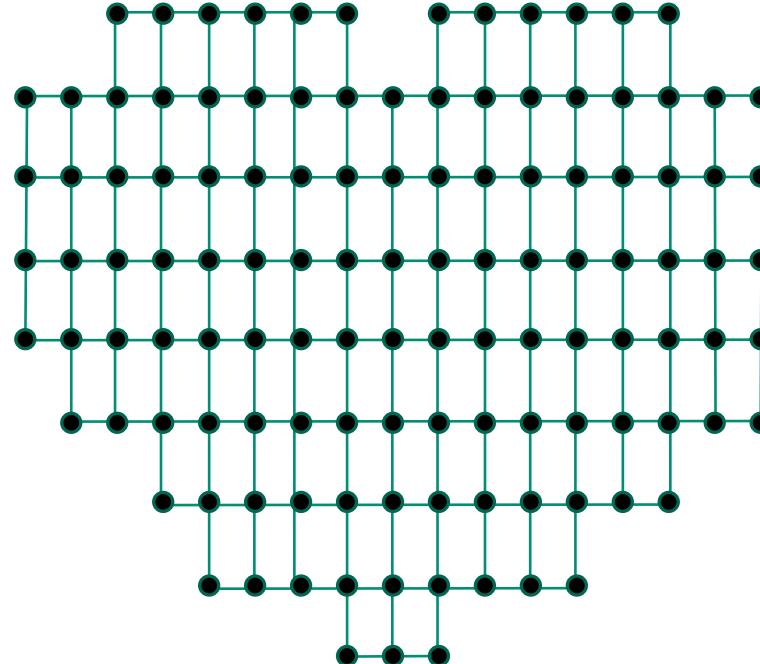
Introducing a [Structured Mesh] over Heart Domain, Ω ;



? What breaks..

- Notes: Geometry is:
 1. Complex
 2. Curved
 3. Sharp

8 | Introducing a [Structured Mesh] over Heart Domain, Ω ;



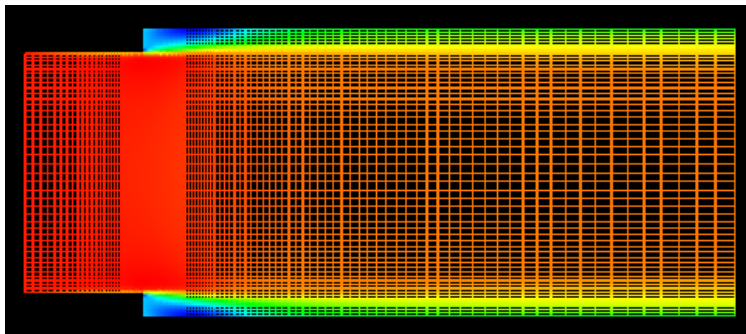
? What breaks..

- Notes: Geometry is:
 1. Complex
 2. Curved
 3. Sharp

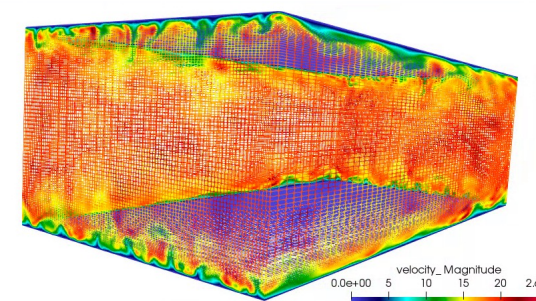
9 | Structured vs Unstructured



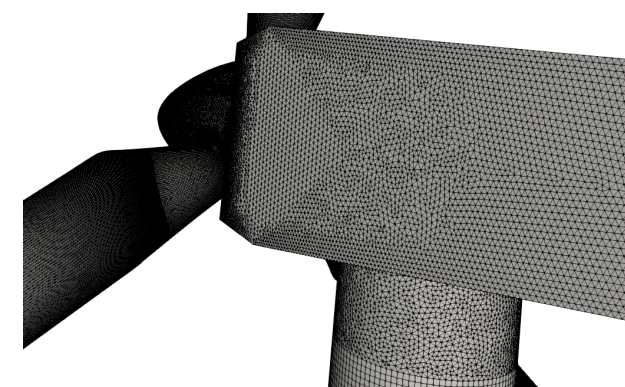
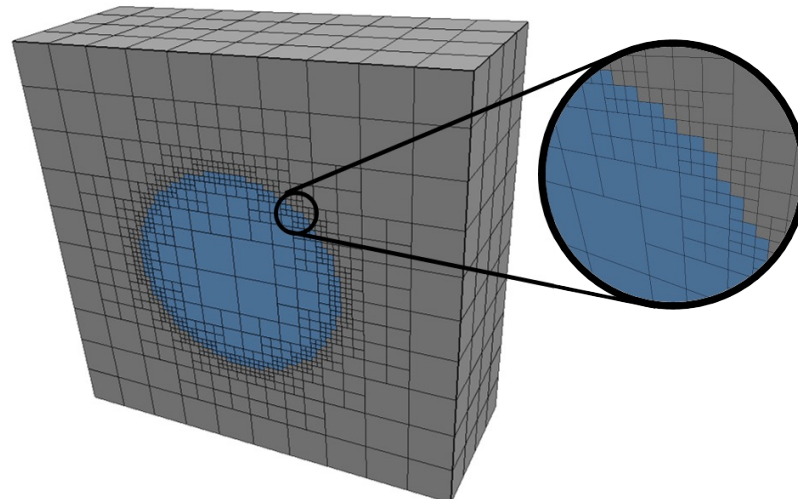
- Many times, the canonical flows of interest are in simplified geometries that allow for cartesian meshes – with “stair-stepping”



RANS-based backward facing step (Domino, 2012)



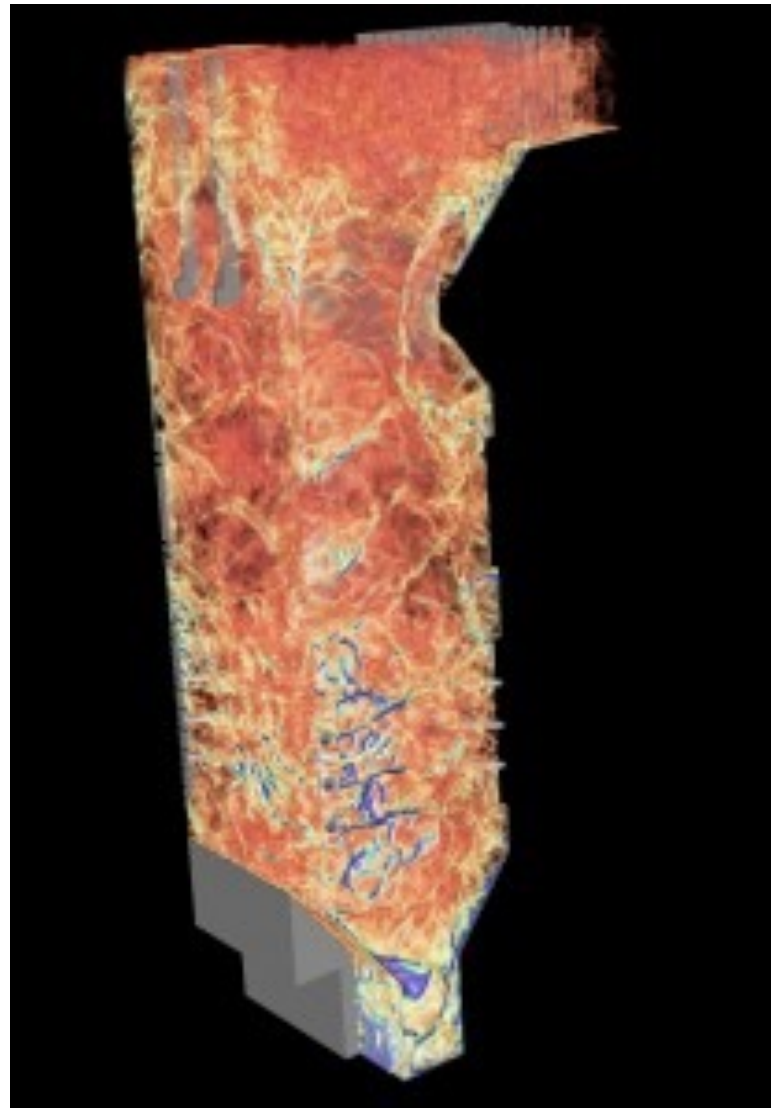
Re^{τ} 395 plane-channel (Jofre, Domino, Iaccarino, 2018)



Often times, not!

In Fairness....

The Carbon-Capture Multidisciplinary Simulation Center

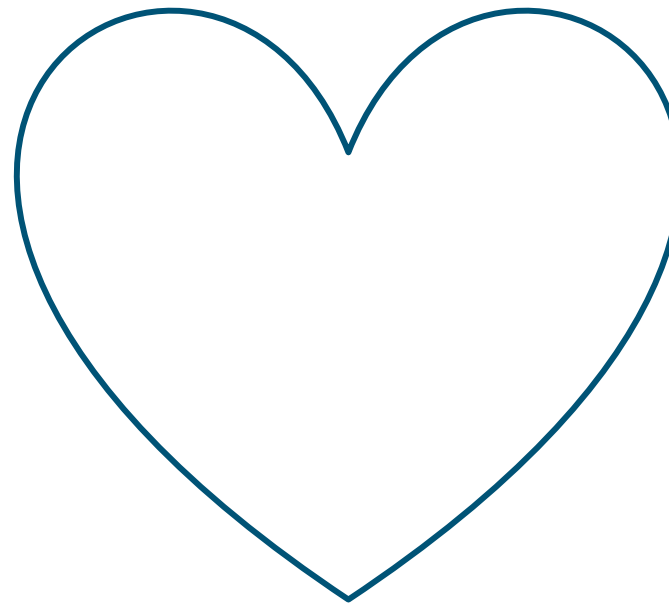


15MW coal-fired boiler volume rendered image of large (90 μm) particles

Staggered schemes have been demonstrated to support complex applications

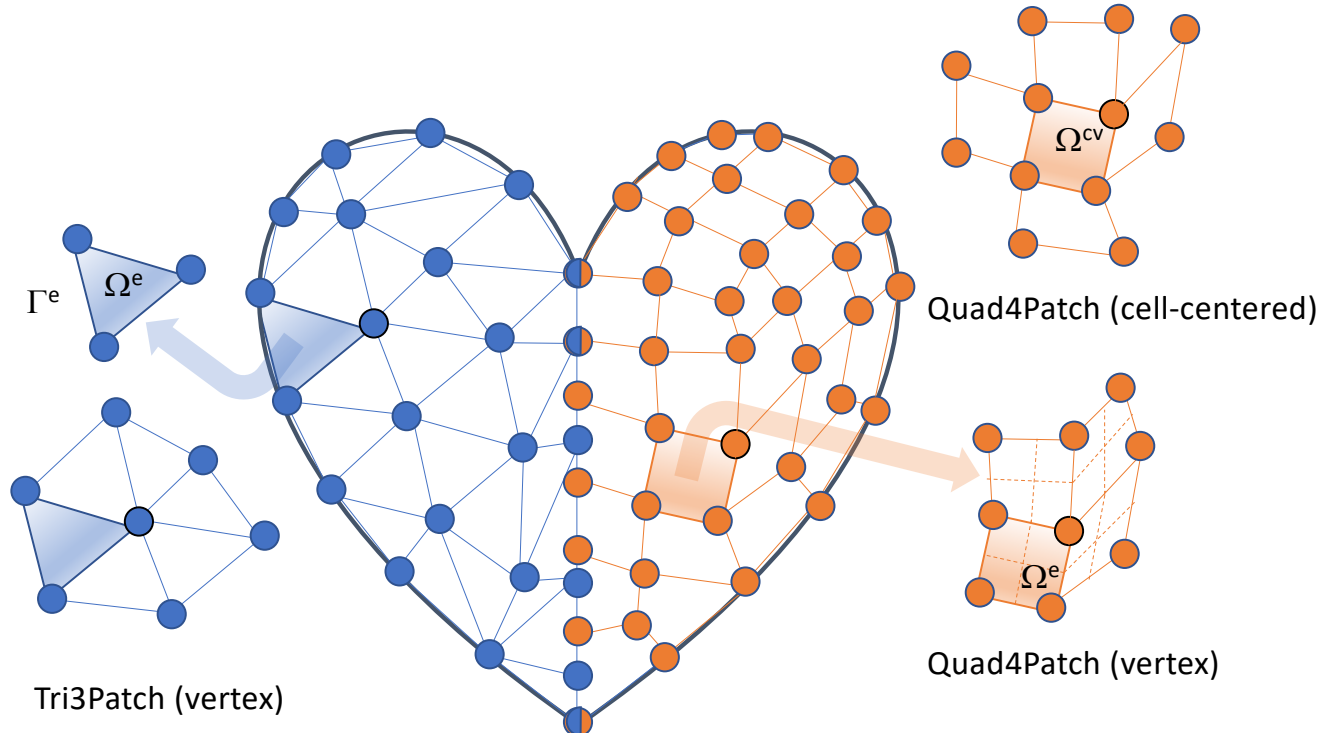
Cut-cells and embedded approaches help

Introducing a Mesh over Heart Domain, Ω



- Elements of size 4 (Quad4) or 3 (Tri3) have been introduced
- Exterior domain is faceted
- Non-conformal interface between the Tri3 and Quad4 block
- Two types of connectivity have been presented: node:element and element:face:element
- Two types of integration: Ω^e vs Ω^{cv}

Introducing a Mesh over Heart Domain, Ω

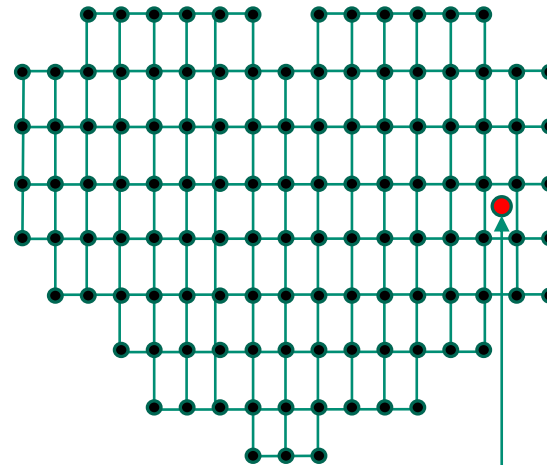


- Elements of size 4 (Quad4) or 3 (Tri3) have been introduced
- Exterior domain is faceted
- Non-conformal interface between the Tri3 and Quad4 block
- Two types of connectivity have been presented: node:element and element:face:element
- Two types of integration: Ω^e vs Ω^{cv}

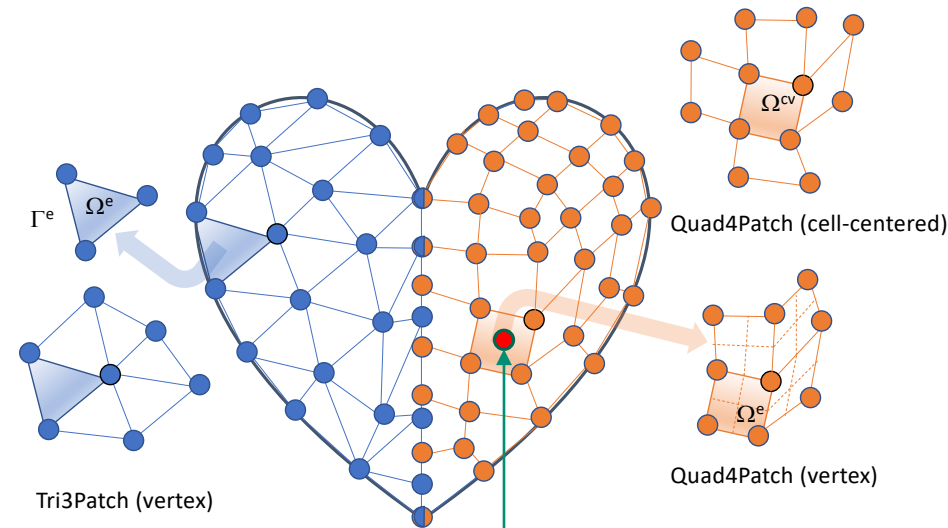
Data Structure Ramifications



- A bit more complicated....



- Element and associated data structures are indexed directly via i^{th} and j^{th} location, e.g., $\text{velocity}_x(i,j)$, over the range: $\text{velocity}_x(0:nX,0:nY)$
- Neighbors are directly indexed, e.g., “north” neighbor of (i,j) is $(i,j+1)$



- Element and associated data structures are indexed indirectly via a data structure, e.g., $\text{velocity}_x(k)$, over the range: $\text{velocity}_x(0:nElem)$
- Neighbors of (k) are obtained via a relationship mapping obtained, e.g.,

```
std::vector<int> neighbor_elems
= elem_relationship(k);
```

Integration Over the Domain



- Consider a simple model equation with the heart domain in mind:

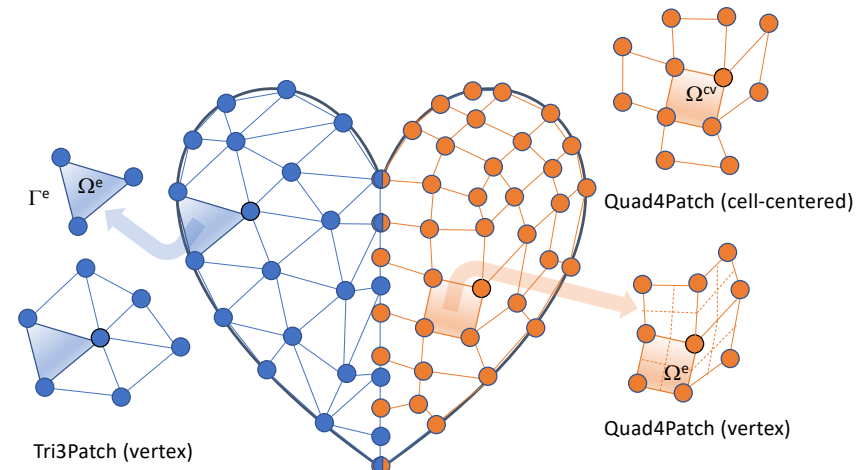
$$\frac{\partial F_j}{\partial x_j} = S, \quad \text{Where } F_j \text{ is a flux and } S \text{ is a source term}$$

- Integrating over the domain, Ω :

$$\int_{\Omega} \frac{\partial F_j}{\partial x_j} dV = \int_{\Omega} S dV.$$

- Without loss of generality, let us define a set of subdomains, Ω_k :

$$\sum_k \int_{\Omega^k} \frac{\partial F_j}{\partial x_j} dV = \sum_k \int_{\Omega_k} S dV,$$

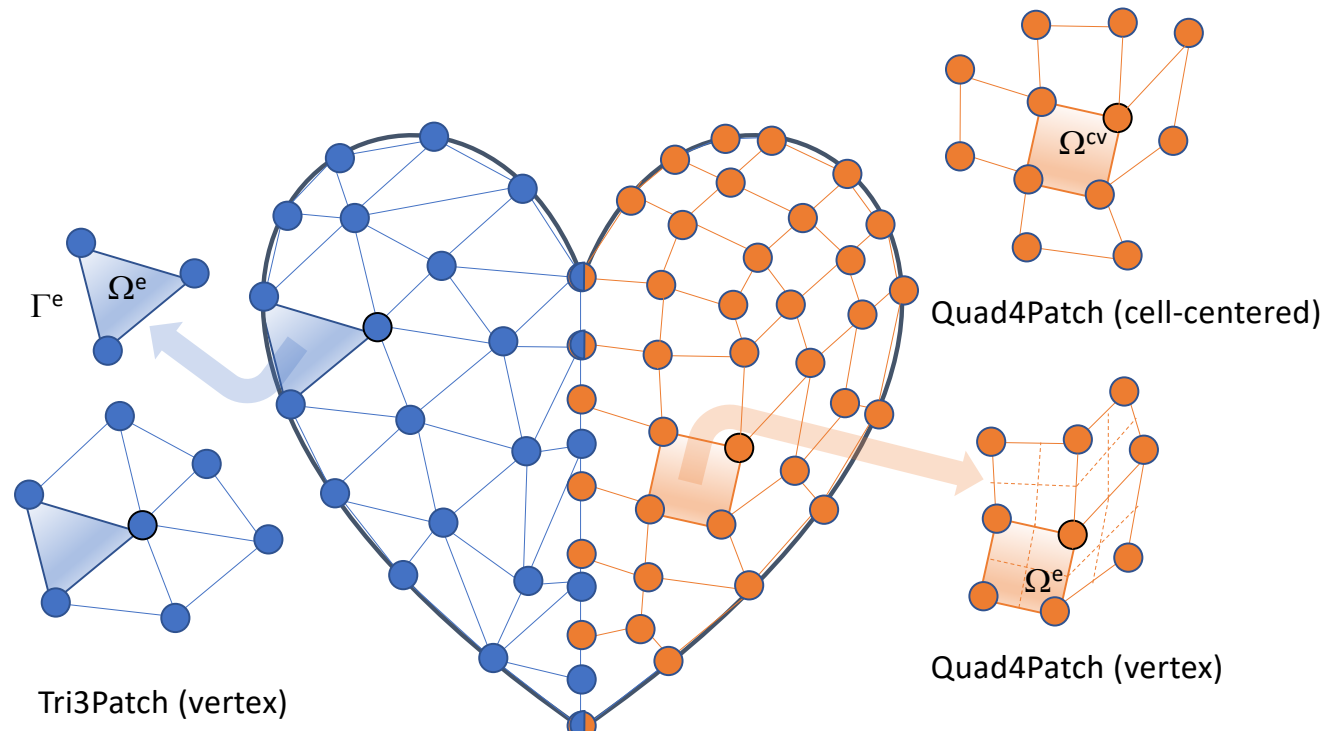


Note: Often the formality of Σ_k and Ω_k is dropped and is implied over the integration

Mesh-based Methods Basic Concept: Sub-divide domain into Finite Elements and Numerically Integrate



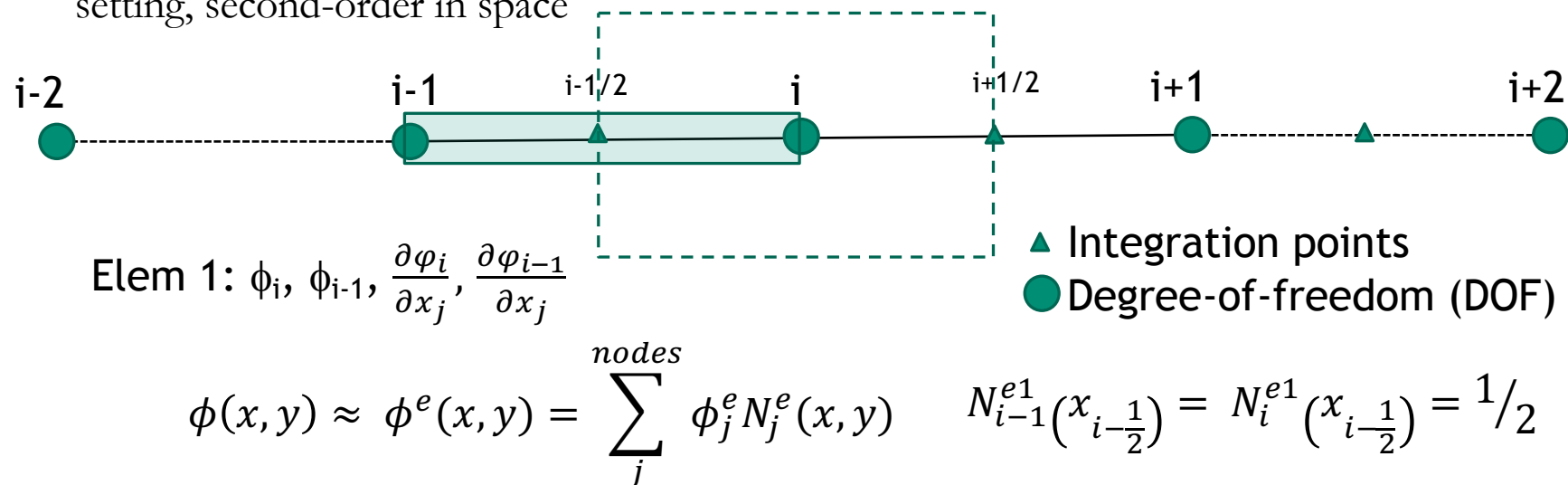
- Define basis within the domain: $\phi(x, y) \approx \phi^e(x, y) = \sum_j^{nodes} \phi_j^e N_j^e(x, y)$
- While restricting to a Lagrange nodal basis, $N_j^e(x_k, y_k) = \delta_{j,k}$





Re-visiting the Underlying Basis: Vertex-centered

- Mindset change for unstructured: the mesh connectivity we have implicitly defines the limiting spatial order of the scheme, here in an unstructured setting, second-order in space



- The “left”/“right” two-state scheme where $i-2$, and $i+1$ values are “reachable” through extrapolation
- Later, in the advection stabilization set of lectures, we will see that such extrapolation is, often “limited”

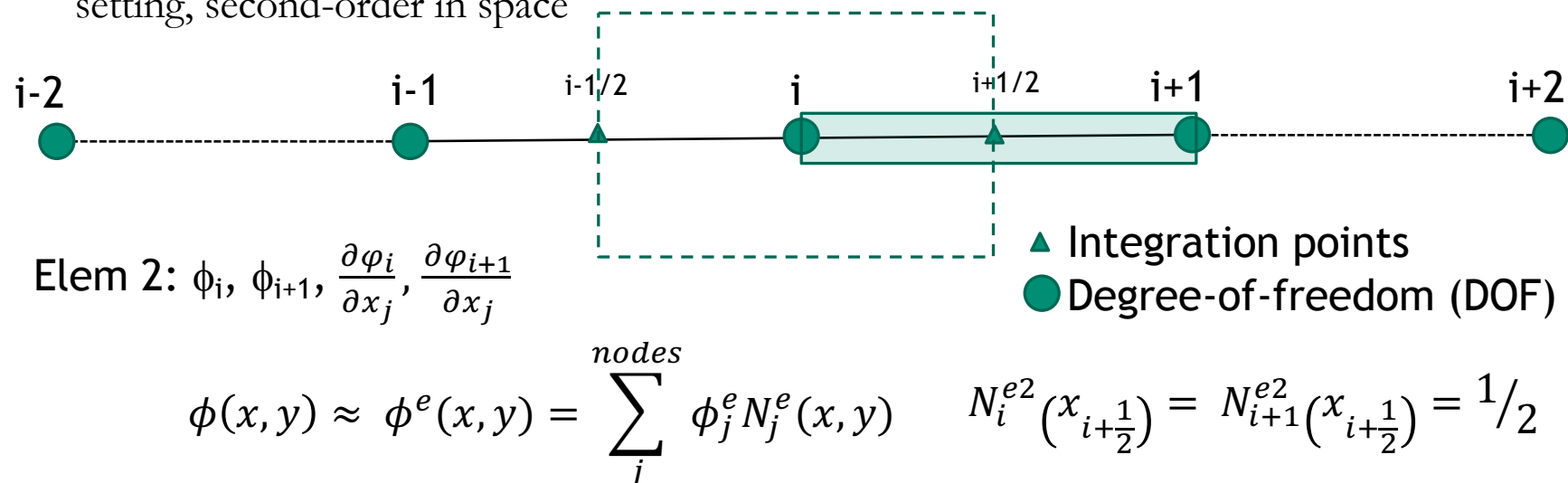
$$\begin{aligned}N_1^{ip} &= \frac{1}{4}(1 - \xi)(1 - \eta) \\N_2^{ip} &= \frac{1}{4}(1 + \xi)(1 - \eta) \\N_3^{ip} &= \frac{1}{4}(1 + \xi)(1 + \eta) \\N_4^{ip} &= \frac{1}{4}(1 - \xi)(1 + \eta)\end{aligned}$$

Iso-parametric coordinate system: -1:+1

Re-visiting the Underlying Basis: Vertex-centered



- Mindset change for unstructured: the mesh connectivity we have implicitly defines the limiting spatial order of the scheme, here in an unstructured setting, second-order in space



- The “left”/“right” two-state scheme where $i-1$, and $i+2$ values are “reachable” through extrapolation
- Later, in the advection stabilization set of lectures, we will see that such extrapolation is, often “limited”

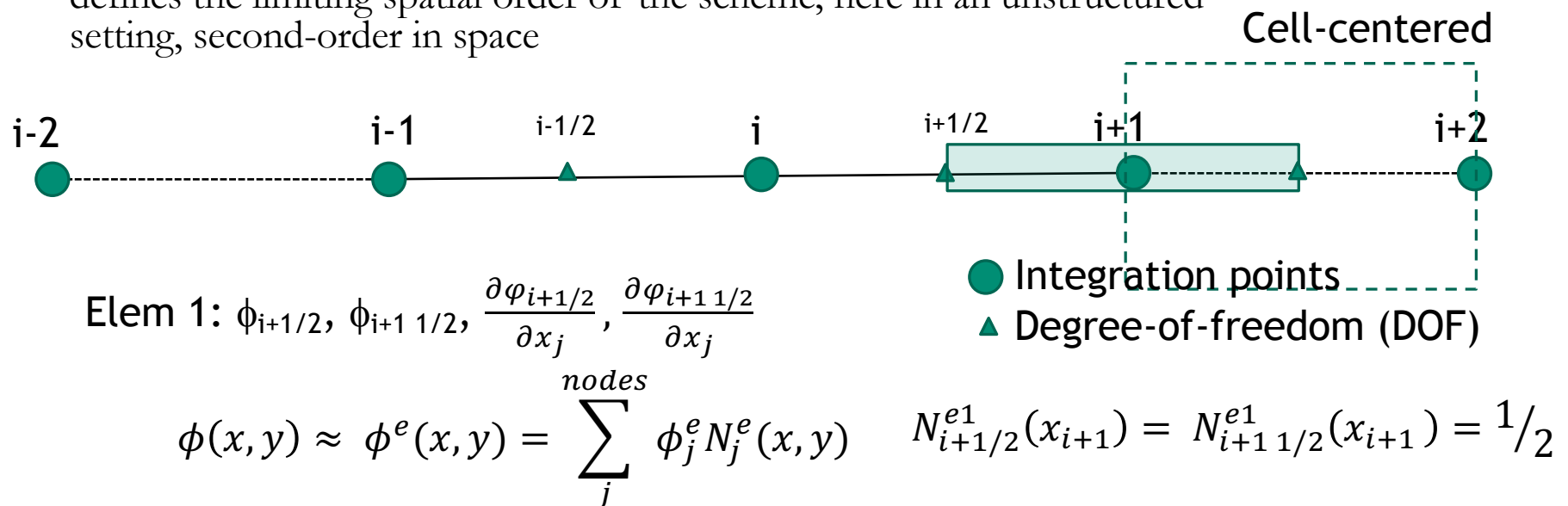
$$\begin{aligned}
 N_1^{ip} &= \frac{1}{4}(1 - \xi)(1 - \eta) \\
 N_2^{ip} &= \frac{1}{4}(1 + \xi)(1 - \eta) \\
 N_3^{ip} &= \frac{1}{4}(1 + \xi)(1 + \eta) \\
 N_4^{ip} &= \frac{1}{4}(1 - \xi)(1 + \eta)
 \end{aligned}$$

Iso-parametric coordinate system: -1:+1

Re-visiting the Underlying Basis: Cell-centered



- Mindset change for unstructured: the mesh connectivity we have implicitly defines the limiting spatial order of the scheme, here in an unstructured setting, second-order in space

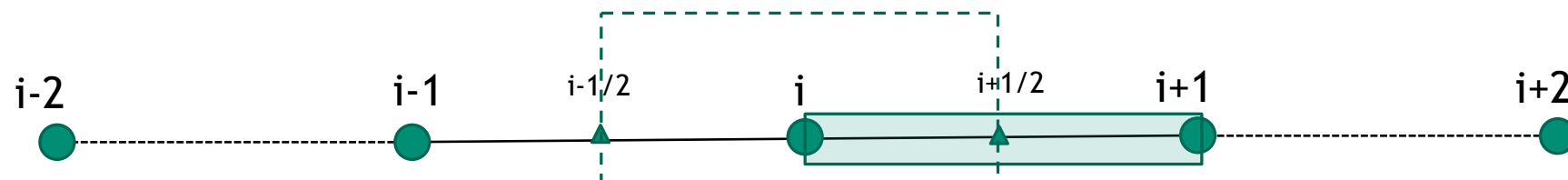


- The “left”/“right” two-state scheme; increased stencil “reachable” - still by extrapolation
- Iterate virtual edges of control volume faces, connected to the left and right DOF location
- Integration point area vector, or at the face of the elements
- What might be a path forward to increase order of accuracy, while maintaining a compact stencil?

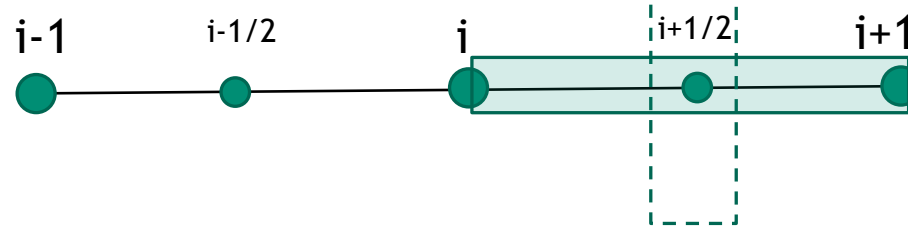
Re-visiting the Underlying Basis: Polynomial Promotion



- From this:



- to that....

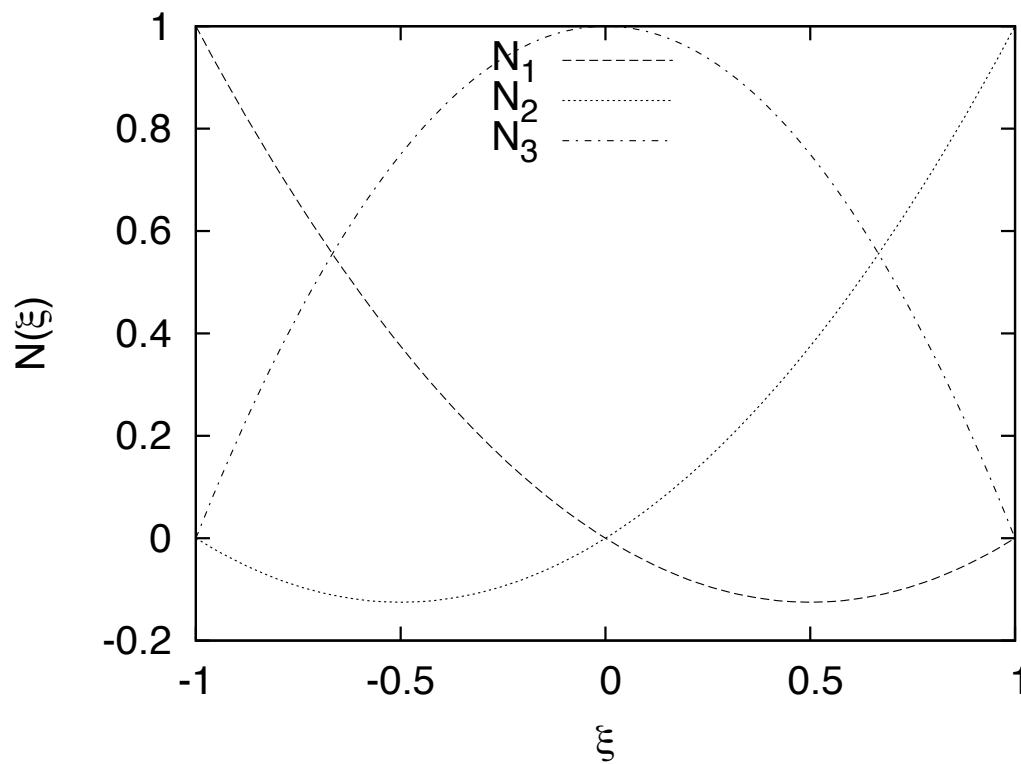
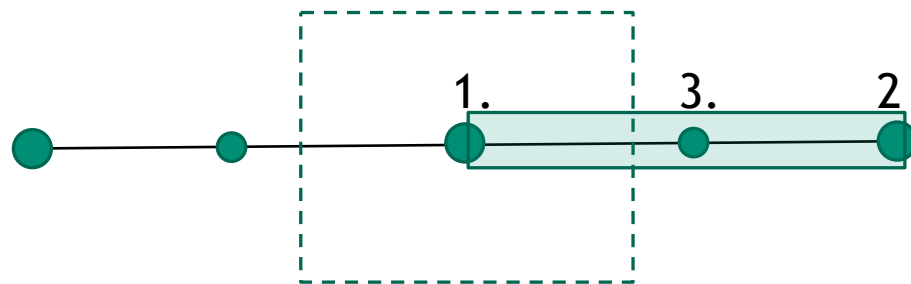


Note:

New promoted nodes “live” at the Gauss-Lobatto points while dual volume lives at the Gauss-Lagrange points: $\pm \sqrt{3}/3$

20

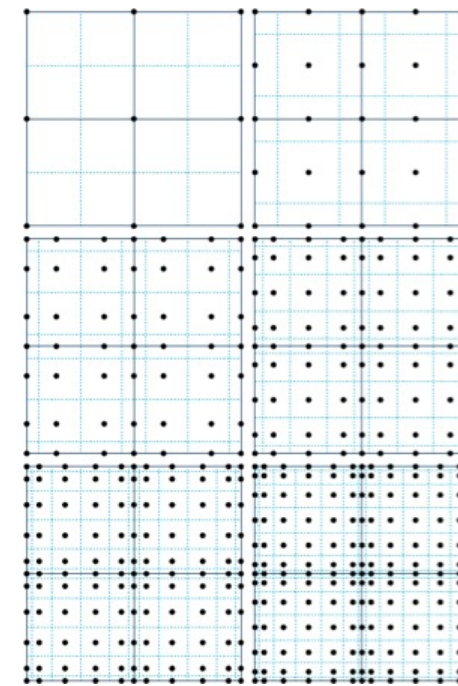
Example of a Quadratic Basis Function



$$N_1 = \frac{-\xi(1-\xi)}{2}$$

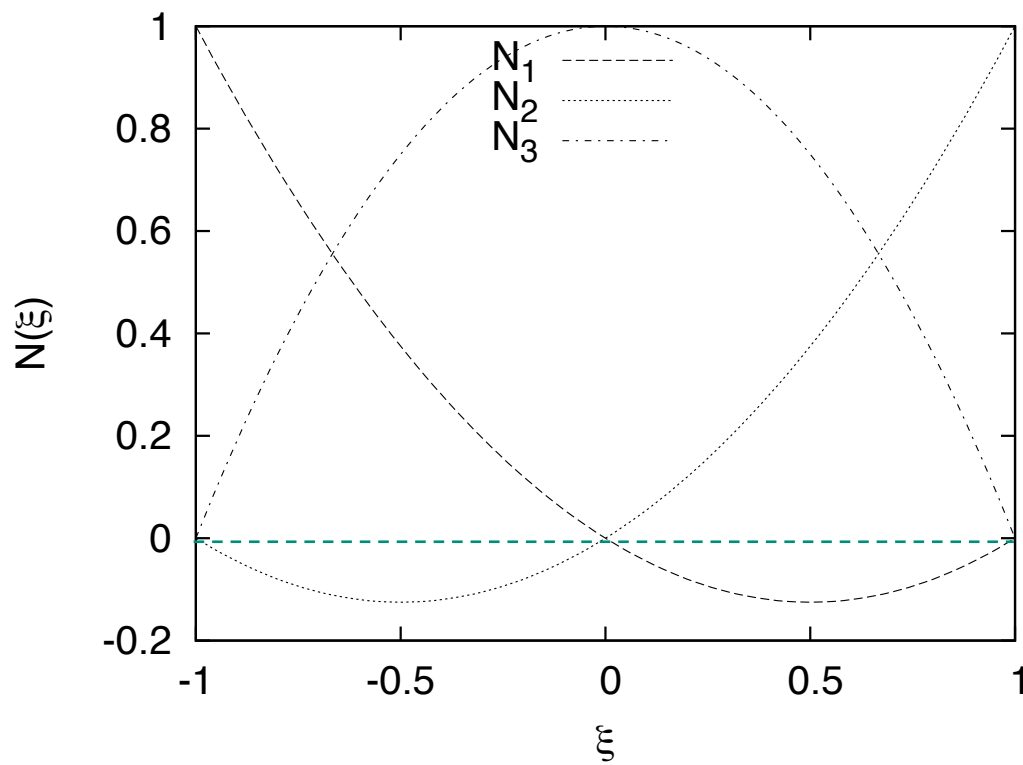
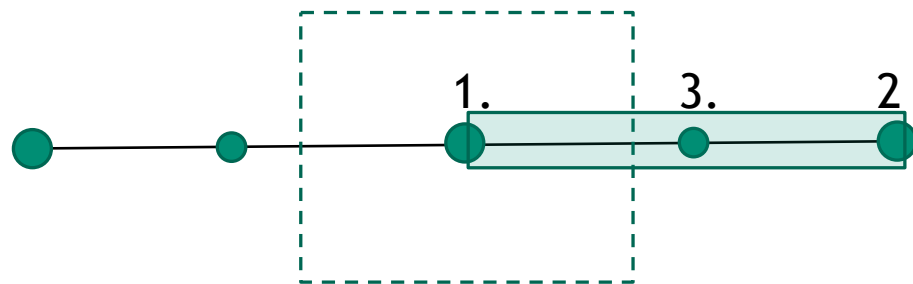
$$N_2 = \frac{\xi(1+\xi)}{2}$$

$$N_3 = (1-\xi)(1+\xi)$$



Two-dimensional promotion

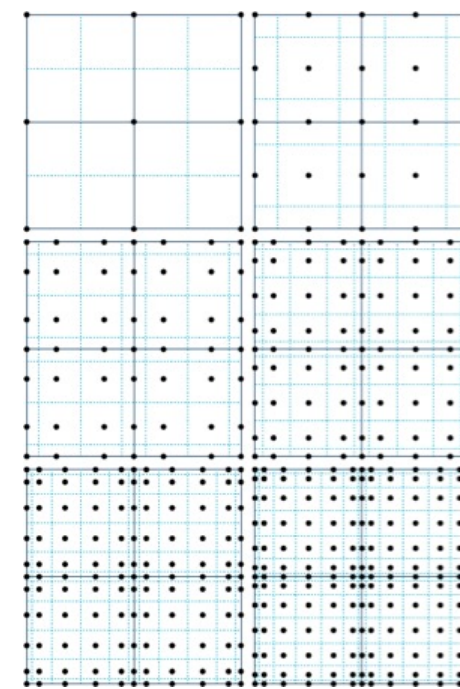
21 Example of a Quadratic Basis Function



$$N_1 = \frac{-\xi(1-\xi)}{2}$$

$$N_2 = \frac{\xi(1+\xi)}{2}$$

$$N_3 = (1-\xi)(1+\xi)$$

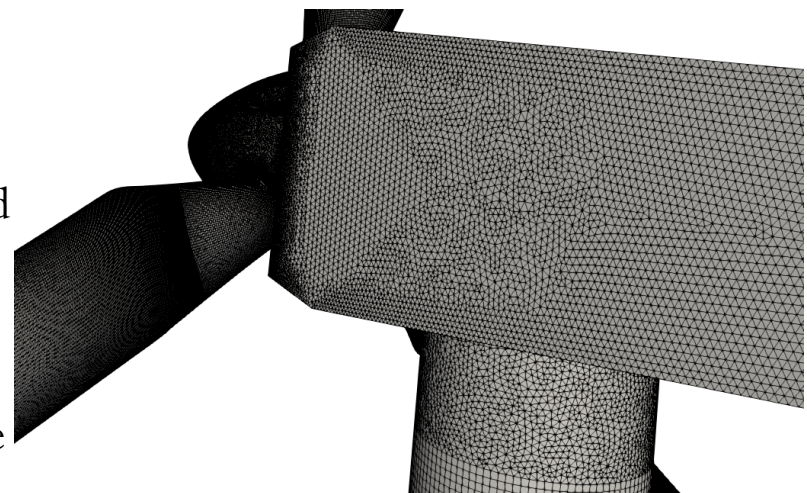


Two-dimensional promotion

Reality: Meshing time for complex applications remains a significant bottleneck!



- Many applications of interest contain complex geometries
- low-Mach fluids users interested in high-quality simulation results tend towards hexahedral-based topologies (if possible)
- However, if a scheme is “design-order” accurate, any topology may suffice as it is simply a matter of mesh size and efficiency – not unlike the active discussion on low- vs higher-order
- Sometimes, the penetration of a low-Mach fluids physics addition in common analysis is high as the meshing can be prohibitively complex



Very complex world - stair-stepped!

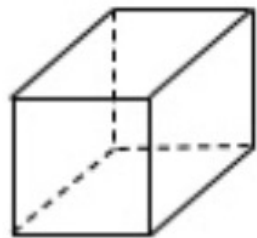


UUR
Example:
Vestas V27
225 kw
hybrid low-
order
hex/tet/pyr
/wedge

Examples of Various Topologies



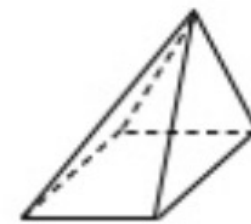
Hex8



Tet4



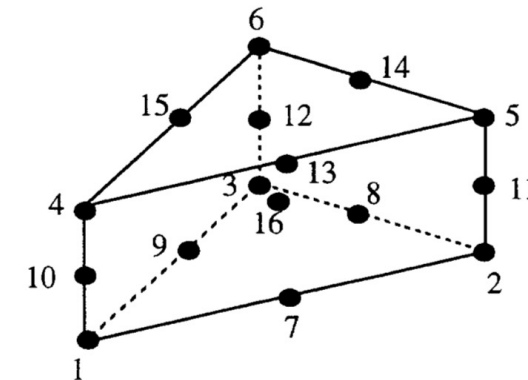
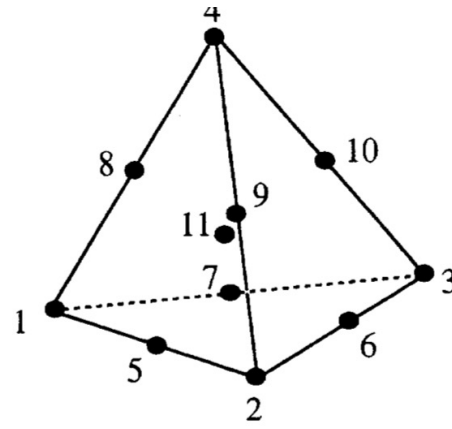
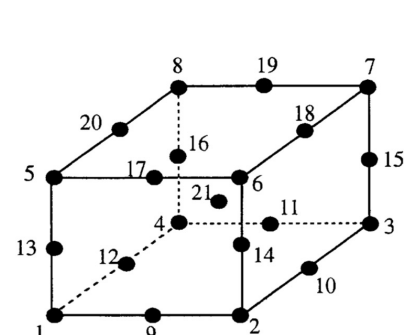
Pyramid5



Wedge6



Arbitrary



Higher-order promoted elements (Hex27, Tet10, Wedge16, Hex64, etc.)

Fundamentals of Discretization (Review)



- Given a partial differential equation (PDE) and associated volumetric form:

$$\rho C_p \frac{\partial T}{\partial t} - \frac{\partial}{\partial x_j} \lambda \frac{\partial T}{\partial x_j} = 0 \quad \int \rho C_p \frac{\partial T}{\partial t} dV - \int \frac{\partial}{\partial x_j} \lambda \frac{\partial T}{\partial x_j} dV = 0$$

- Applying Gauss Divergence provides the standard finite volume form:

$$\int \frac{\partial q_j}{\partial x_j} dV = \int q_j n_j dS \quad \int \rho C_p \frac{\partial T}{\partial t} dV - \int \lambda \frac{\partial T}{\partial x_j} n_j dS = 0$$

- We can also multiple PDE by an arbitrary test function, w , and integrate over a volume,

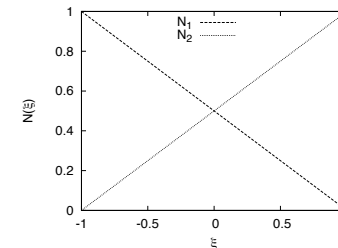
$$\int w \rho C_p \frac{\partial T}{\partial t} dV - \int w \frac{\partial}{\partial x_j} \lambda \frac{\partial T}{\partial x_j} dV = 0$$

$$\int w \rho C_p \frac{\partial T}{\partial t} dV + \int \frac{\partial w}{\partial x_j} \lambda \frac{\partial T}{\partial x_j} dV - \int w \lambda \frac{\partial T}{\partial x_j} dS = 0$$

Next, integrate by parts and apply Gauss-Divergence. Note, that test function must be differentiable – shown here, at least once..

Sometimes, one notes T as T^h - the trial space on given mesh size, h

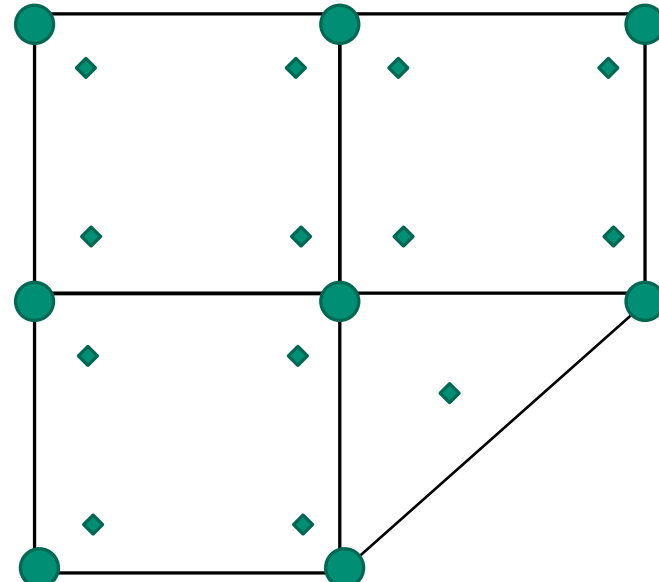
The Finite Element Method (FEM)



- Consider the example in which the finite element method (FEM) is employed
- Define an underlying nodal basis with the element:

$$T(x_k) \approx \sum_{i=1}^{npe} N_i(x_k) T_i \quad \frac{\partial T(x_k)}{\partial x_j} \approx \sum_{i=1}^{npe} \frac{\partial N_i(x_k)}{\partial x_j} T_i$$

$$\rho C_p \frac{\partial T}{\partial t} - \frac{\partial}{\partial x_j} \lambda \frac{\partial T}{\partial x_j} = 0$$



- Gaussian Quadrature is used
 - using a $-1:1$ range, $\pm \sqrt{3}/3$

- Consider a simple heat conduction model PDE,

$$\int w \rho C_p \frac{\partial T}{\partial t} dV - \int w \frac{\partial}{\partial x_j} \lambda \frac{\partial T}{\partial x_j} dV = 0$$

- Integration-by-parts (with G-D) provides:

$$\int w \rho C_p \frac{\partial T}{\partial t} dV + \int \frac{\partial w}{\partial x_j} \lambda \frac{\partial T}{\partial x_j} dV - \int w \lambda \frac{\partial T}{\partial x_j} n_j dS = 0$$

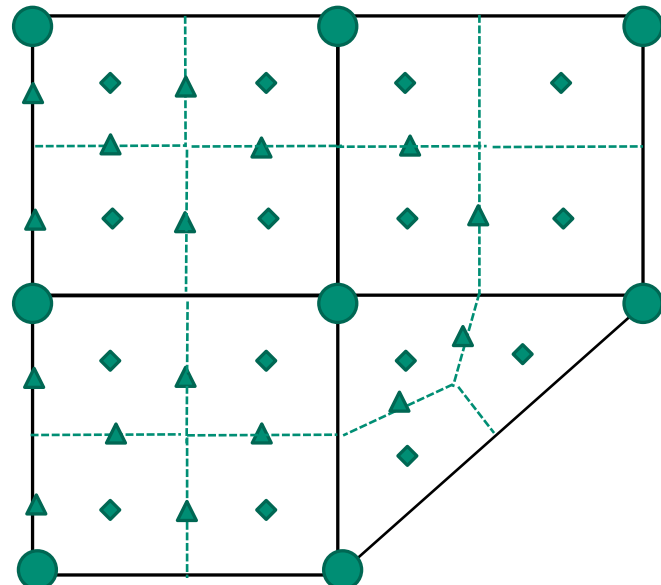
- Iterate element quadrature points
- Note that N can be arbitrary in order (shown here for a linear)

The Hybrid Control-Volume Finite Element Method (CVFEM)



- A combination between a vertex-centered finite volume and FEM is the method known as Control Volume Finite Element
- A dual mesh is constructed to obtain flux and volume quadrature locations
- As with FEM, a basis is defined:

$$T(x_k) \approx \sum_{i=1}^{npe} N_i(x_k) T_i \quad \frac{\partial T(x_k)}{\partial x_j} \approx \sum_{i=1}^{npe} \frac{\partial N_i(x_k)}{\partial x_j} T_i$$



Dual-volume definition

- Integration-by-parts over test function w:

$$\int w \rho C_p \frac{\partial T}{\partial t} dV + \int \frac{\partial w}{\partial x_j} \lambda \frac{\partial T}{\partial x_j} dV - \int w \lambda \frac{\partial T}{\partial x_j} n_j dS = 0$$

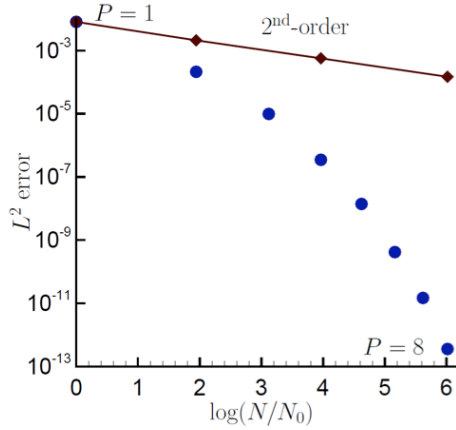
- However, define a test function, w, as a piece-wise constant function (Heaviside) to be 1 inside the dual volume and 0 outside. Gradient is a Dirac-delta function:

$$\frac{\partial w}{\partial x_j} = -n_j \delta(x_j - xIP_j)$$

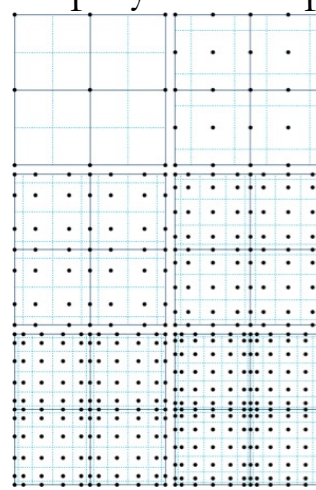
- Leading to: $\int \rho C_p \frac{\partial T}{\partial t} dV - \int \lambda \frac{\partial T}{\partial x_j} n_j dS = 0$



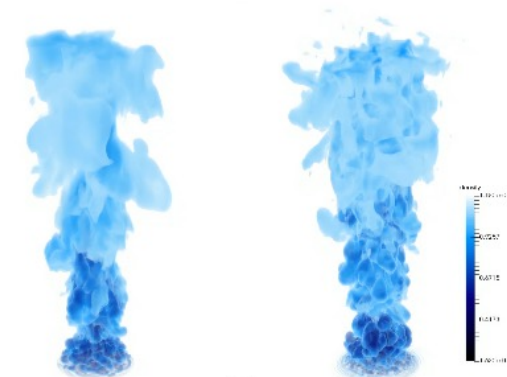
- The CVFEM method, therefore, is a finite volume scheme that is locally conservative, i.e., momentum leaving one dual volume face enters the adjacent dual volume
- However, the diffusion operator, like its FEM counterpart is absent of any error due to non-orthogonality
- Suffers on high-aspect ratio meshes in presence of high gradients: $\sqrt{3}$
- Since the test-function, w , is different from the underlying basis representation, this method can be considered a Petrov-Galerkin method
- The method can also be promoted in polynomial space (firs



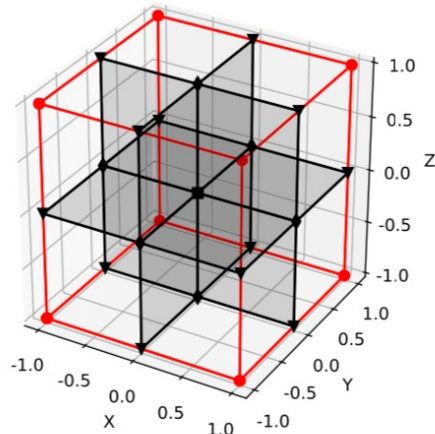
Spectral convergence



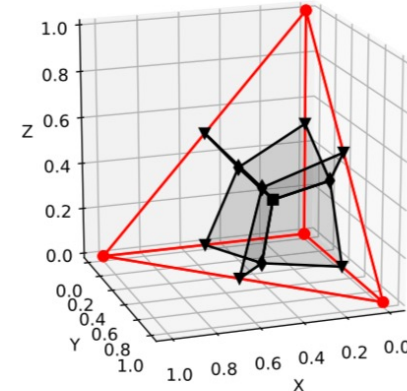
Dual-volume for promoted quad4

 $P=1$ (left) and $P=4$ (right)
Helium plume (VR-density)

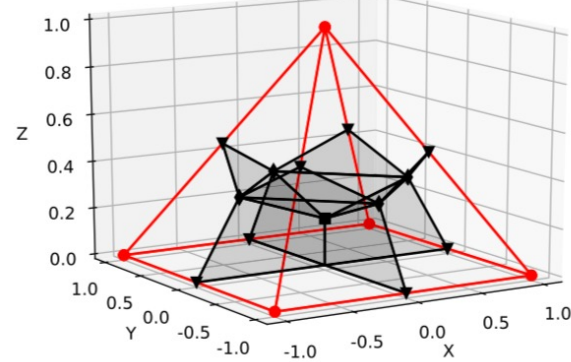
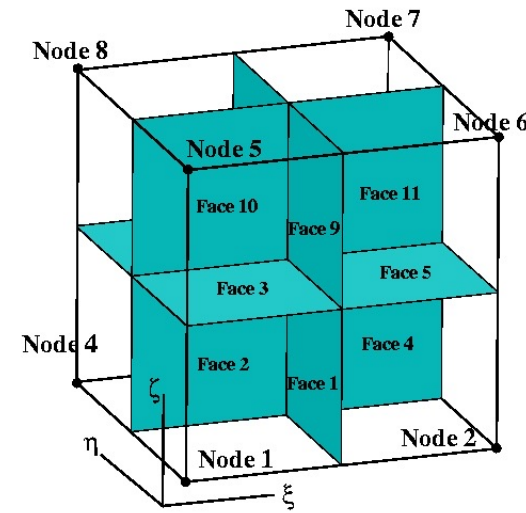
Dual Volume Definitions for Hybrid Meshes



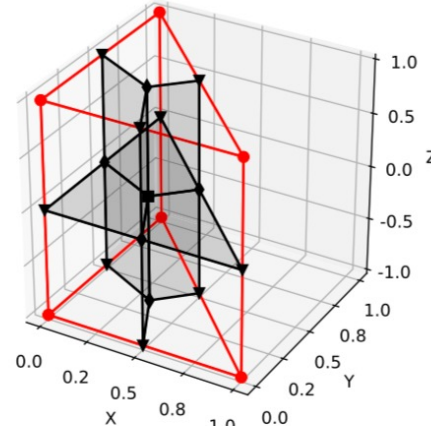
(a) Hexahedral topology (Hex8).



(b) Tetrahedral topology (Tet4).



(c) Pyramid topology (Pyramid5).



(d) Wedge topology (Wedge6).

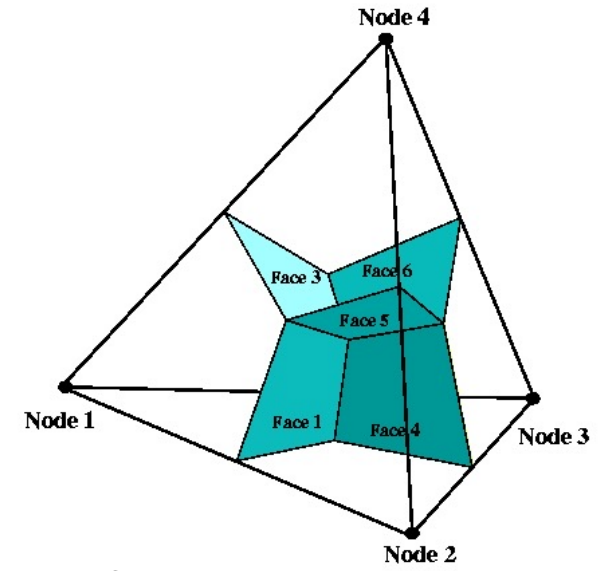


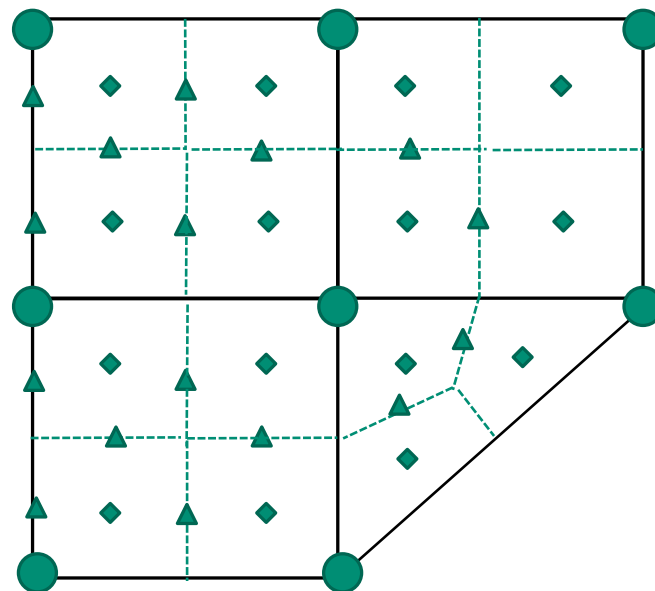
Fig. 1. CVFEM element and dual-volume definition for the low-order topologies.

Domino, et. al, “An assessment of atypical mesh topologies for low-Mach large-eddy simulation” 2019

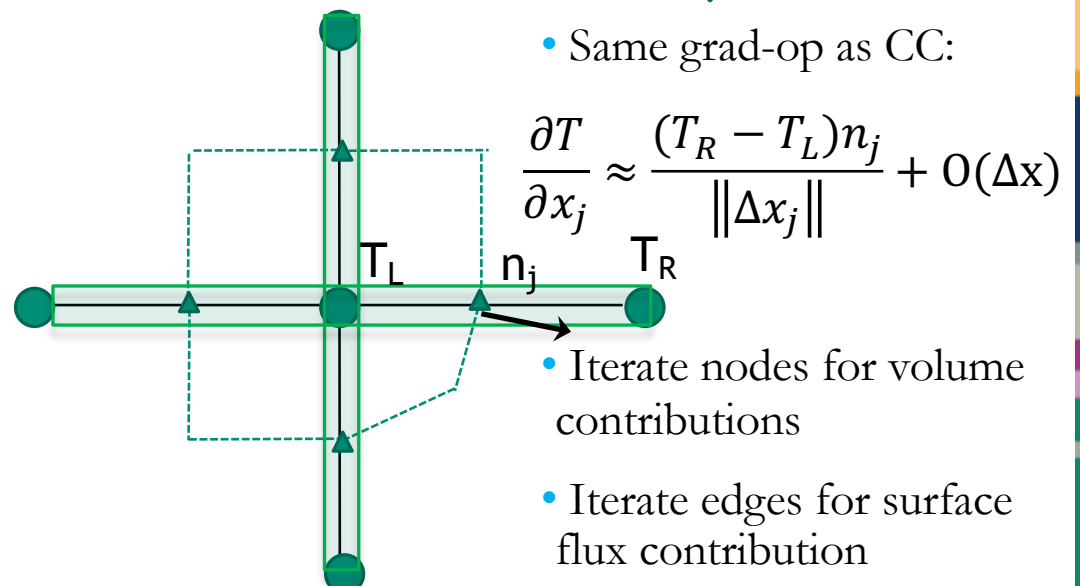
Equal Order Interpolation Edge-Based Vertex-Centered (EBVC) Finite Volume



- All primitives are collocated at the vertices of the elements with equal-order interpolation
- A dual mesh is constructed to obtain flux and volume quadrature locations
- Classic two-state, “L” and “R” approach provides spatially second-order accuracy
 - ▲ Surface quadrature point (area summed to edge)
 - ◆ Volume quadrature point (sub-vol summed to node)



Dual-volume definition

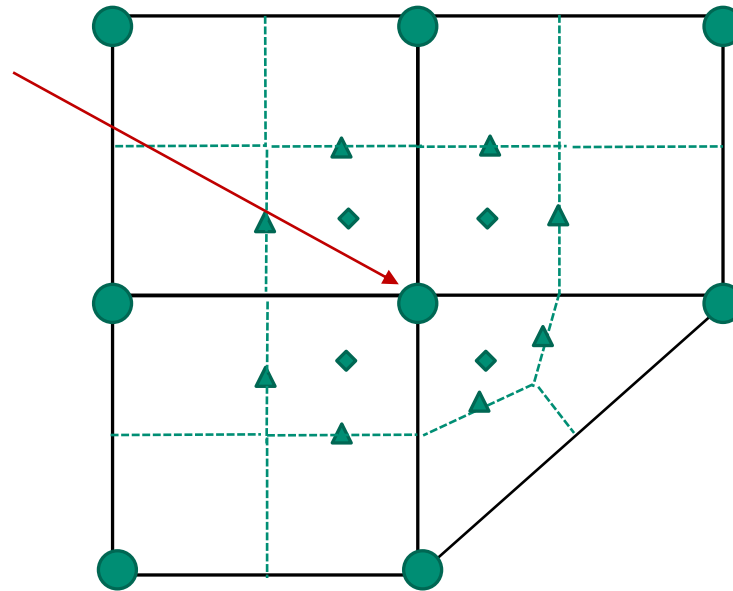


Edge-based stencil

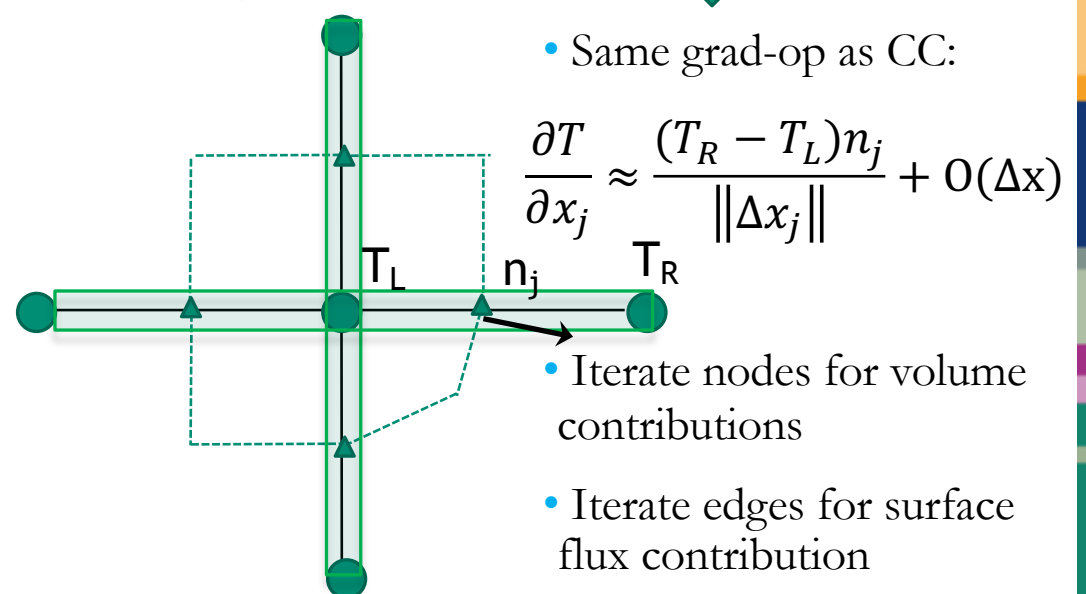
Equal Order Interpolation Edge-Based Vertex-Centered (EBVC) Finite Volume



- All primitives are collocated at the vertices of the elements with equal-order interpolation
- A dual mesh is constructed to obtain flux and volume quadrature locations
- Classic two-state, “L” and “R” approach provides spatially second-order accuracy
 - ▲ Surface quadrature point (area summed to edge)
 - ◆ Volume quadrature point (sub-vol summed to node)



Dual-volume definition

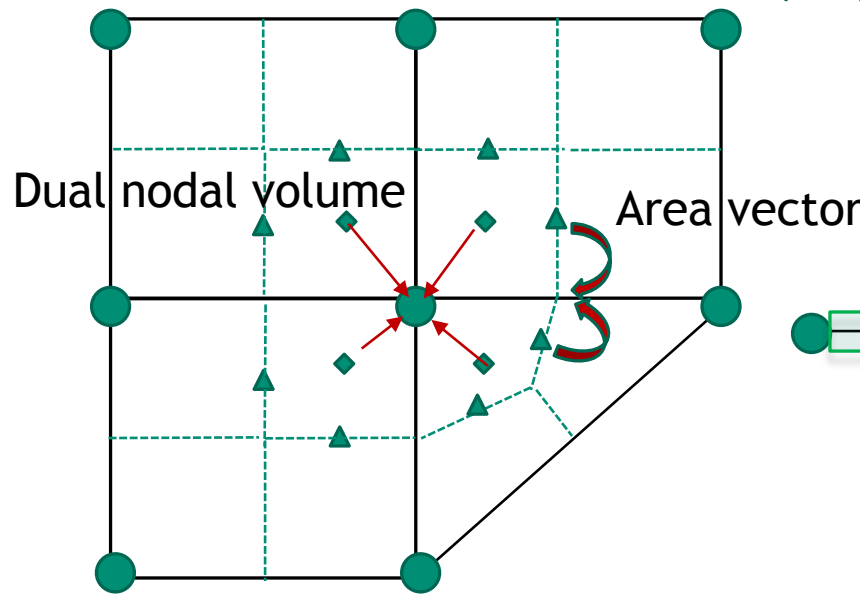


Edge-based stencil

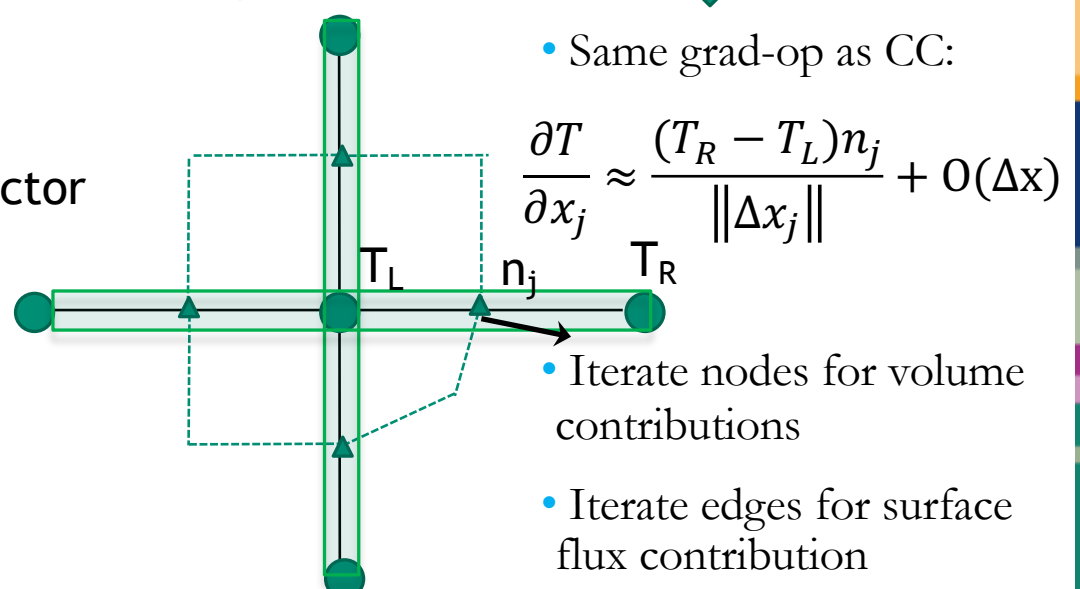
Equal Order Interpolation Edge-Based Vertex-Centered (EBVC) Finite Volume



- All primitives are collocated at the vertices of the elements with equal-order interpolation
- A dual mesh is constructed to obtain flux and volume quadrature locations
- Classic two-state, “L” and “R” approach provides spatially second-order accuracy
 - ▲ Surface quadrature point (area summed to edge)
 - ◆ Volume quadrature point (sub-vol summed to node)



Dual-volume definition



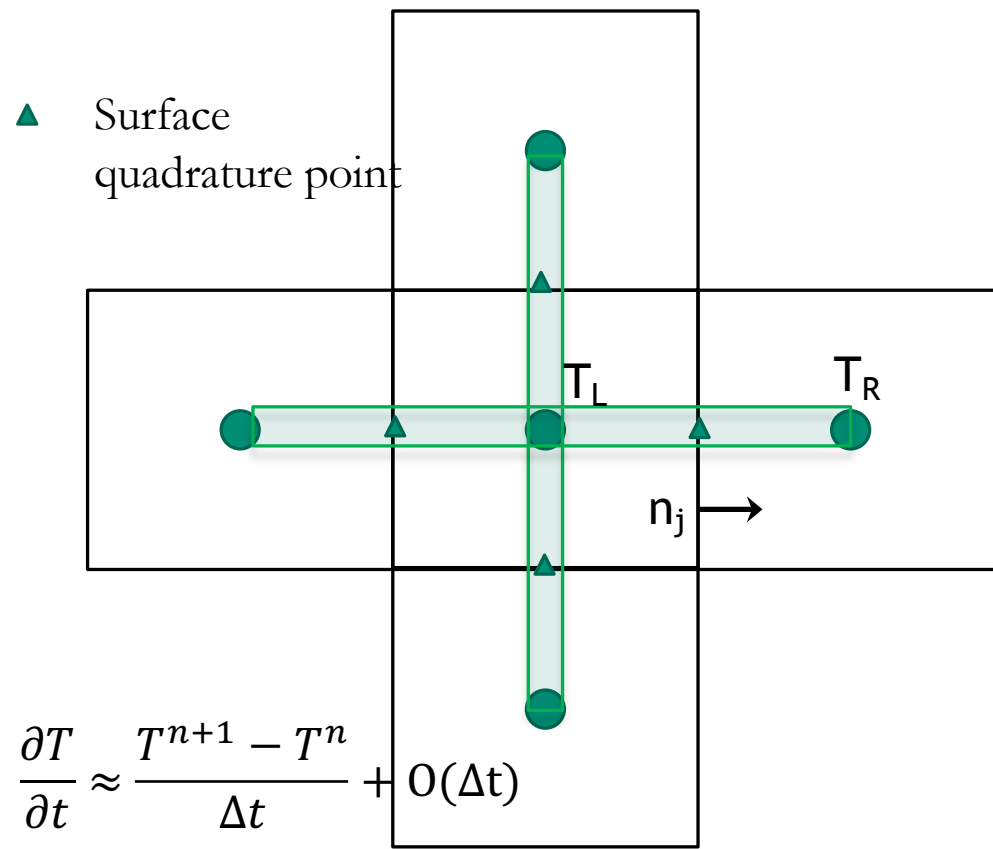
Edge-based stencil

Equal-Order Interpolation Cell-Centered (CC) Finite Volume



- All primitives are collocated at the cell-center of the element with equal-order interpolation
- Classic two-state, “L” and “R” approach provides spatially second-order accuracy

▲ Surface quadrature point



- Consider a simple heat conduction model PDE,

$$\rho C_p \frac{\partial T}{\partial t} - \frac{\partial}{\partial x_j} \lambda \frac{\partial T}{\partial x_j} = 0$$

- Integrate over a control volume and use Gauss-Divergence,

$$\int \rho C_p \frac{\partial T}{\partial t} dV - \int \lambda \frac{\partial T}{\partial x_j} n_j dS = 0$$

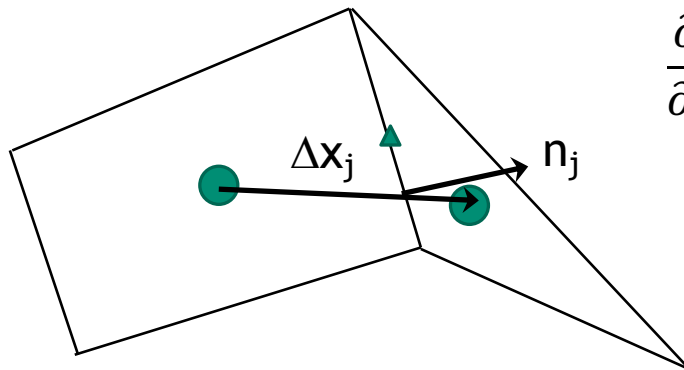
$$\text{with: } \frac{\partial T}{\partial x_j} \approx \frac{(T_R - T_L)n_j}{\|\Delta x_j\|} + O(\Delta x)$$

- Iterate element cell-centers for volume contributions (time/source)
- Iterate element faces for surface flux contribution

Typical Failings for Two-State Discretization Methods



- With two points, only a linear basis can be used.
- Therefore, unstructured CC and EBVC are limited to second-order spatial accuracy
- Non-orthogonality is problematic for gradient-operator



$$\frac{\partial T}{\partial x_j} = G_j T + [(T_R - T_L) - G_k T \Delta x_k] \frac{A_j}{A_l \Delta x_l}$$

With area vector defined by: $A_j = n_j dS$

- Above, $G_j T$ is a projected nodal gradient at the cell-center, or vertex center:
- Non-orthogonality is simply defined as the mis-alignment of the distance vector between the two "L" and "R" states and the surface normal
- Both edge- and cell centered-based schemes show degraded accuracy on typical production meshes
- Several non-orthogonality approaches are available, for the best source, see Jasak
 - Jasak, "Error analysis and error estimation for the finite volume method with applications to fluid flow", Imperial College Dissertation, 1996
- One Significant Advantage: Monotonicity preserving on high-aspect ratio meshes...

$$G_j T = \frac{\int T A_j}{\int dV}$$

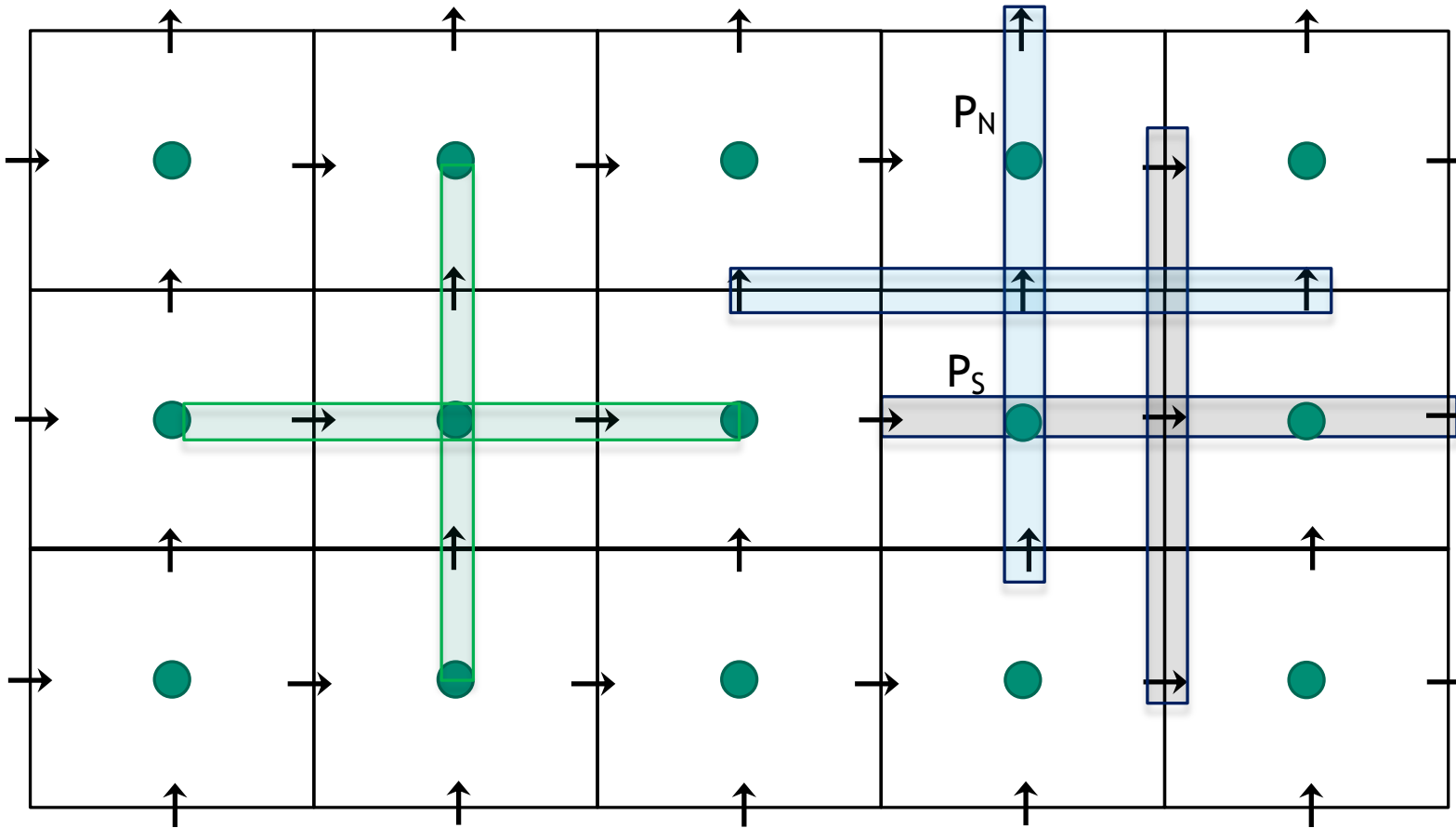
Classic Staggered Finite Volume

Stencil for CC-quantities

Stencil for x-velocity →

Stencil for y-velocity ↑

- Velocity degree-of-freedom is staggered relative to pressure and other primitives, e.g., enthalpy, mixture fraction, etc.



Attributes of a Staggered Scheme



- By design, non-orthogonality is absent, however, complex geometry will be stair-stepped
- From a fluids perspective, the operators are ideal, i.e., pressure gradient for momentum is compact, e.g., $(P_E - P_W)\Delta x^{-1}$
 - As will be seen in future lecture topics, the skew-adjoint nature of the Divergence operator, **D**, and Gradient operator, **G**, allows for a Laplace operator, **L = DG**
- Can be extended to higher-order
- Frequently, meshing complex geometries can be extremely difficult (consider our V27 example)

An Informal Survey....



- Cell-Centered: (Sometimes generalized Polyhedra)
 - Ansys Fluent, OpenFOAM (FireFOAM, NavyFOAM), CD-Adapco (Star-CCM), Soleil-X (Stanford)
- EBVC: (Most typical in the acoustically compressible space)
 - SU2, FUN3D, CHAD, Nalu-Wind (production), Nalu (option to explore discretizations)
- CVFEM
 - Fluent (originally!), CFX-TASC-FLOW, Sierra Fuego (SNL), Nalu
- FEM
 - FIDAP, COMSOL, EDDY (NASA), AcuSim, PHASTA
- Staggered
 - Arches (Utah)

An Informal Survey....



- Cell-Centered: (Sometimes generalized Polyhedra)
 - Ansys Fluent, OpenFOAM (FireFOAM, NavyFOAM), CD-Adapco (Star-CCM), Soleil-X (Stanford)
 - EBVC: (Most typical in the acoustically compressible space)
 - SU2, FUN3D, CHAD, Nalu-Wind (production), Nalu (option to explore discretizations)
 - CVFEM
 - Fluent (originally!), CFX-TASC-FLOW, Sierra Fuego (SNL), Nalu
 - FEM
 - FIDAP, COMSOL, EDDY (NASA), AcuSim, PHASTA
 - Staggered
 - Arches (Utah)
- Common Water-Cooler CFD Arguments:**
- Structured vs. Un-structured
 - FEM vs. Finite Volume
 - Node-centered vs. Cell-centered
 - Monolithic vs. Operator Split
 - Compressible vs. (acoustically) Incompressible
 - Explicit vs. Implicit



- Cell-Centered: (Sometimes generalized Polyhedra)
 - Ansys Fluent, OpenFOAM (FireFOAM, NavyFOAM), CD-Adapco (Star-CCM), Soleil-X (Stanford)
- • EBVC: (Most typical in the acoustically compressible space)
 - SU2, FUN3D, CHAD, Nalu-Wind (production), Nalu (option to explore discretizations)
- • CVFEM
 - Fluent (originally!), CFX-TASC-FLOW, Sierra Fuego (SNL), Nalu
- • FEM
 - FIDAP, COMSOL, EDDY (NASA), AcuSim, PHASTA
- • Staggered
 - Arches (Utah)



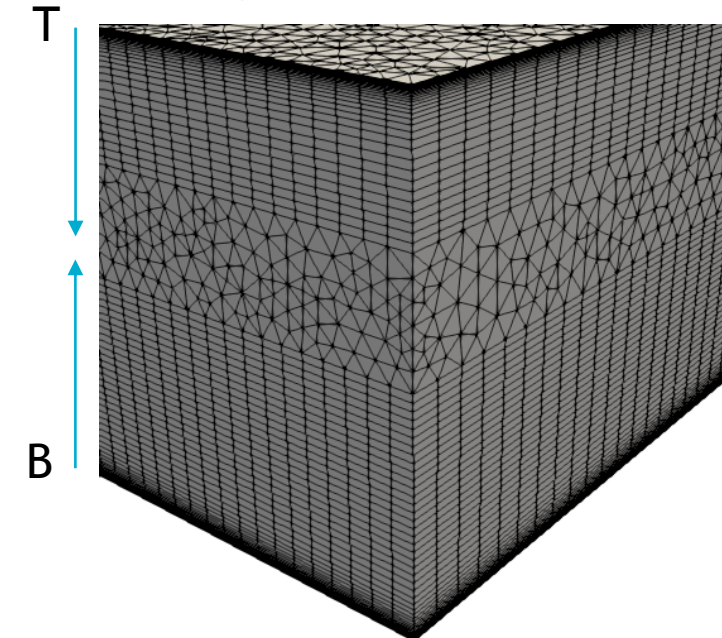
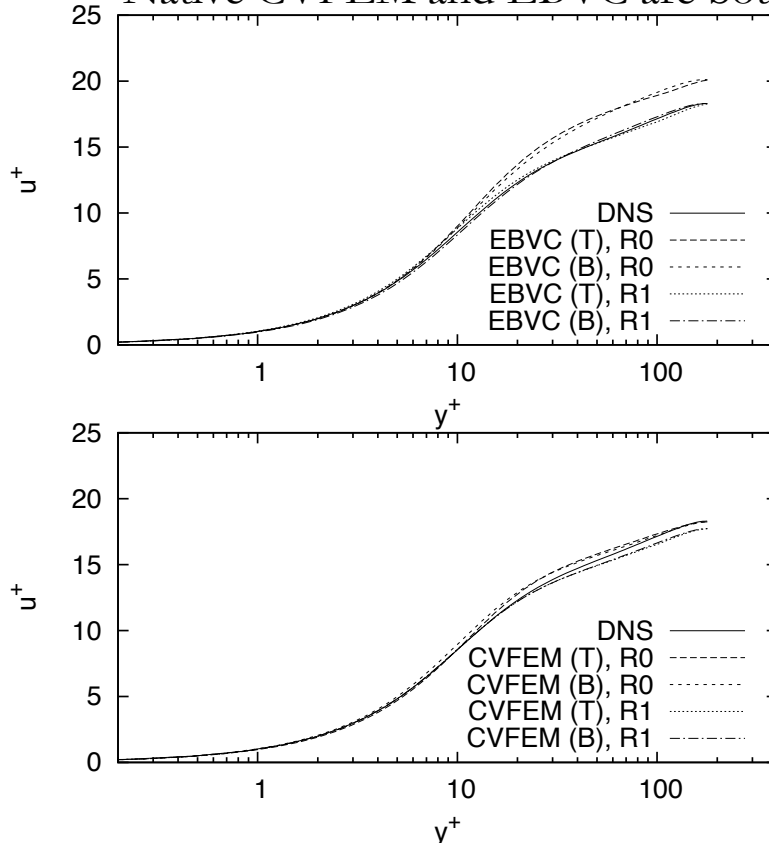
Common Water-Cooler CFD Arguments:

- Structured vs. Un-structured
- FEM and Finite Volume
- Node-centered vs. Cell-centered
- Monolithic and Operator Split
- Compressible vs. (acoustically) Incompressible
- Explicit and Implicit

Hybrid Meshes, Even for LES!



- Hybrid mesh study based on Ham and Iaccarino, *CTR Annual Brief*, 2006, found that simulations were extremely sensitive to mesh topology
 - Non-symmetric time mean flow found for cell-centered; better for the CTR node-centered formulation
 - Native CVFEM and EBVC are both symmetric in mean quantities

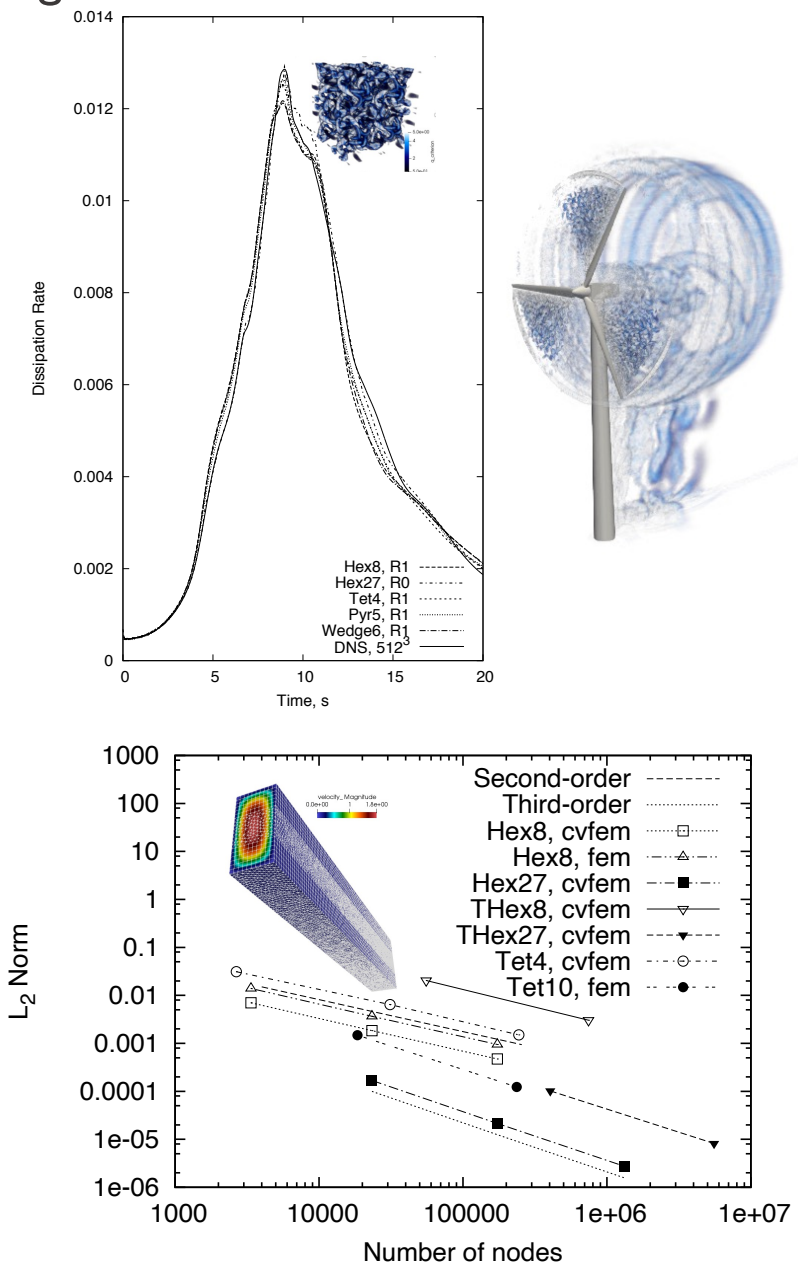
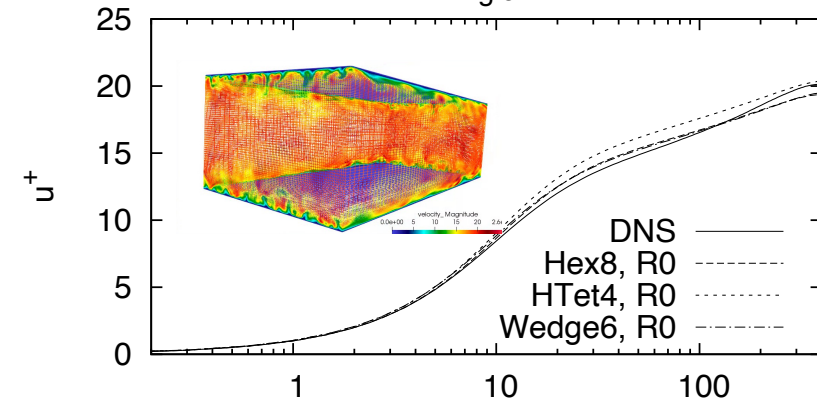
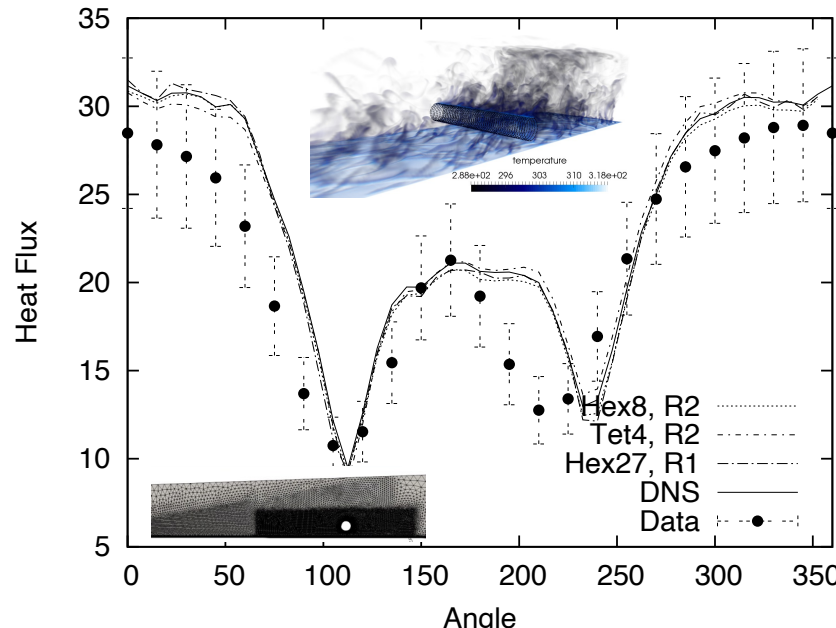


Domino, et. al, “The suitability of hybrid meshes for low-Mach large-eddy simulation” Stanford CTR Summer Program, 2018

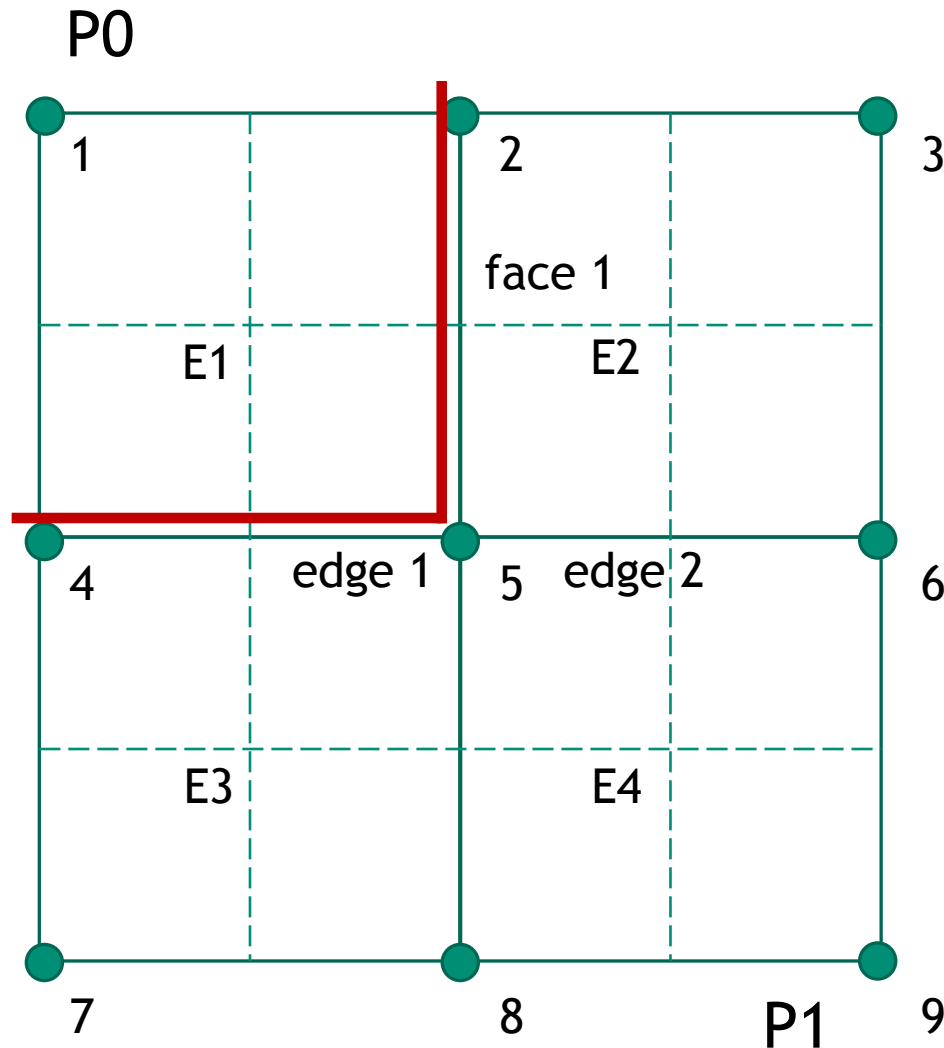
Recent Generalized Unstructured Findings



- Domino, et. al, “An assessment of atypical mesh topologies for low-Mach large-eddy simulation” 2019



A Note on Parallelism... Vertex-based



Sierra Toolkit/Standard Ownership rules: Mesh object (nodes, edges, faces, elements) owned by lower-rank. For example:

- P0 locally owns E1 and nodes 1, 2, 4, and 5
- P1 locally owns E2, E3, and E4 and nodes 3, 6, 7, 8, and 9
- P0 and P1 share nodes 2, 4, and 5

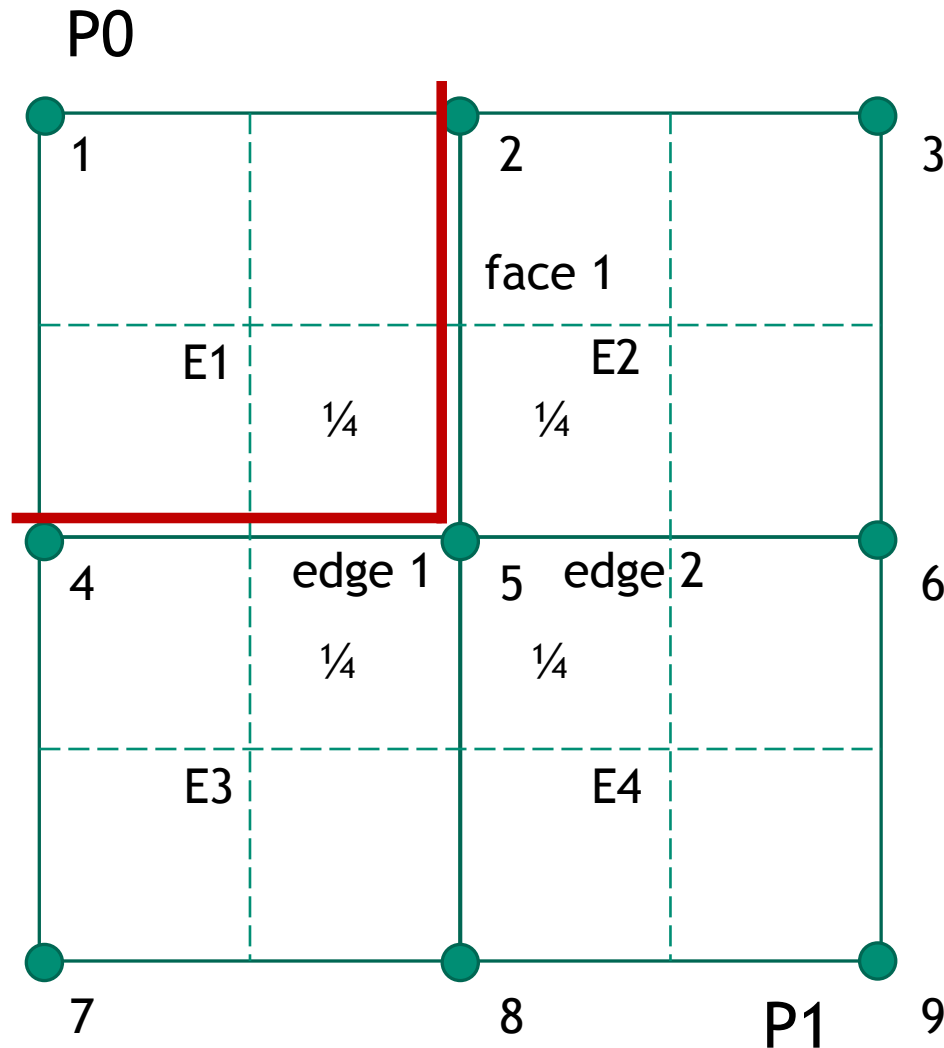
Desired Control-Volume Finite Element (CVFEM) Operation:

- “nodal volume” assemble for node 5 via iteration of each 1cmx1cm element. Desired nodal volume for node 5 = 1 cm² exactly the same on both parallel ranks

Options:

1. Iterate over locally owned elements and locally accumulate nodal volume field followed by a parallel sum and copy owned to shared.
2. Ghost element E2, E3, and E4 to P0 and E1 to P1 (along with coordinates) and iterate locally owned and ghosted elements. Locally accumulate nodal volume field followed by a copy owned to shared.

A Note on Parallelism... Vertex-based



Sierra Toolkit/Standard Ownership rules: Mesh object (nodes, edges, faces, elements) owned by lower-rank. For example:

- P0 locally owns E1 and nodes 1, 2, 4, and 5
- P1 locally owns E2, E3, and E4 and nodes 3, 6, 7, 8, and 9
- P0 and P1 share nodes 2, 4, and 5

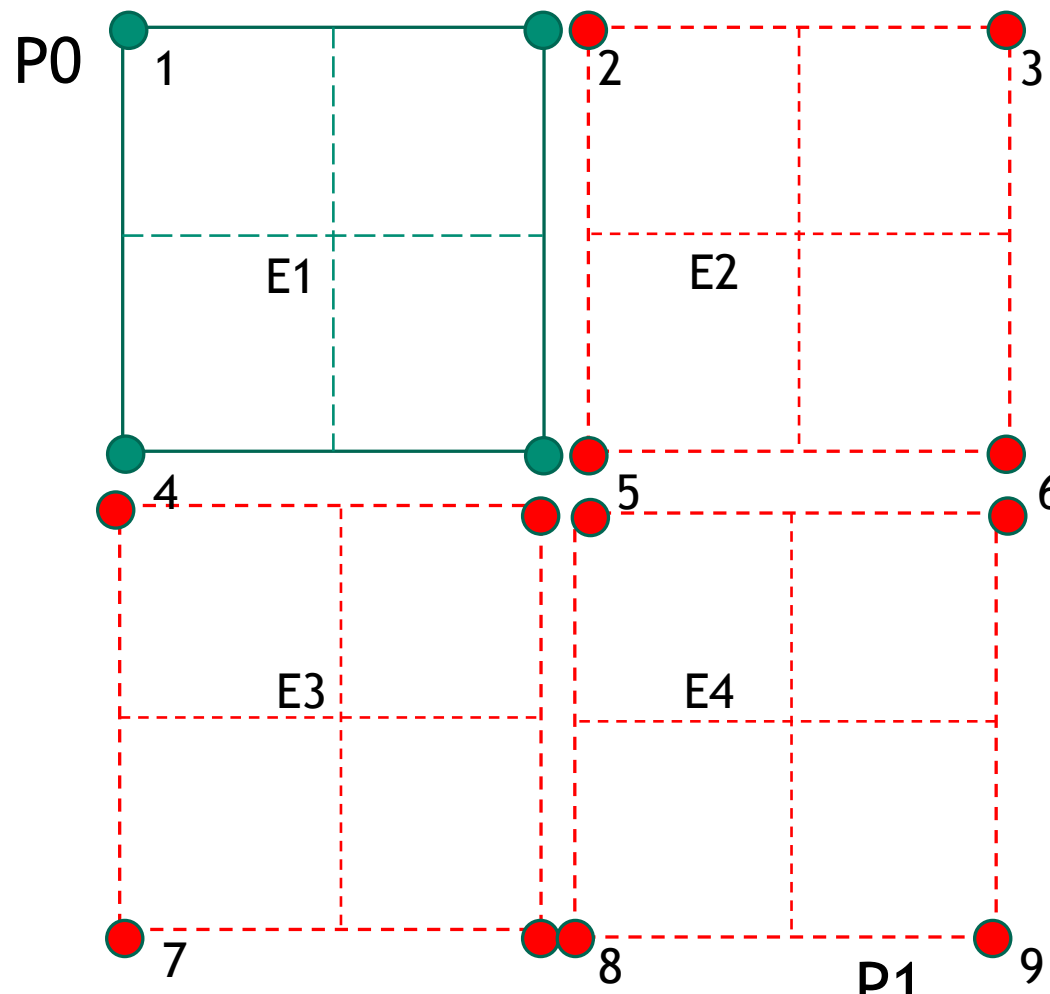
Desired Control-Volume Finite Element (CVFEM) Operation:

- “nodal volume” assemble for node 5 via iteration of each 1cmx1cm element. Desired nodal volume for node 5 = 1 cm² exactly the same on both parallel ranks

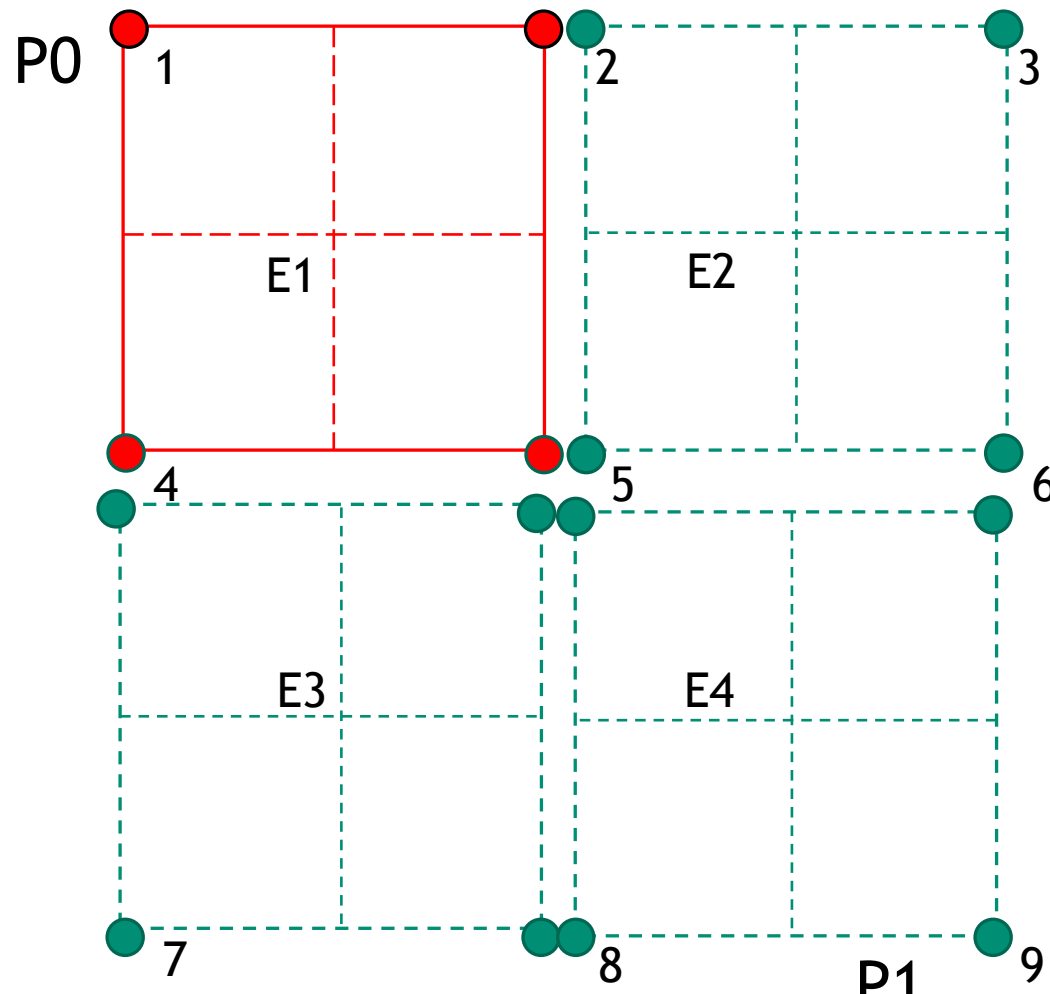
Options:

1. Iterate over locally owned elements and locally accumulate nodal volume field followed by a parallel sum and copy owned to shared.
2. Ghost element E2, E3, and E4 to P0 and E1 to P1 (along with coordinates) and iterate locally owned and ghosted elements. Locally accumulate nodal volume field followed by a copy owned to shared.

A Note on Parallelism... Aura-based; View from P0



Ghost $P_1 \rightarrow P_0$



Ghost P0 -> P1

Common low-Mach Discretization Approaches: Conclusions



- Two-state methods, e.g., cell-centered and EBVC are attractive due to simplicity, however, suffer from non-orthogonality issues in the diffusion operator
- Generally, CC or EBVC is 2x faster on a given mesh size
 - Less accurate/stable on generalized unstructured mesh topologies
 - Better diffusion operator on high-aspect ratio meshes
 - Simple, single topology (virtual-, or full-edge)
- FEM provides a machinery to provide accurate discretizations on non-ideal meshes, however, the same diffusion operator suffers on high-aspect ratio meshes
- CVFEM is a hybrid method that contains the likeable attributes of both FV and FEM (same high-aspect ratio diffusion operator finding)
- Staggered arrangement is well suited for a class of fluid mechanics applications where low-order or simple geometries are found
- Examples for time/source/advection and diffusion provided for EBVC, CVFEM, and FEM
- Recall that Nalu iterates over locally-owned mesh objects as apposed to local+ghosted
 - This is a choice; however, the STK infrastructure allows for both approaches
 - Test yourself on a dual nodal volume assembly?



Stanford ME469: Common low-Mach Discretization Approaches: EBVC

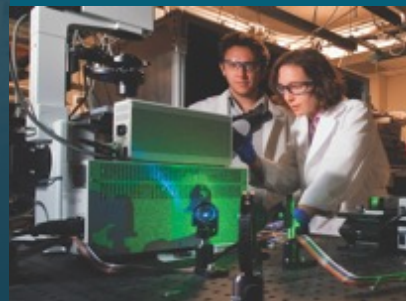


PRESENTED BY

Stefan P. Domino

Computational Thermal and Fluid Mechanics

Sandia National Laboratories SAND2018-4536 PE



Sandia National Laboratories is a multimission laboratory managed and operated by National Technology & Engineering Solutions of Sandia, LLC, a wholly owned subsidiary of Honeywell International Inc., for the U.S. Department of Energy's National Nuclear Security Administration under contract DE-NA0003525.



- Time/Src/Advection/Diffusion equation for scalar ϕ

$$\frac{\partial \rho\phi}{\partial t} + \frac{\partial \rho u_j \phi}{\partial x_j} - \frac{\partial}{\partial x_j} \left(\frac{\mu}{Sc} \frac{\partial \phi}{\partial x_j} \right) = S^\phi$$

$$\int w \left(\frac{\partial \rho\phi}{\partial t} + \frac{\partial}{\partial x_j} \left(\rho u_j \phi - \frac{\mu}{Sc} \frac{\partial \phi}{\partial x_j} \right) - S^\phi \right) dV = 0.$$

- Here, w is the weight function, or an arbitrary function that is differentiable - at least once
 - Any ideas why? What are the properties of the above PDE?
- In this example, let density, velocity, and diffusive flux coefficient be prescribed
- This equation, with a prescribed velocity, can be used to model trace species contaminant transport, smoke, etc.
- The above equation is termed a weighted-residual statement of the original PDE
- Thus far, it is exact

Model Passive Scalar Transport; Heaviside Test Function



- Time/Src/Advection/Diffusion equation for scalar ϕ

$$\int w \left(\frac{\partial \rho \phi}{\partial t} + \frac{\partial}{\partial x_j} \left(\rho u_j \phi - \frac{\mu}{Sc} \frac{\partial \phi}{\partial x_j} \right) - S^\phi \right) dV = 0.$$

$$\int w \frac{\partial \rho u_j \phi}{\partial x_j} dV = - \int \rho u_j \phi \frac{\partial w}{\partial x_j} dV + \int w \rho u_j \phi n_j dS$$

$$\frac{\partial w}{\partial x_j} = -n_j \delta(x_j - x_j^{ip}),$$

- Recall, the CVFEM and EBVC test function meets our requirement in that it is differentiable once
- This definition also allows us to view such methods as Petrov-Galerkin schemes

Model Passive Scalar Transport: Fully Implicit



- Time/Src/Advection/Diffusion equation for scalar ϕ

$$\int \frac{\partial \rho \phi}{\partial t} dV + \int \left(\rho u_j \phi - \frac{\mu}{Sc} \frac{\partial \phi}{\partial x_j} \right) n_j dS = \int S^\phi dV,$$

Model Passive Scalar Transport: Fully Implicit



- Time/Src/Advection/Diffusion equation for scalar ϕ

$$\int \frac{\partial \rho \phi^{n+1}}{\partial t} dV + \int \left(\rho u_j \phi^{n+1} - \frac{\mu}{Sc} \frac{\partial \phi^{n+1}}{\partial x_j} \right) n_j dS = \int S^\phi dV,$$

Model Passive Scalar Transport: Coupling



- Our fully coupled implicit system consists of: continuity, momentum, and mixture fraction

For a given time step:

$$\left\{ \begin{array}{l} \text{do while (!converged) \{} \\ \quad \left[\begin{array}{cccc} \frac{\partial C}{\partial p} & \frac{\partial C}{\partial \tilde{u}_x} & \frac{\partial C}{\partial \tilde{u}_y} & \frac{\partial C}{\partial \tilde{z}} \\ \frac{\partial \tilde{U}_x}{\partial p} & \frac{\partial \tilde{U}_x}{\partial \tilde{u}_x} & \frac{\partial \tilde{U}_x}{\partial \tilde{u}_y} & \frac{\partial \tilde{U}_x}{\partial \tilde{z}} \\ \frac{\partial \tilde{U}_y}{\partial p} & \frac{\partial \tilde{U}_y}{\partial \tilde{u}_x} & \frac{\partial \tilde{U}_y}{\partial \tilde{u}_y} & \frac{\partial \tilde{U}_y}{\partial \tilde{z}} \\ \frac{\partial \tilde{Z}}{\partial p} & \frac{\partial \tilde{Z}}{\partial \tilde{u}_x} & \frac{\partial \tilde{Z}}{\partial \tilde{u}_y} & \frac{\partial \tilde{Z}}{\partial \tilde{z}} \end{array} \right] \left[\begin{array}{c} \Delta p \\ \Delta \tilde{u}_x \\ \Delta \tilde{u}_y \\ \Delta \tilde{z} \end{array} \right] = - \left[\begin{array}{c} resC \\ res\tilde{U}_x \\ res\tilde{U}_y \\ res\tilde{Z} \end{array} \right] \\ \text{\}} \end{array} \right.$$

Left-hand-side (LHS) or Jacobian is simplified for the passive scalar system

$$\left[\frac{\partial \tilde{Z}}{\partial \tilde{z}} \right] [\Delta \tilde{z}] = - [res\tilde{Z}] \quad A\Delta x = b - Ax^* = -res$$



- Our fully coupled implicit system consists of: continuity, momentum, and mixture fraction; shown below in “residual form”

For a given time step:

Left-hand-side (LHS) or Jacobian is simplified for the passive scalar system

$$\left[\frac{\partial}{\partial \tilde{z}} \tilde{Z} \right] \left[\Delta \tilde{z} \right] = - \left[res \tilde{Z} \right] \quad A \Delta x = b - Ax^* = -res \sim M \Delta x$$

Deep Dive on EBVC: Example Case

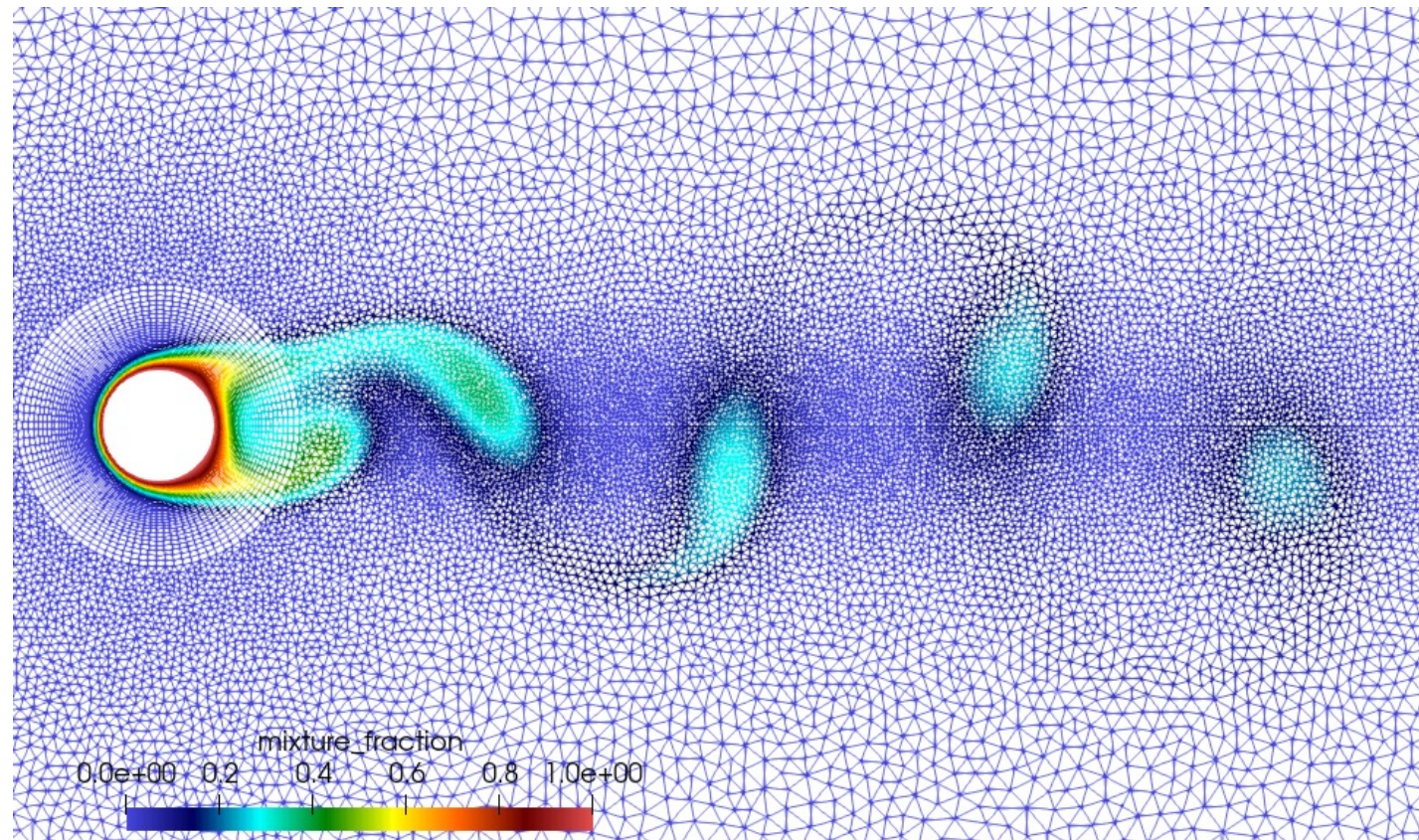


- For a mid-term set of example cases, we have selected a flow past a two-dimensional cylinder at a Reynolds number of 150
- Mesh and input files can be found in the Nalu/examples/street directory
- Familiarize yourself with this physics set via literature surveys
 - As a starting place, see: https://en.wikipedia.org/wiki/Kármán_vortex_street
 - Also look at the Canvas Nalu lecture notes for a brief write-up
- In this test case, we have added a passive scalar field whose inflow is zero and wall boundary condition unity. For your final project, feel free to modify inflow and wall parameters as you choose.
- Note that this case uses a conformal hybrid mesh, or a mesh of disparate element topologies, Quad4 and Tri3
- See:
https://canvas.stanford.edu/courses/137697/files/folder/additional_reading?preview=7730176

Deep Dive on EBVC: Example Viz (Passive Scalar)



- Hybrid mesh (quad4/tri3)





Time Integrators:

- ```
- StandardTimeIntegrator:
 name: ti_1
 start_time: 0
 termination_step_count: 2000
 time_step: 1.0e-3
 time_stepping_type: adaptive
 time_step_count: 0
 second_order_accuracy: yes
```

`second_order_accuracy`: yes/no



- limiter: Upwind using projected nodal gradients is limited

```
velocity: yes
```

```
mixture_fraction: no
```

- laminar\_schmidt:

```
mixture_fraction: 0.9
```

$$-\frac{\partial}{\partial x_j} \left( \frac{\mu}{Sc} \frac{\partial \phi}{\partial x_j} \right)$$

- peclet\_function\_form:

```
velocity: tanh
```

```
mixture_fraction: tanh
```

- peclet\_function\_tanh\_transition:

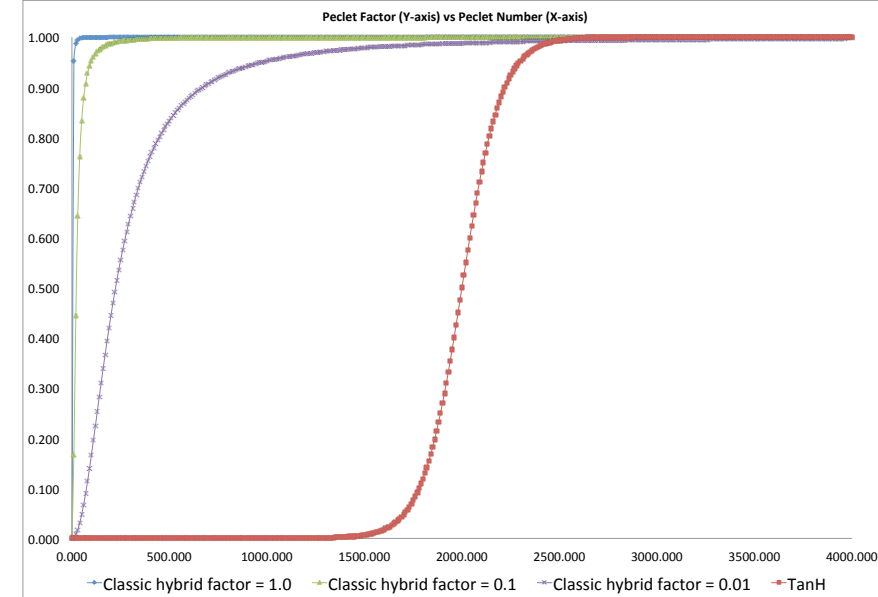
```
velocity: 2.0
```

```
mixture_fraction: 1000.0
```

- peclet\_function\_tanh\_width:

```
velocity: 4.0
```

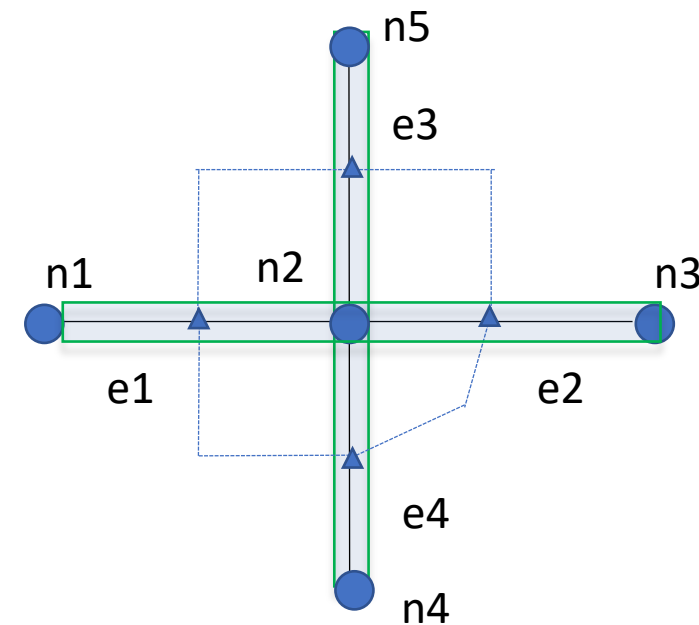
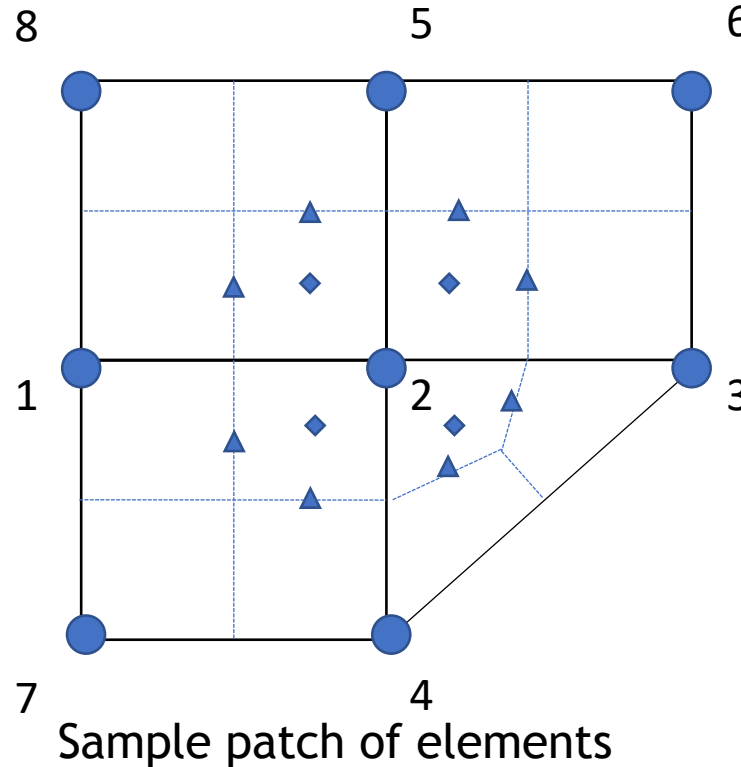
```
mixture_fraction: 100.0
```



## Deep Dive on EBVC



- Recall, EBVC is a discretization scheme that:
  - Iterates over locally-owned nodes for Time/Source/etc. (volumetric-based terms)
  - Iterates over locally-owned edges for Advection/Diffusion/etc. (integrated by parts terms)
  - Below is the patch of elements connected to node 2 (a global matrix row number)
  - Area vector at the edge and dual volume at the node require the node:element connectivity whose quantities are determined in a pre-processing step

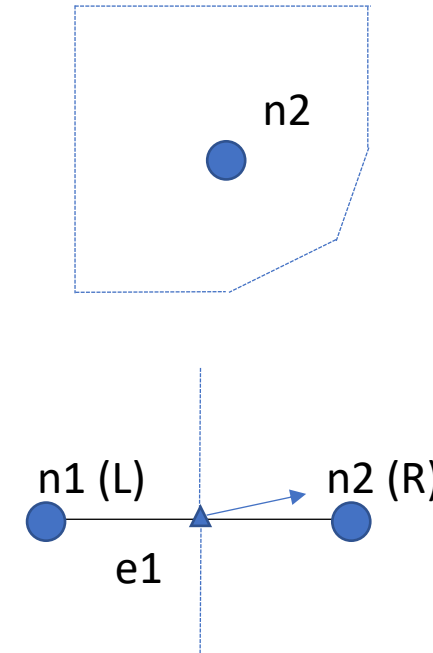
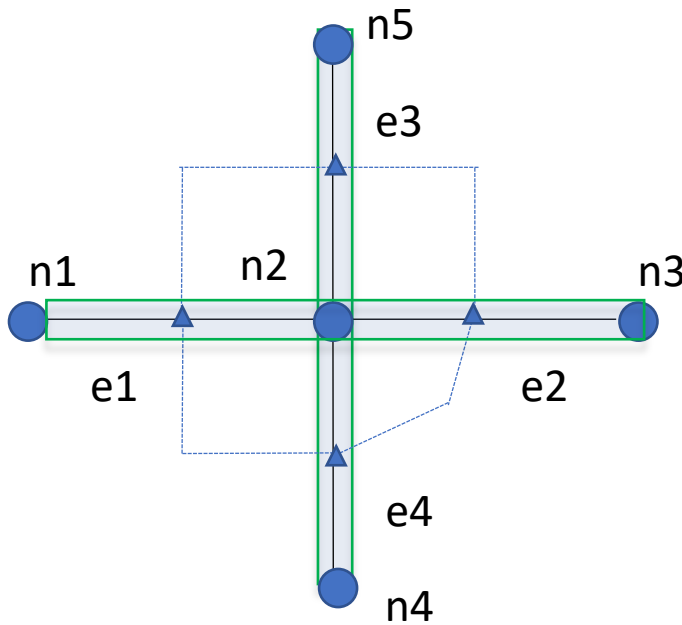


Note: No expectation of nodal ordering..

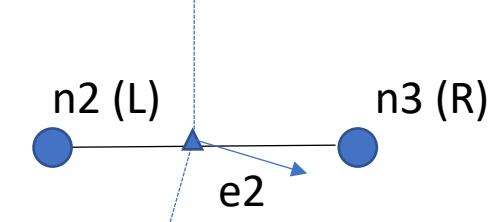
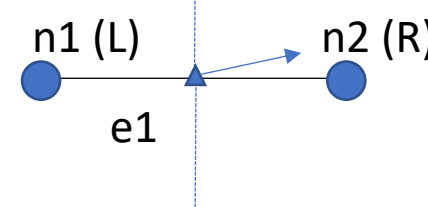
## Deep Dive on EBVC: Node and Edge-loops



- Recall, EBVC is a discretization scheme that:
  - Iterates over locally-owned nodes for Time/Source/etc. (volumetric-based terms)
  - Iterates over locally-owned edges for Advection/Diffusion/etc. (integrated by parts terms)



$$\int S^\phi dV \approx \sum_{nd} S_{nd}^\phi V_{nd}.$$

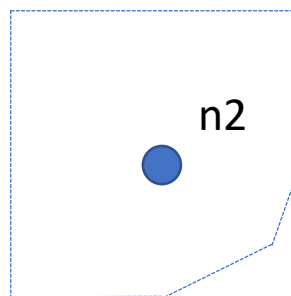


$$\int w \frac{\partial \rho u_j \phi}{\partial x_j} dV \approx \sum_{ip} (\rho u_j)_{ip} \phi_{ip} n_j dS \approx \sum_{ip} \dot{m}_{ip} \phi_{ip}$$

## Deep Dive on EBVC: Implicit Time Discretization



- Let us define a general implicit time integrator that is A-stable
  - For  $y' = k y$ ;  $y(0) = 1$ ;  $y(t) = e^{kt}$  solution approaches zero as time increases for  $k < 0$
- Backward Euler (two state) and is first-order accurate (A-stable)
- BDF2 (three state) is second-order accurate (A-stable)
- This term is assembled over a nodal iteration



$$\int \frac{\partial \rho \phi}{\partial t} dV \approx \sum_{nd} \frac{(\gamma_1 \rho_{nd}^{n+1} \phi_{nd}^{n+1} + \gamma_2 \rho_{nd}^n \phi_{nd}^n + \gamma_3 \rho_{nd}^{n-1} \phi_{nd}^{n-1})}{\Delta t} V_{nd}.$$

- For uniform time steps:

$$\gamma_1 = 3/2$$

$$\gamma_2 = -2$$

$$\gamma_3 = 1/2$$

## Deep Dive on EBVC: Implicit Time Discretization (Code)



- <https://github.com/NaluCFD/Nalu/blob/master/src/ScalarMassBDF2NodeSupAlg.C>

```
//-----
//----- node_execute -----
//-----

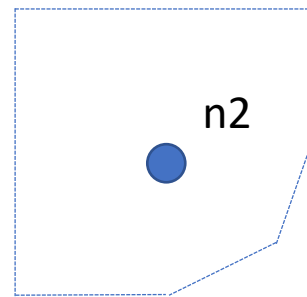
void
ScalarMassBDF2NodeSupAlg::node_execute(
 double *lhs,
 double *rhs,
 stk::mesh::Entity node)
{
 // deal with lumped mass matrix
 const double qNm1 = *stk::mesh::field_data(*scalarQNm1_, node);
 const double qN = *stk::mesh::field_data(*scalarQN_, node);
 const double qNp1 = *stk::mesh::field_data(*scalarQNp1_, node);
 const double rhoNm1 = *stk::mesh::field_data(*densityNm1_, node);
 const double rhoN = *stk::mesh::field_data(*densityN_, node);
 const double rhoNp1 = *stk::mesh::field_data(*densityNp1_, node);
 const double dualVolume = *stk::mesh::field_data(*dualNodalVolume_, node);
 const double lhsTime = gamma1_*rhoNp1*dualVolume/dt_;
 rhs[0] -= (gamma1_*rhoNp1*qNp1 + gamma2_*qN*rhoN + gamma3_*qNm1*rhoNm1)*dualVolume/dt_;
 lhs[0] += lhsTime;
}
```

Note the implicit term

## Deep Dive on EBVC: Source Term Discretization



- Source terms for the edge-based scheme are also assembled over a nodal loop



$$\int S^\phi dV \approx \sum_{nd} S_{nd}^\phi V_{nd}.$$

- Note that in this scheme, we are using single point quadrature, i.e., the function is evaluated at a single point
- $p = 2N - 1$ 
  - Where  $N$  is the number of integration points and  $p$  is the polynomial order
  - For a linear basis, using one-point quadrature is design-order

## Deep Dive on EBVC: Source Term Discretization (Code)



- [https://github.com/NaluCFD/Nalu/blob/master/src/user\\_functions/VariableDensityMixFracSrcNodeSupAlg.C](https://github.com/NaluCFD/Nalu/blob/master/src/user_functions/VariableDensityMixFracSrcNodeSupAlg.C)

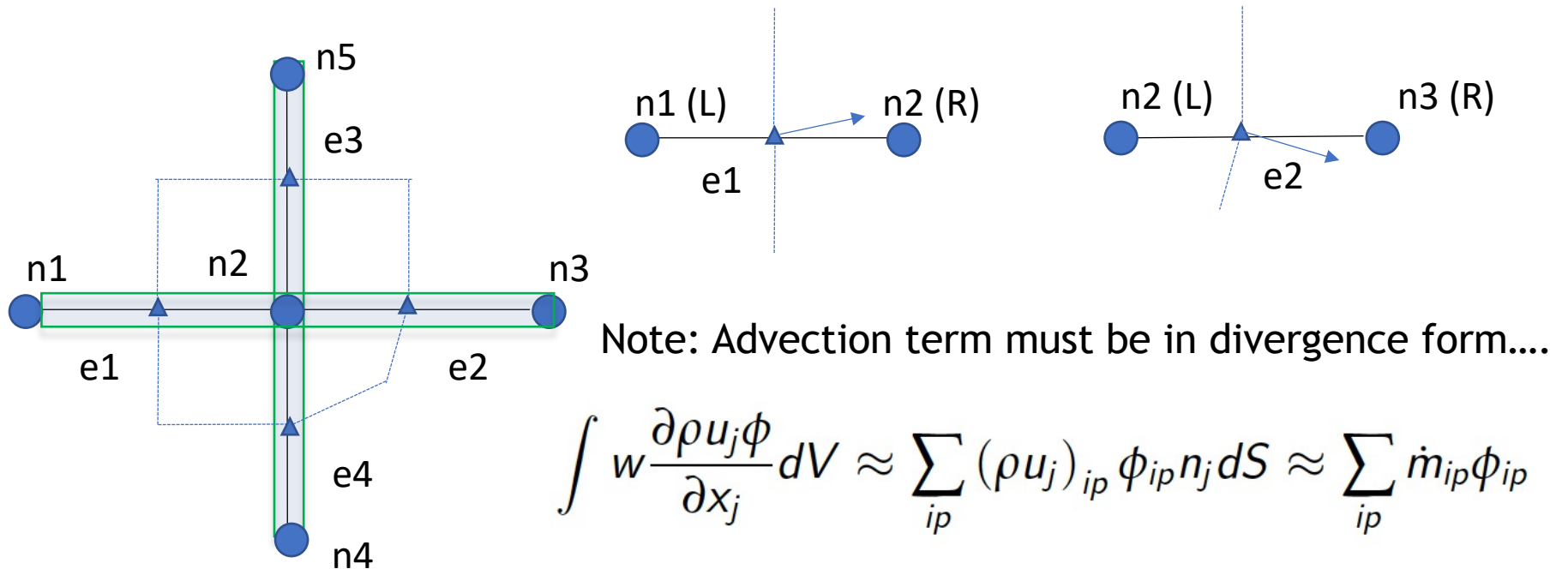
```
//-----
//----- node_execute -----
//-----
void
VariableDensityMixFracSrcNodeSupAlg::node_execute(
 double /*lhs*/,
 double *rhs,
 stk::mesh::Entity node)
{
 // deal with lumped mass matrix
 const double *coords = stk::mesh::field_data(*coordinates_, node);
 const double dualVolume = *stk::mesh::field_data(*dualNodalVolume_, node);
 const double x = coords[0];
 const double y = coords[1];
 const double z = coords[2];

 const double src = 0.10e1 * pow(znot_ * cos(amf_ * pi_ * x) * cos(amf_ * pi_ * y) * cos(amf_
 rhs[0] += src*dualVolume;
}
```

## Deep Dive on EBVC: Advection Discretization (no stabilization)



- For advection, we have transformed the volume integral to a surface integration
- Therefore, a patch of edges are required for the full assembly at node 2



- Recall, that the mass flow rate at an integration point is prescribed
- Moreover, since the integration point is at the edge mid-point,  $\phi_{ip} = (\phi^R + \phi^L)/2$
- This is a *central-* or *Galerkin-based* advection operator; shown in conservative form

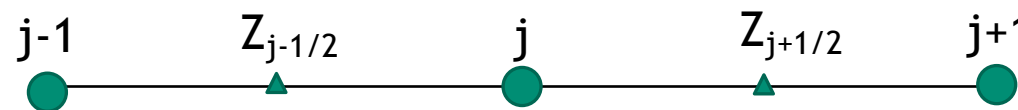
## Deep Dive on EBVC: Advection Discretization (Code)



- <https://github.com/NaluCFD/Nalu/blob/master/src/AssembleScalarEdgeSolverAlgorithm.C>
- This routine includes advection and diffusion



- Upwind advection operators can provide diagonal dominance (at the cost of accuracy)



$$Z_{j+1/2} = \begin{cases} Z_j; u > 0 \\ Z_{j+1}; u < 0 \end{cases}$$

“as the wind blows”

- However, upwind operators, even if higher-order, are numerically diffuse
- Higher-order upwind (second-order in space) can be obtained on an unstructured mesh by use of projected nodal gradients and extrapolation:

$$G_x Z_j = \frac{Z_{j+1} - Z_{j-1}}{2\Delta x} \quad G_x Z_{j-1} = \frac{Z_j - Z_{j-2}}{2\Delta x}$$

for  $u > 0$

$$Z_{j+1/2} = \alpha \left( Z_j + G_x Z_j \frac{\Delta x}{2} \right) + (1 - \alpha) \left[ \frac{1}{2} (Z_j + Z_{j+1}) \right]$$

$\alpha$  is a blending parameter

$$Z_{j-1/2} = \alpha \left( Z_{j-1} + G_x Z_{j-1} \frac{\Delta x}{2} \right) + (1 - \alpha) \left[ \frac{1}{2} (Z_j + Z_{j-1}) \right]$$



- Blending extrapolated upwind with central  $(Z_L + Z_R)/2$  provides:

$$\text{for } u > 0 \quad Z_{j+1/2} = \alpha \left( Z_j + G_x Z_j \frac{\Delta x}{2} \right) + (1 - \alpha) \left[ \frac{1}{2} (Z_j + Z_{j+1}) \right]$$

$$Z_{j-1/2} = \alpha \left( Z_{j-1} + G_x Z_{j-1} \frac{\Delta x}{2} \right) + (1 - \alpha) \left[ \frac{1}{2} (Z_j + Z_{j-1}) \right]$$

$$\text{for } u < 0 \quad Z_{j+1/2} = \alpha \left( Z_{j+1} + G_x Z_{j+1} \frac{\Delta x}{2} \right) + (1 - \alpha) \left[ \frac{1}{2} (Z_j + Z_{j+1}) \right]$$

$$Z_{j-1/2} = \alpha \left( Z_j + G_x Z_j \frac{\Delta x}{2} \right) + (1 - \alpha) \left[ \frac{1}{2} (Z_j + Z_{j-1}) \right]$$

Resulting  
1-D Stencil

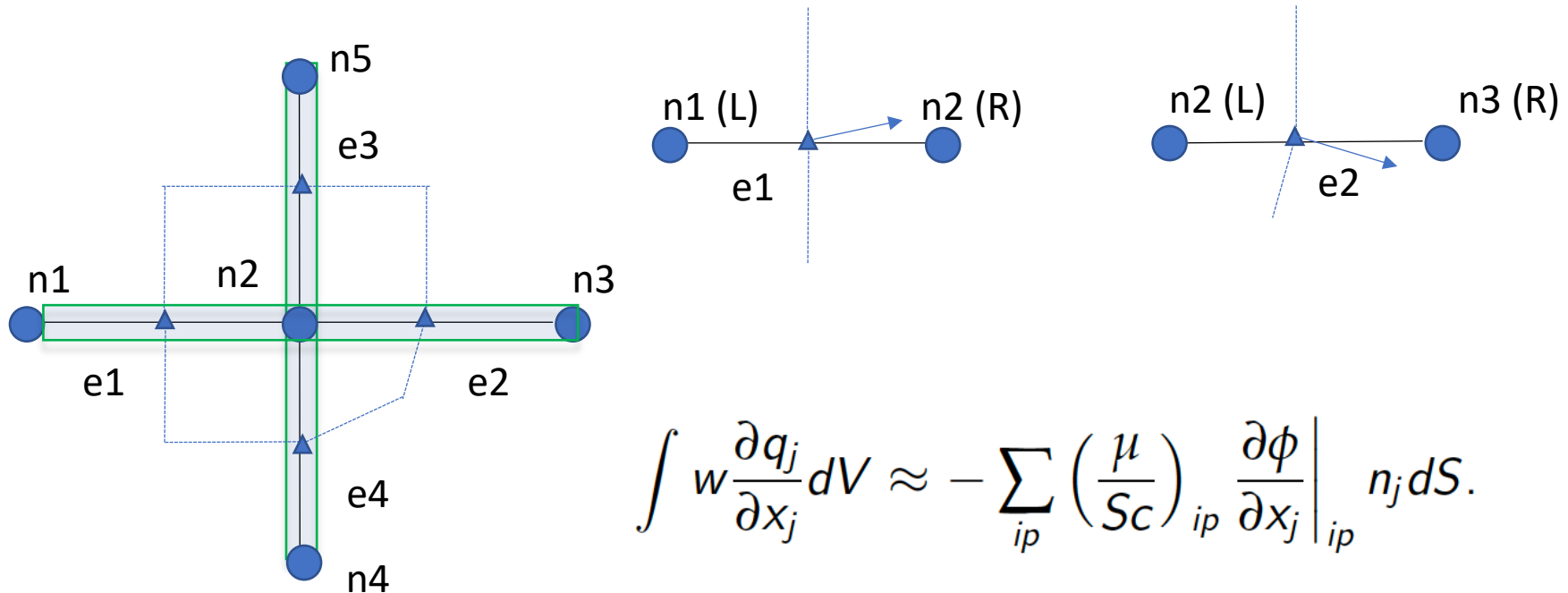
| j-2  | j-1  | j    | j+1  | j+2  | $\alpha$ | $m$ |
|------|------|------|------|------|----------|-----|
| 1/4  | -5/4 | +3/4 | +1/4 | 0    | 1        | >0  |
| 0    | -1/4 | -3/4 | +5/4 | -1/4 | 1        | >0  |
| +1/6 | -6/6 | +3/6 | +2/6 | 0    | 1/2      | <0  |
| 0    | -2/6 | -3/6 | +6/6 | -1/6 | 1/2      | <0  |

- Slope limiting required when gradients are not smooth (Berger et al, 2005, 43<sup>rd</sup> AIAA)

## Deep Dive on EBVC: Diffusion Discretization



- For diffusion, we have transformed the volume integral to a surface integration
- Therefore, a patch of edges are required for the full assembly at node 2

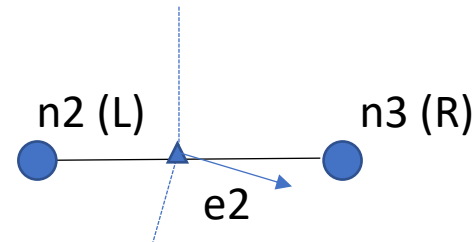


## Deep Dive on EBVC: Diffusion Discretization



- The edge-based diffusion operator is a bit more complex in that we are computing a gradient at the integration point while using two nodes, the left and right
- In many practical meshes, the distance vector between the edges ( $\mathbf{dx}_j$ ) and the edge area vector will not be perfectly orthogonal
- This non-orthogonality causes inaccuracy when using a simplified approach

$$\frac{\partial \phi_{ip}}{\partial x} = \frac{(\phi_R - \phi_L)}{dx}.$$



- The non-orthogonality approach of Jasek (Ph.D. Imperial College) is a standard cell-centered approach that has been adopted for edge-based schemes
  - CC and EBVC are each two-state schemes and share non-orthogonality issues

$$\left. \frac{\partial \phi}{\partial x_j} \right|_{ip} = \overline{G_j \phi} + [(\phi_R - \phi_L) - \overline{G_I \phi} dx_I] \frac{A_j}{A_k dx_k}.$$

## Deep Dive on EBVC: Diffusion Discretization (code)



- <https://github.com/NaluCFD/Nalu/blob/master/src/AssembleScalarEdgeDiffSolverAlgorithm.C>

$$\begin{aligned} - \int w \frac{\mu}{Sc} \frac{\partial \phi}{\partial x_j} dV &\approx - \left. \frac{\mu}{Sc} \right|_{ip} \left[ (\overline{G_x \phi} A_x + \overline{G_y \phi} A_y) + (\phi_R - \phi_L) \frac{A_x A_x + A_y A_y}{A_x \Delta x_x + A_y \Delta x_y} \right. \\ &\quad \left. - (\overline{G_x \phi} dx + \overline{G_y \phi} dy) \frac{A_x A_x + A_y A_y}{A_x dx + A_y dy} \right]. \end{aligned} \quad (21)$$

## Types of Boundary Conditions



- Inflow: values are known and enforced via a Dirichlet
- Open: pressure known: flow in or out of the domain; zero gradient for diffusion
- Wall: values are known and enforced via a Dirichlet
- Symmetry: Normal stress specified; tangential stress zero
- Non-conformal: hybrid DG/CVFEM
- “overset”: Constraint-based

See: <https://nalu.readthedocs.io/en/latest/source/theory/boundaryConditions.html>

## Common low-Mach Discretization Approaches: Conclusions



- Two-state methods, e.g., cell-centered and EBVC are attractive due to simplicity, however, suffer from non-orthogonality issues in the diffusion operator
- Generally, CC or EBVC is 2x faster on a given mesh size
- Less accurate/stable on generalized unstructured mesh topologies
- Better diffusion operator on high-aspect ratio meshes



# Stanford ME469: Common low-Mach Discretization Approaches: CVFEM/FEM

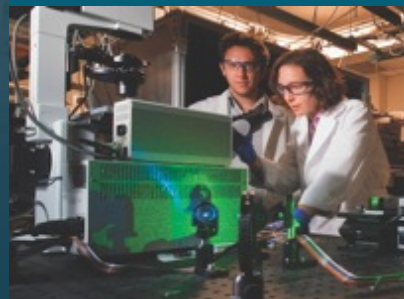


*PRESENTED BY*

Stefan P. Domino

Computational Thermal and Fluid Mechanics

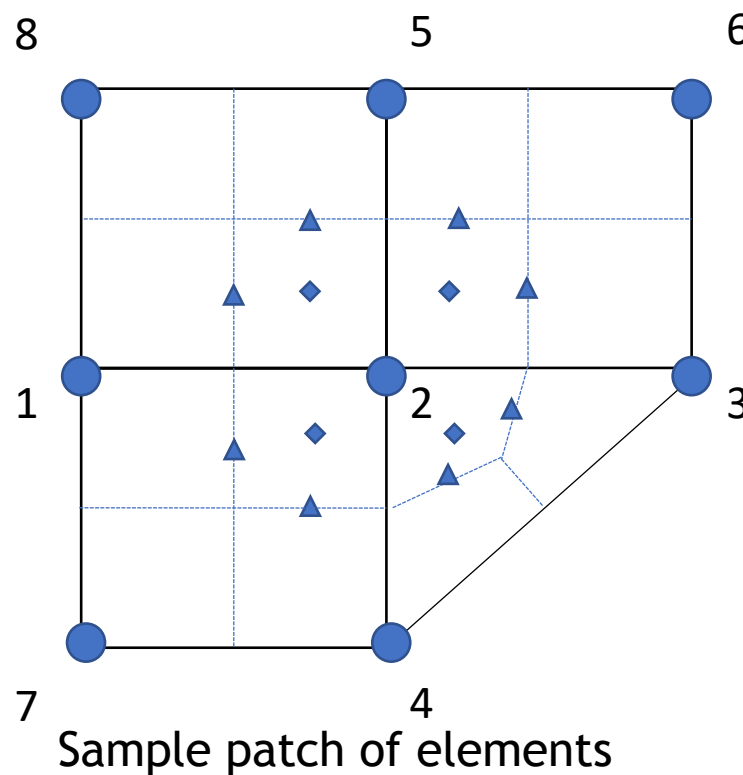
Sandia National Laboratories SAND2018-4536 PE



Sandia National Laboratories is a multimission laboratory managed and operated by National Technology & Engineering Solutions of Sandia, LLC, a wholly owned subsidiary of Honeywell International Inc., for the U.S. Department of Energy's National Nuclear Security Administration under contract DE-NA0003525.



- Recall, CVFEM is a discretization scheme that:
  - Iterates over locally-owned elements for Time/Source/etc. (volumetric-based terms)
  - Iterates over locally-owned elements for Advection/Diffusion/etc. (integrated by parts terms)
- Below is the patch of elements connected to node 2 (a global matrix row number)

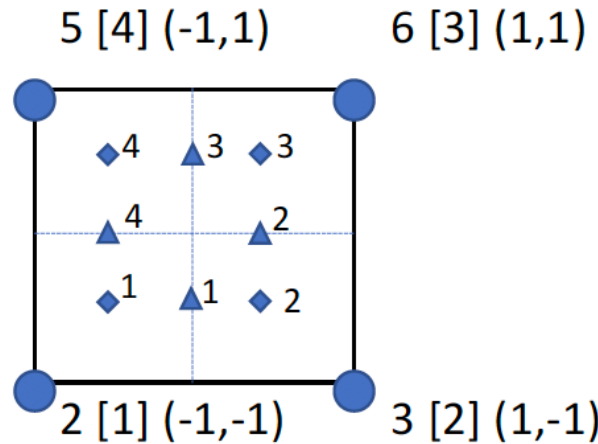


Note: Time and source terms can also be evaluated at nodes without loss of accuracy

## Deep Dive on CVFEM: Element-loops



- For each element, recall that a dual volume has been constructed
- Volume-based contributions are evaluated at the subcontrol volume integration points (diamonds)
- Surface-based contributions are evaluated at the subcontrol surface integration points (triangles)
- We define an isoparametric element than ranges from -1:1 in the  $\xi$ - (x-direction) and  $\eta$ - (y-direction) direction



Basis Functions for a Quad4

$$\begin{aligned}
 N_1^{ip} &= \frac{1}{4}(1 - \xi)(1 - \eta) \\
 N_2^{ip} &= \frac{1}{4}(1 + \xi)(1 - \eta) \\
 N_3^{ip} &= \frac{1}{4}(1 + \xi)(1 + \eta) \\
 N_4^{ip} &= \frac{1}{4}(1 - \xi)(1 + \eta)
 \end{aligned}$$

For example, the isoparametric coordinate for ip 1 is (0.0, -0.5)

## Deep Dive on CVFEM: Implicit Time Discretization



- Backward Euler (two state) and is first-order accurate (A-stable)
- BDF2 (three state) is second-order accurate (A-stable)
- This term is assembled over an element iteration and drives a consistent mass matrix with a full node:element:node connectivity

$$\int \frac{\partial \rho \phi}{\partial t} dV \approx \sum_{scvip} \frac{(\gamma_1 \rho_{scvip}^{n+1} \phi_{scvip}^{n+1} + \gamma_2 \rho_{scvip}^n \phi_{scvip}^n + \gamma_3 \rho_{scvip}^{n-1} \phi_{scvip}^{n-1})}{\Delta t} V_{scvip},$$

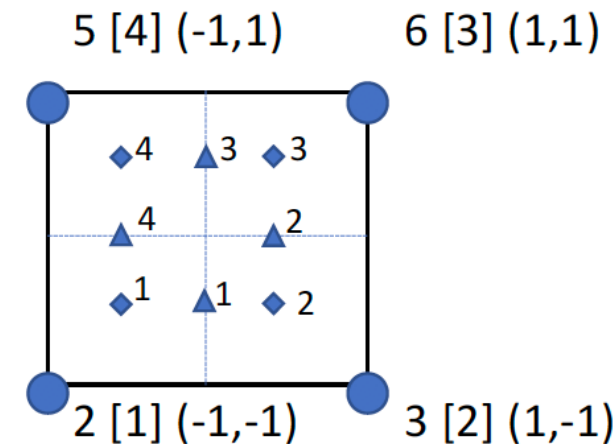
- For uniform time steps:

$$\gamma_1 = 3/2$$

$$\gamma_2 = -2$$

$$\phi_{scvip} = \sum_{nd} N_{nd}^{scvip} \phi_{nd}.$$

$$\gamma_3 = 1/2$$



## Deep Dive on CVFEM: Implicit Time Discretization



- Backward Euler (two state) and is first-order accurate (A-stable)
- BDF2 (three state) is second-order accurate (A-stable)
- This term is assembled over an element iteration and drives a consistent mass matrix with a full node:element:node connectivity

$$\int \frac{\partial \rho \phi}{\partial t} dV \approx \sum_{scvip} \frac{(\gamma_1 \rho_{scvip}^{n+1} \phi_{scvip}^{n+1} + \gamma_2 \rho_{scvip}^n \phi_{scvip}^n + \gamma_3 \rho_{scvip}^{n-1} \phi_{scvip}^{n-1})}{\Delta t} V_{scvip},$$

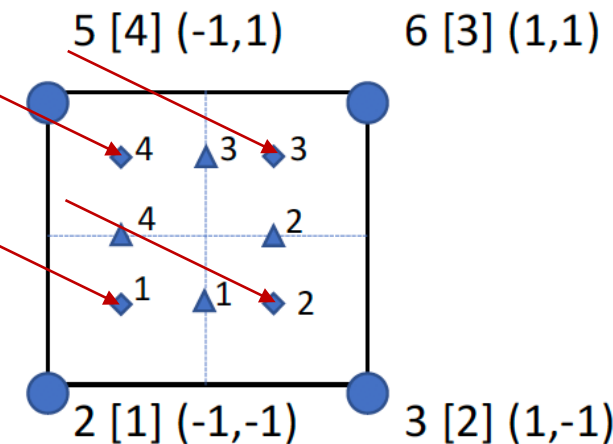
- For uniform time steps:

$$\gamma_1 = 3/2$$

$$\gamma_2 = -2$$

$$\phi_{scvip} = \sum_{nd} N_{nd}^{scvip} \phi_{nd}.$$

$$\gamma_3 = 1/2$$



## Deep Dive on CVFEM: Implicit Time Discretization (Code)

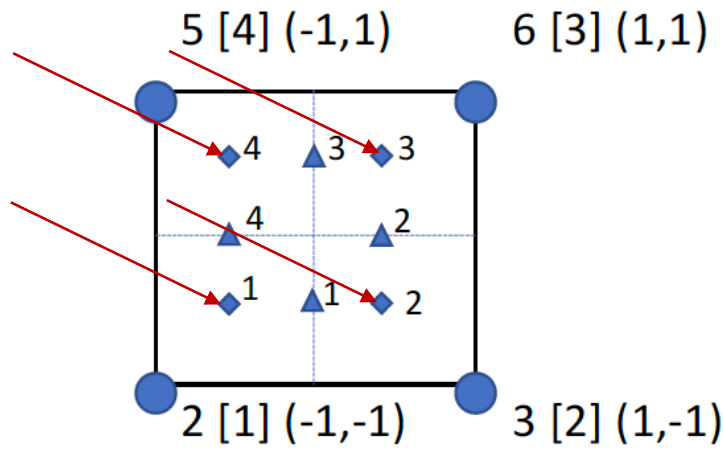


- <https://github.com/NaluCFD/Nalu/blob/master/src/kernel/ScalarMassElemKernel.C>

## Deep Dive on CVFEM: Source Term Discretization



- Source terms for CVFEM are also assembled over an element or nodal loop
- In some cases, the source term is complex, i.e., includes gradients, which drives either a nodal assembly of these quantities to the nodes or local evaluation



$$\int w S^\phi dV \approx \sum_{scvip} S_{scvip}^\phi V_{scvip},$$

$$S_{scvip}^\phi = \sum_{nd} N_{nd}^{scvip} S_{nd}^\phi.$$

# Deep Dive on CVFEM: Source Term Discretization (Code)



- [https://github.com/NaluCFD/Nalu/blob/master/src/user\\_functions/SteadyThermal3dContactSrcElemKernel.C](https://github.com/NaluCFD/Nalu/blob/master/src/user_functions/SteadyThermal3dContactSrcElemKernel.C)

```

template<typename AlgTraits>
void
SteadyThermal3dContactSrcElemKernel<AlgTraits>::execute(
 SharedMemView<DoubleType**>& /* lhs */,
 SharedMemView<DoubleType *>& rhs,
 ScratchViews<DoubleType>& scratchViews)
{

 // Forcing nDim = 3 instead of using AlgTraits::nDim_ here to avoid compiler
 // warnings when this template is instantiated for 2-D topologies.
 NALU_ALIGNED DoubleType w_scvCoords[3];

 SharedMemView<DoubleType**>& v_coordinates = scratchViews.get_scratch_view_2D(*coordinates_);
 SharedMemView<DoubleType*>& v_scv_volume = scratchViews.get_me_views(CURRENT_COORDINATES).scv_volume;

 // interpolate to ips and evaluate source
 for (int ip = 0; ip < AlgTraits::numScvIp_; ++ip) {

 // nearest node to ip
 const int nearestNode = ipNodeMap_[ip];

 // zero out
 for (int j = 0; j < AlgTraits::nDim_; ++j)
 w_scvCoords[j] = 0.0;

 for (int ic = 0; ic < AlgTraits::nodesPerElement_; ++ic) {
 const DoubleType r = v_shape_function_(ip,ic);
 for (int j = 0; j < AlgTraits::nDim_; ++j)
 w_scvCoords[j] += r*v_coordinates(ic,j);
 }

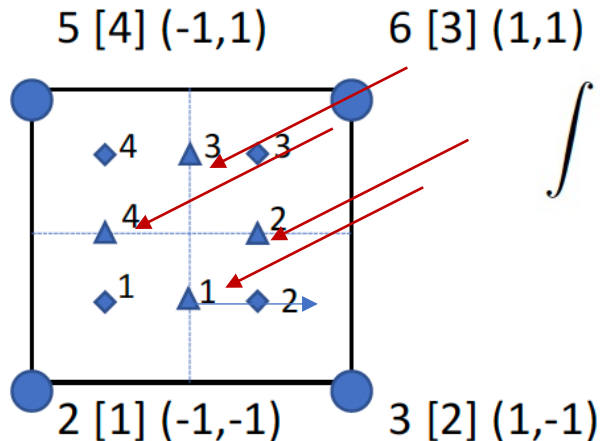
 rhs(nearestNode) += k_/4.0*(2.0*a_*pi_)*(2.0*a_*pi_)*(
 stk::math::cos(2.0*a_*pi_* w_scvCoords[0])
 + stk::math::cos(2.0*a_*pi_* w_scvCoords[1])
 + stk::math::cos(2.0*a_*pi_* w_scvCoords[2]))*v_scv_volume(ip);
 }
}

```

## Deep Dive on CVFEM: Advection Discretization (no stabilization)



- For advection, we have transformed the volume integral to a surface integration
- Therefore, a patch of elements are required for the full assembly at node 2



$$\int w \frac{\partial \rho u_j \phi}{\partial x_j} dV \approx \sum_{ip} (\rho u_j)_{ip} \phi_{ip} n_j dS \approx \sum_{ip} \dot{m}_{ip} \phi_{ip}$$

Note:

1. Common to integrate-by-parts, however, not required
2. Advection term need not be in divergence form (non-conserved form is suitable)

- Recall, that the mass flow rate at an integration point is prescribed
- Integration points can also be shifted from the subcontrol surface to the edge mid-point (while still using the integration point area vector)
- This is a *central-* or *Galerkin-based* advection operator

## Deep Dive on CVFEM: Advection Discretization Non-Conserved Form



- The advection term can be integrated by parts, or not; moreover, the PDE can drive a non-conservative equation form

$$\int w \frac{\partial \rho u_j \phi}{\partial x_j} dV = \int w \rho u_j \phi n_j dS - \int \rho u_j \phi \frac{\partial w}{\partial x_j} dV,$$



$$\int w \rho u_j \frac{\partial \phi}{\partial x_j} dV + \int w \phi \frac{\partial \rho u_j}{\partial x_j} dV,$$

IBP - or not...

This is now a choice

Non-conserved form, unlike cell-centered FV, poses no complexity

$$\int w \frac{\partial \rho \phi}{\partial t} dV = \int w \rho \frac{\partial \phi}{\partial t} dV + \int w \phi \frac{\partial \rho}{\partial t} dV$$

$$\int w \left( \rho \frac{\partial \phi}{\partial t} + \rho u_j \frac{\partial \phi}{\partial x_j} \right) dV,$$



• <https://github.com/NaluCFD/Nalu/blob/master/src/kernel/ScalarAdvDiffElemKernel.C>

- This routine includes advection and diffusion
- Recall that integration point value is provided by nodal loop over the underlying nodal basis for this element
- Also note that this routine is valid for all types of supported elements – both low- and higher-order

### Basis Functions for a Quad4

$$N_1^{ip} = \frac{1}{4}(1 - \xi)(1 - \eta)$$

$$N_2^{ip} = \frac{1}{4}(1 + \xi)(1 - \eta)$$

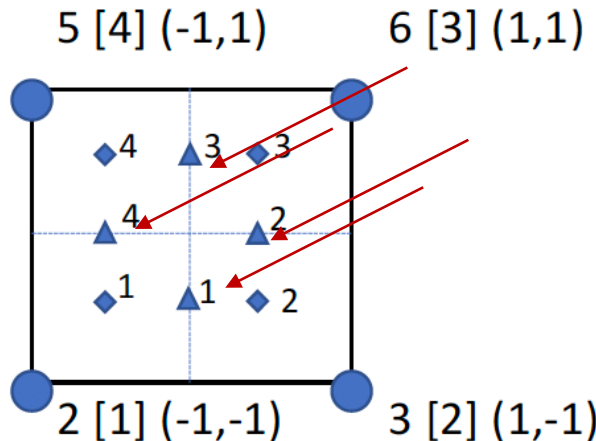
$$N_3^{ip} = \frac{1}{4}(1 + \xi)(1 + \eta)$$

$$N_4^{ip} = \frac{1}{4}(1 - \xi)(1 + \eta)$$

## Deep Dive on CVFEM: Diffusion Discretization



- For diffusion, we have transformed the volume integral to a surface integration
- Therefore, a patch of elements are required for the full assembly at node 2



$$\begin{bmatrix} \frac{\partial x}{\partial \xi} & \frac{\partial y}{\partial \xi} \\ \frac{\partial x}{\partial \eta} & \frac{\partial y}{\partial \eta} \end{bmatrix} \begin{bmatrix} \frac{\partial N}{\partial x} \\ \frac{\partial N}{\partial y} \end{bmatrix} = \begin{bmatrix} \frac{\partial N}{\partial \xi} \\ \frac{\partial N}{\partial \eta} \end{bmatrix} \quad \mathbf{J}^{-1} = \begin{bmatrix} \frac{\partial x}{\partial \xi} & \frac{\partial y}{\partial \xi} \\ \frac{\partial x}{\partial \eta} & \frac{\partial y}{\partial \eta} \end{bmatrix}^{-1}$$

$$\begin{bmatrix} \frac{\partial N}{\partial x} \\ \frac{\partial N}{\partial y} \end{bmatrix} = \begin{bmatrix} \frac{\partial x}{\partial \xi} & \frac{\partial y}{\partial \xi} \\ \frac{\partial x}{\partial \eta} & \frac{\partial y}{\partial \eta} \end{bmatrix}^{-1} \begin{bmatrix} \frac{\partial N}{\partial \xi} \\ \frac{\partial N}{\partial \eta} \end{bmatrix}$$

$$\int w \frac{\partial q_j}{\partial x_j} dV \approx - \sum_{ip} \frac{\mu}{Sc_{ip}} \frac{\partial \phi}{\partial x_j}_{ip} n_j dS = - \sum_{ip} \frac{\mu}{Sc_{ip}} \sum_{nd} \frac{\partial N_{nd}^{ip}}{\partial x_j} \phi_{nd} A_j^{ip},$$

Note that the CVFEM approach is absent any non-orthogonality corrections; However, high aspect ratio elements are now challenging...

## Deep Dive on CVFEM: Diffusion Discretization (code)

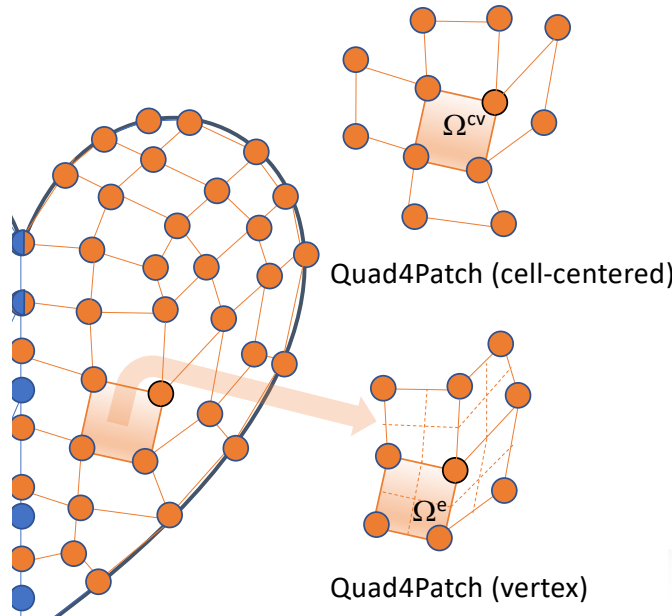


- <https://github.com/NaluCFD/Nalu/blob/master/src/kernel/ScalarAdvDiffElemKernel.C>

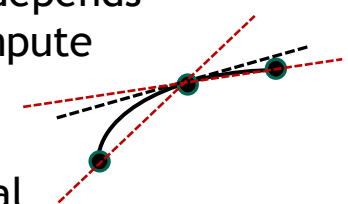
## Deep Dive on Nodal Gradient Operator: An Alternative View



- Recall, that the edge-based diffusion operator, and for some choices for the advection operator, a nodal gradient is required
- What is a nodal gradient? As formerly described in the *Computing Gradients* lecture, in a cell-centered context we obtained this via a number of ways, e.g., Green-Gauss, Least Squares, etc.
- Let's take another view...



First, the gradient of a function (other than linear) is discontinuous, i.e., the value at a shared element face depends on which element is used to compute the gradient



Therefore, we can view the nodal gradient a continuous at the nodes and discontinuous within the elements

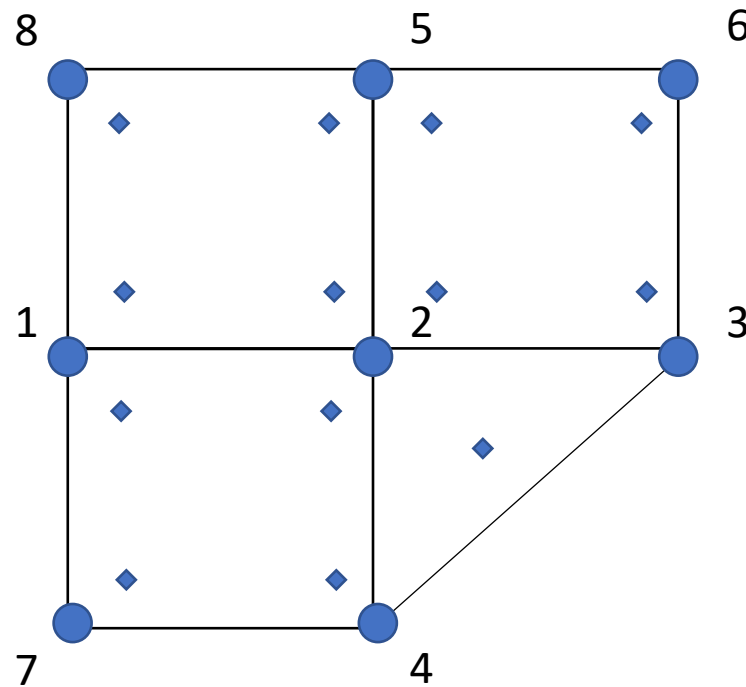
Let's minimize this difference:  $\frac{1}{2} \left( \frac{\partial \phi}{\partial x_j} - G_j \phi \right)^2$ .  
by solving:

$$\int w G_j \phi dV = \int w \frac{\partial \phi}{\partial x_j} dV \rightarrow G_j \phi = \frac{\sum_{ip} \phi_{ip} n_j dS}{V}$$

Lumped-mass



- Recall, FEM is a discretization scheme that:
  - Iterates over locally-owned elements for Time/Source/etc (volumetric-based terms)
  - Iterates over locally-owned elements for Advection/Diffusion/etc. (integrated by parts terms)
  - Below is the patch of elements connected to node 2 (a global matrix row number)

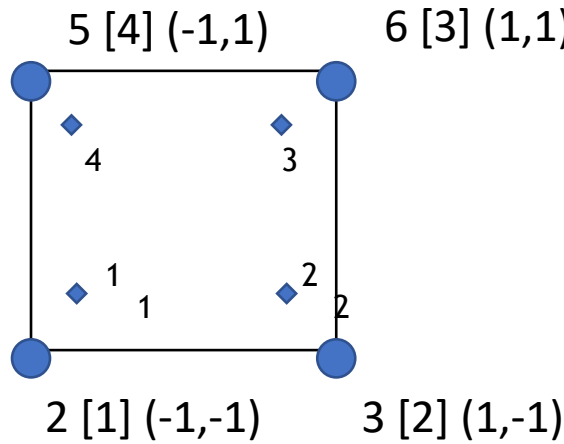


Note: Single integration point location for all terms

Sample patch of elements



- For each element, we have a set of integration or quadrature points (no dual-notion)
- We define an isoparametric element than ranges from -1:1 in the  $\xi$ - (x-direction) and  $\eta$ - (y-direction) direction
- Gaussian quadrature on a -1:1 range is defined, +/-  $\sqrt{3}/3$



Basis Functions for a Quad4

$$\begin{aligned}
 N_1^{ip} &= \frac{1}{4}(1 - \xi)(1 - \eta) \\
 N_2^{ip} &= \frac{1}{4}(1 + \xi)(1 - \eta) \\
 N_3^{ip} &= \frac{1}{4}(1 + \xi)(1 + \eta) \\
 N_4^{ip} &= \frac{1}{4}(1 - \xi)(1 + \eta)
 \end{aligned}$$

## Deep Dive on FEM: Implicit Time Discretization



- Backward Euler (two state) and is first-order accurate (A-stable)
- BDF2 (three state) is second-order accurate (A-stable)
- This term is assembled over an element iteration and drives a consistent mass matrix with a full node:element:node connectivity

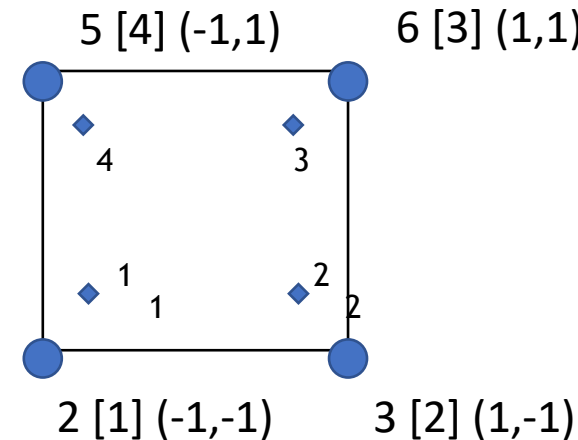
$$\int w \frac{\partial \rho \phi}{\partial t} dV,$$

- For uniform time steps:

$$\gamma_1 = 3/2$$

$$\gamma_2 = -2$$

$$\gamma_3 = 1/2$$

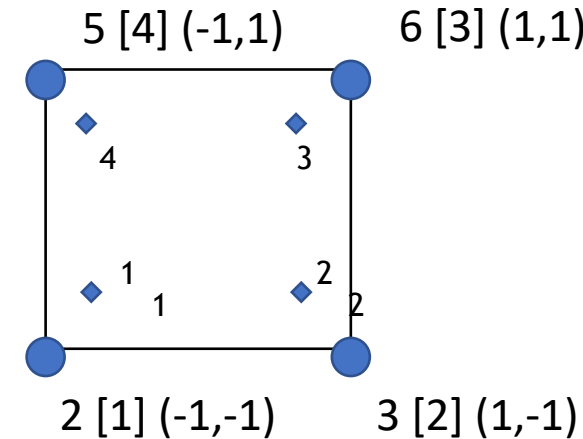


## Deep Dive on FEM: Source Term Discretization



- Source terms for FEM are assembled over an element loop
- In some cases, the source term is complex, i.e., includes gradients, which drives either a nodal assembly of these quantities to the nodes or local evaluation

$$\int w S dV.$$



## Deep Dive on FEM: Advection Discretization



- Advection terms for FEM are assembled over an element loop
- The advection term can be integrated by parts, or not; moreover, the PDE can drive a non-conservative equation form

$$\int w \frac{\partial \rho u_j \phi}{\partial x_j} dV = \int w \rho u_j \phi n_j dS - \int \rho u_j \phi \frac{\partial w}{\partial x_j} dV,$$

IBP - or not...

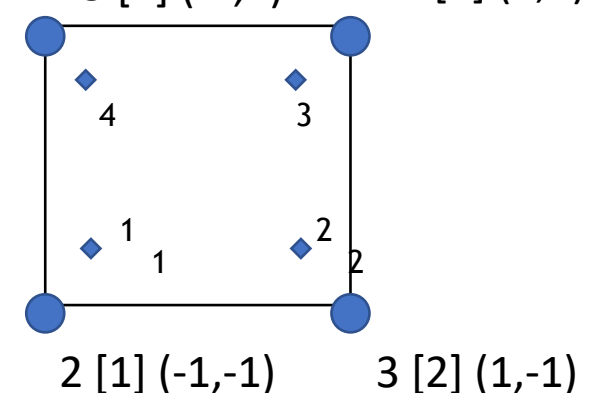
This is now a choice

$$\int w \rho u_j \frac{\partial \phi}{\partial x_j} dV + \int w \phi \frac{\partial \rho u_j}{\partial x_j} dV,$$

Non-conserved form, like  
CVFEM, poses no  
complexity

$$\int w \frac{\partial \rho \phi}{\partial t} dV = \int w \rho \frac{\partial \phi}{\partial t} dV + \int w \phi \frac{\partial \rho}{\partial t} dV$$

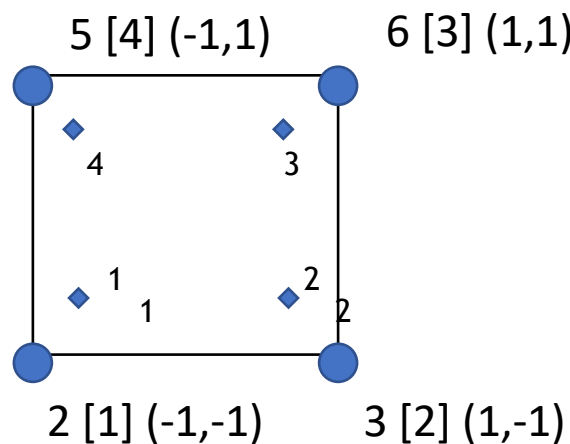
$$\int w \left( \rho \frac{\partial \phi}{\partial t} + \rho u_j \frac{\partial \phi}{\partial x_j} \right) dV,$$



## Deep Dive on FEM: Diffusion Discretization



- For diffusion, we will again use the nodal basis to support a diffusion operator
- Integration-by-parts is desired to remove the second-derivative requirement that would not be possible for a linear basis



$$\begin{bmatrix} \frac{\partial x}{\partial \xi} & \frac{\partial y}{\partial \xi} \\ \frac{\partial x}{\partial \eta} & \frac{\partial y}{\partial \eta} \end{bmatrix} \begin{bmatrix} \frac{\partial N}{\partial x} \\ \frac{\partial N}{\partial y} \end{bmatrix} = \begin{bmatrix} \frac{\partial N}{\partial \xi} \\ \frac{\partial N}{\partial \eta} \end{bmatrix} \quad \mathbf{J}^{-1} = \begin{bmatrix} \frac{\partial x}{\partial \xi} & \frac{\partial y}{\partial \xi} \\ \frac{\partial x}{\partial \eta} & \frac{\partial y}{\partial \eta} \end{bmatrix}^{-1}$$

$$\begin{bmatrix} \frac{\partial N}{\partial x} \\ \frac{\partial N}{\partial y} \end{bmatrix} = \begin{bmatrix} \frac{\partial x}{\partial \xi} & \frac{\partial y}{\partial \xi} \\ \frac{\partial x}{\partial \eta} & \frac{\partial y}{\partial \eta} \end{bmatrix}^{-1} \begin{bmatrix} \frac{\partial N}{\partial \xi} \\ \frac{\partial N}{\partial \eta} \end{bmatrix}$$

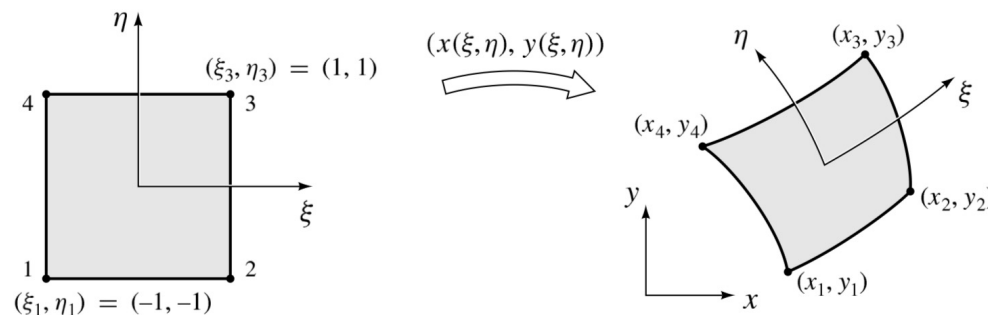
$$\int w \frac{\partial q_j}{\partial x_j} dV = \int w q_j n_j dS - \int q_j \frac{\partial w}{\partial x_j} dV.$$

Note that the FEM approach is absent any non-orthogonality corrections

## Element Integration: Physical to Transformed Space



Let us define a linear basis over a representative two-dimensional quadrilateral with iso-parametric range of  $\xi$ : -1:+1 and  $\eta$ : -1:+1



Transformation:

$$\begin{pmatrix} x \\ y \end{pmatrix} = \begin{pmatrix} x(\xi, \eta) \\ y(\xi, \eta) \end{pmatrix} \quad \mathbf{J} = \begin{pmatrix} \frac{\partial x}{\partial \xi} & \frac{\partial x}{\partial \eta} \\ \frac{\partial y}{\partial \xi} & \frac{\partial y}{\partial \eta} \end{pmatrix}$$

$|\mathbf{J}|$  is determinant of the transformation matrix

$$|\mathbf{J}| = \frac{\partial x}{\partial \xi} \frac{\partial y}{\partial \eta} - \frac{\partial x}{\partial \eta} \frac{\partial y}{\partial \xi}$$

With weight  $w_g$

$$I = \int_{\hat{\Omega}^e} \hat{f}(\xi, \eta) |\mathbf{J}| d\xi d\eta \approx \sum_{g=1}^G w_g \hat{f}(\xi_g, \eta_g) |\mathbf{J}|_{(\xi_g, \eta_g)},$$

Goal: Evaluate an integral:

$$I = \int_{\Omega^e} f(x, y) dx dy$$

Change of variables:

$$I = \int_{\hat{\Omega}^e} \hat{f}(\xi, \eta) |\mathbf{J}| d\xi d\eta$$

$$\begin{pmatrix} \frac{\partial N}{\partial x} \\ \frac{\partial N}{\partial y} \end{pmatrix} = J^{-1} \begin{pmatrix} \frac{\partial N}{\partial \xi} \\ \frac{\partial N}{\partial \eta} \end{pmatrix}$$

## Deep Dive on FEM: Discretization Kernels (Code)



- Time
  - <https://github.com/NaluCFD/Nalu/blob/master/src/kernel/ScalarMassFemKernel.C>
- Advection
  - <https://github.com/NaluCFD/Nalu/blob/master/src/kernel/ScalarAdvFemKernel.C>
- Diffusion
  - <https://github.com/NaluCFD/Nalu/blob/master/src/kernel/ScalarDiffFemKernel.C>

## Common low-Mach Discretization Approaches: Conclusions



- FEM provides a machinery to provide accurate discretizations on non-ideal meshes, however, the same diffusion operator suffers on high-aspect ratio meshes
- CVFEM is a hybrid method that contains the likeable attributes of both FV and FEM (same high-aspect ratio diffusion operator finding)



# Stanford ME469: Common low-Mach Discretization Approaches: Comparisons

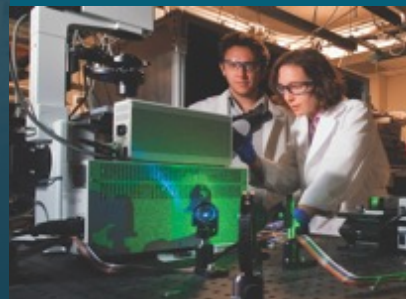


*PRESENTED BY*

Stefan P. Domino

Computational Thermal and Fluid Mechanics

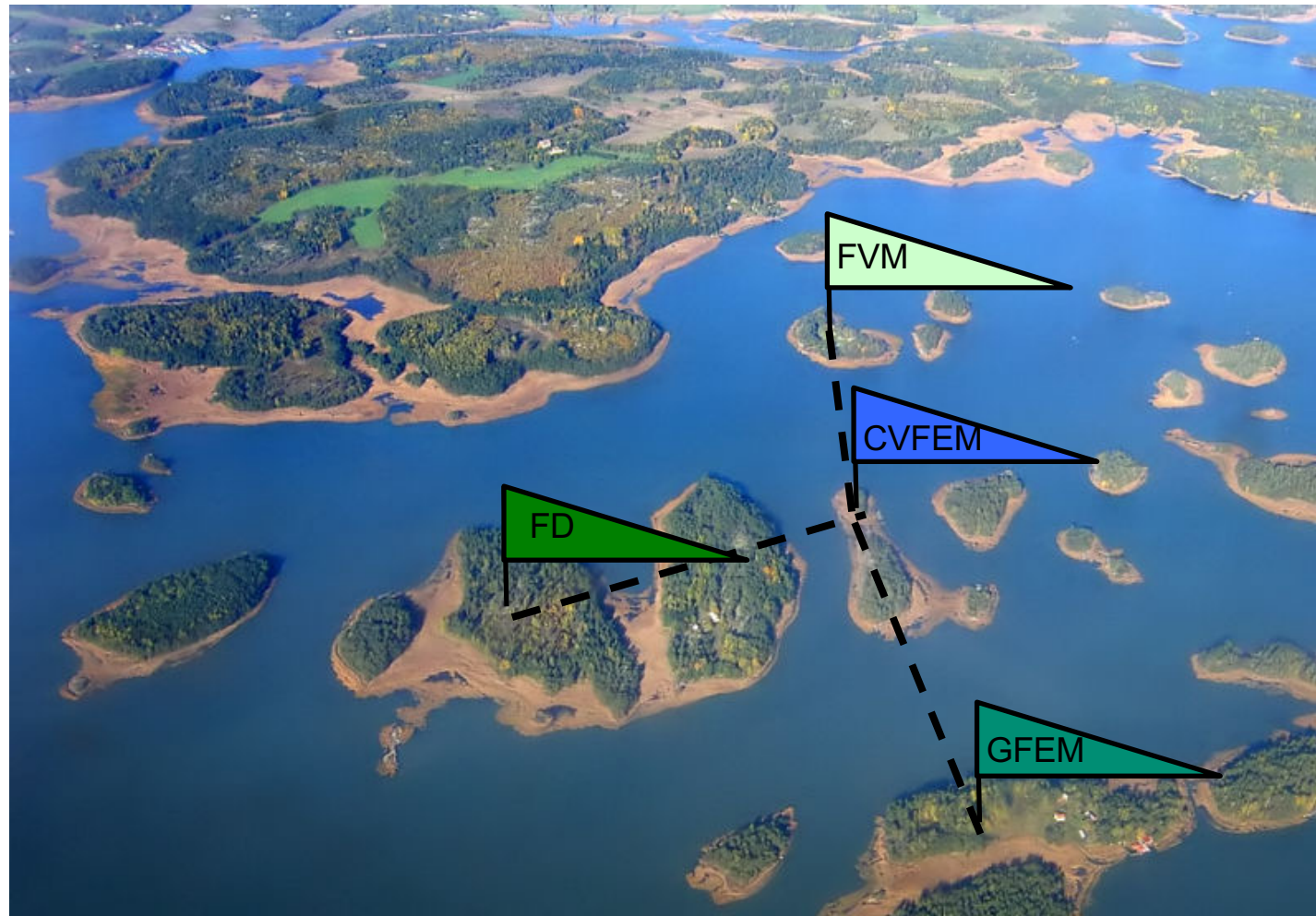
Sandia National Laboratories SAND2018-4536 PE



Sandia National Laboratories is a multimission laboratory managed and operated by National Technology & Engineering Solutions of Sandia, LLC, a wholly owned subsidiary of Honeywell International Inc., for the U.S. Department of Energy's National Nuclear Security Administration under contract DE-NA0003525.



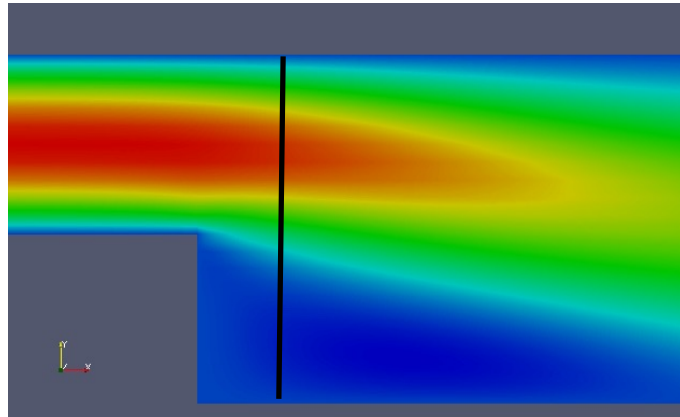
- Me469 Tenant: Let's work to understand how each method relate to one another



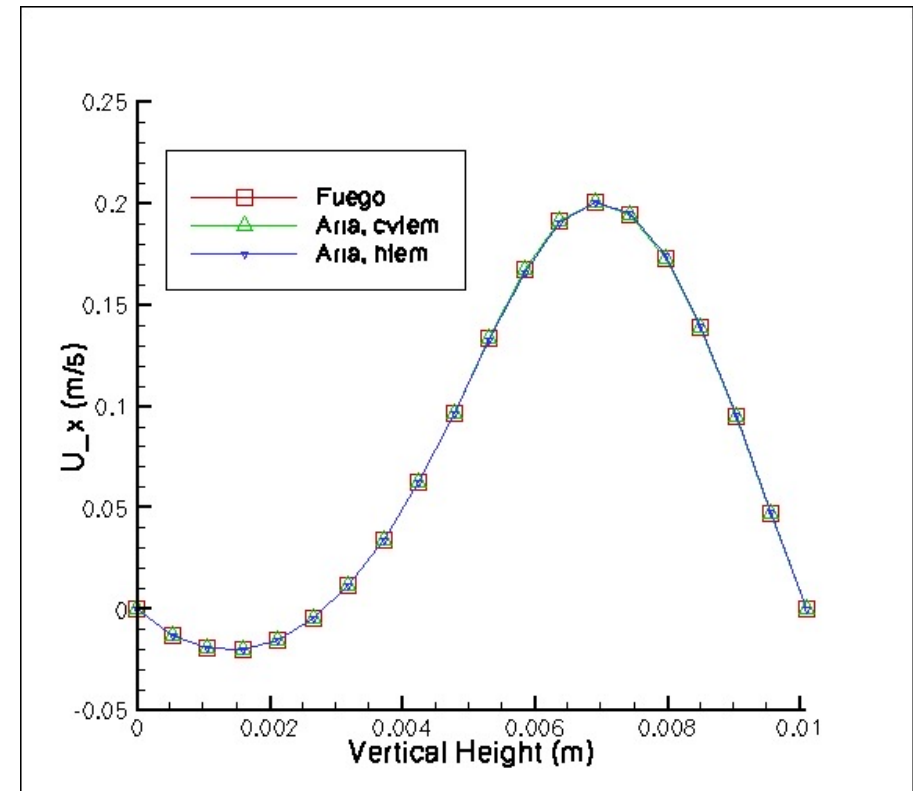
## Laminar Backstep

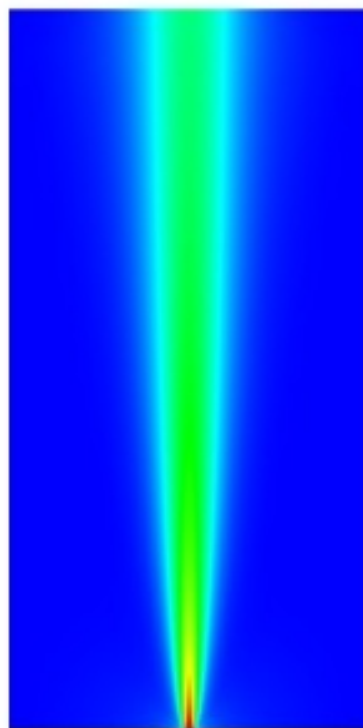


- Laminar back step ( $Re = 389$  based on step height) comparing two code implementations for CVFEM (Sierra/Fuego and Sierra Aria), FEM (within Aria – here termed, “hybrid” FEM, or HFEM – essentially, the same low-Mach CVFEM approach with full integration-by-parts).

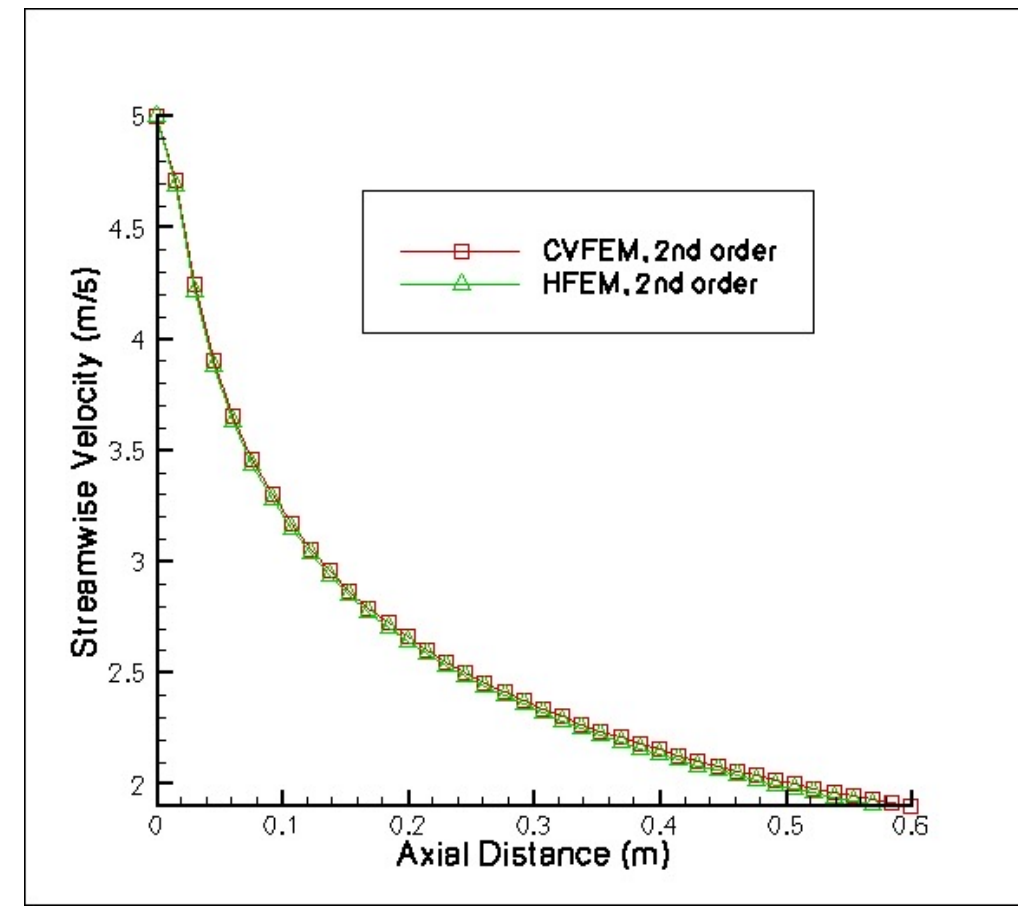


X-component of velocity  
Vertical line represents one-D  
line plot location

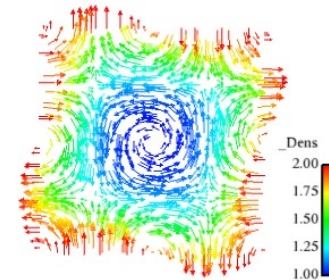




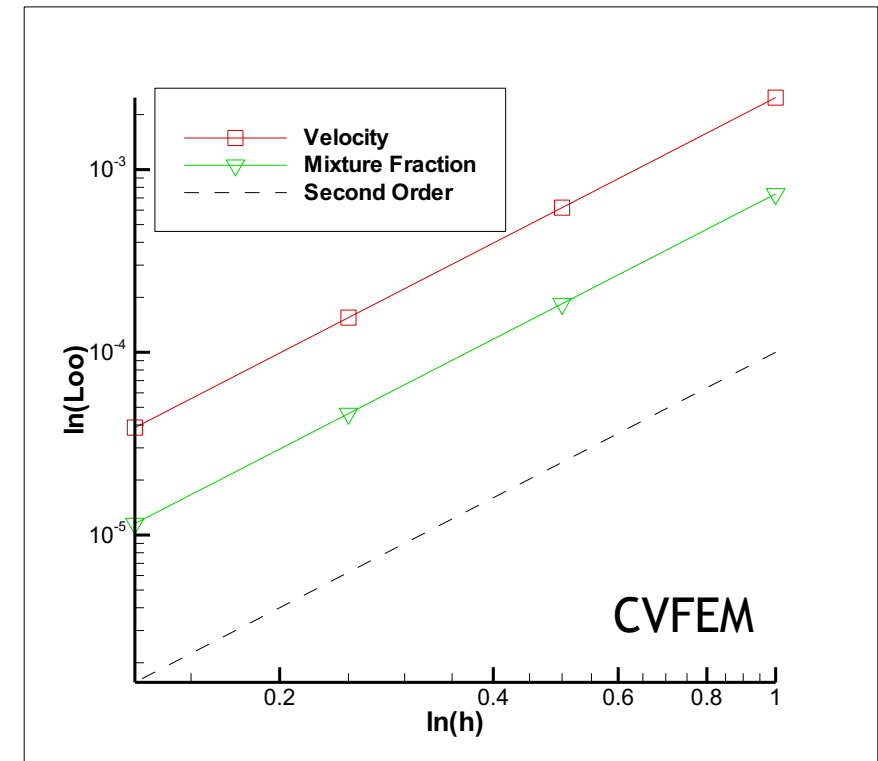
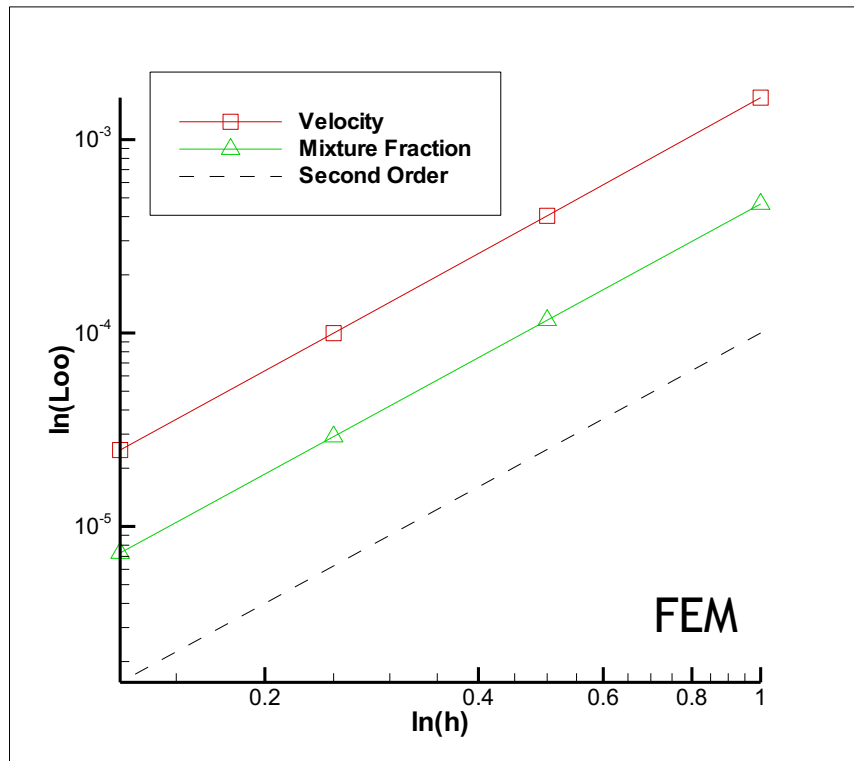
Y-component of velocity



## Order-of-Accuracy



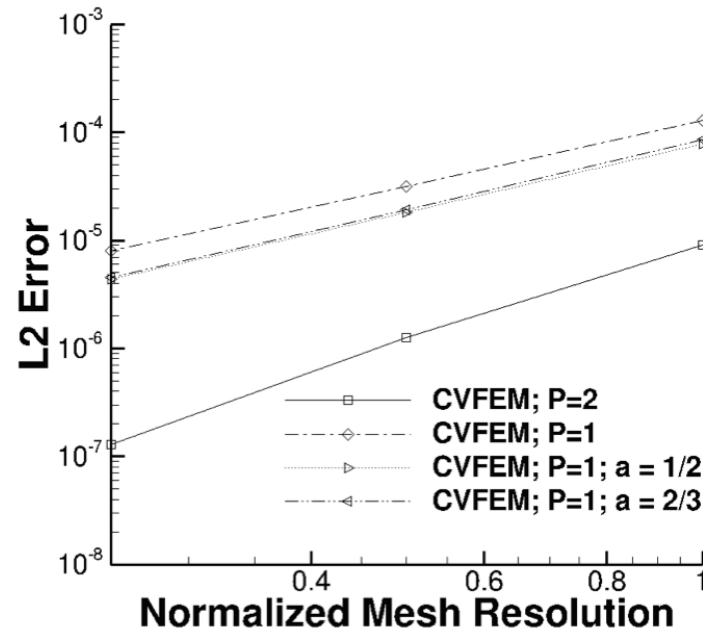
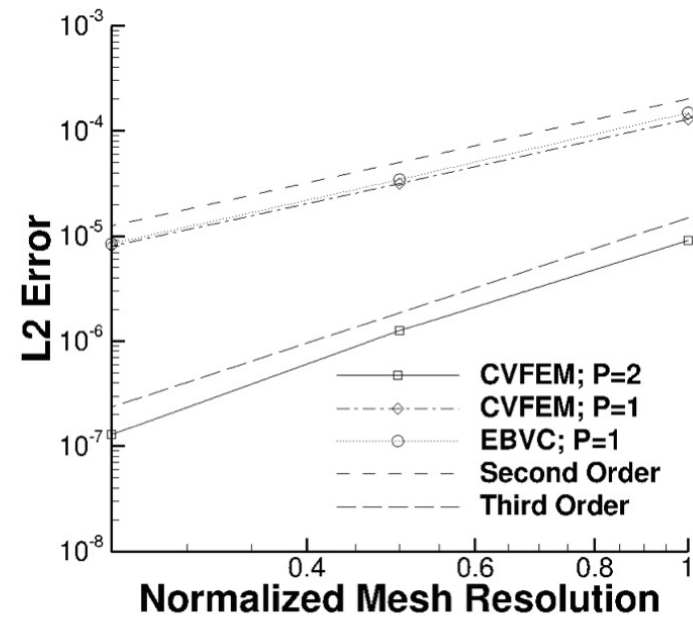
- Difficult two dimensional variable density low-Mach flow using method of manufactured solutions; DOFS:  $u, v, p$  and  $Z$ ; density =  $f(Z)$



## Isothermal Taylor-Vortex Decay



- Exercising the low-and high-order ( $P=1$  and  $P=2$  CVFEM) along with EBVC with and without pseudo-higher-order upwind)

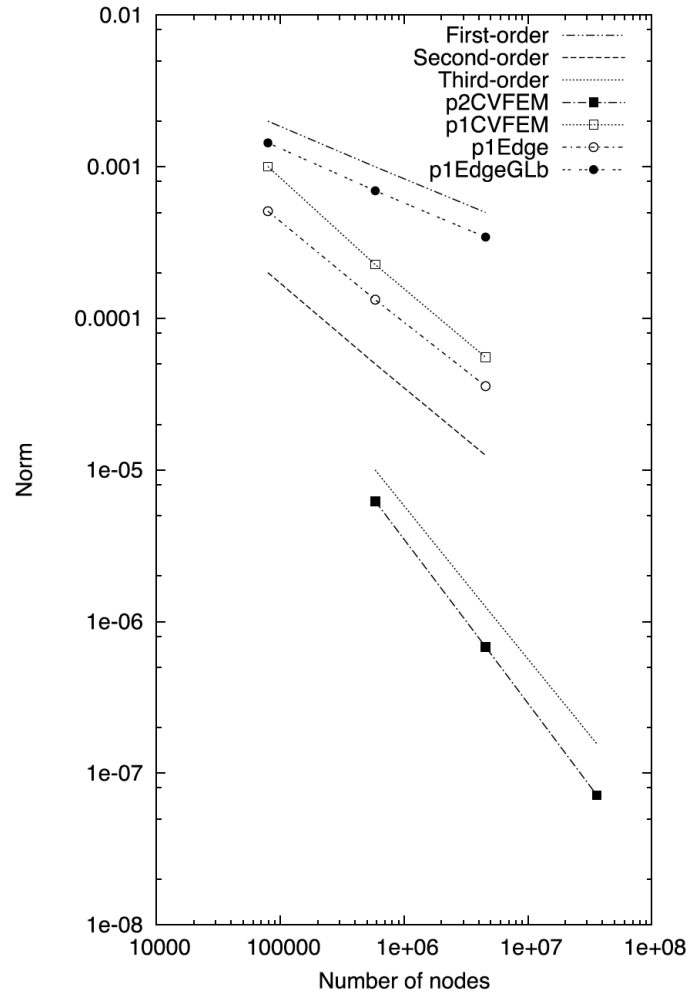
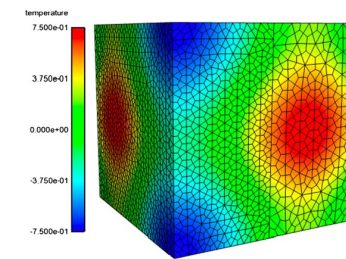


Domino, 2014 “A comparison between low-order and higher-order low-Mach discretization approaches”, Proceedings of CTR Summer Program.

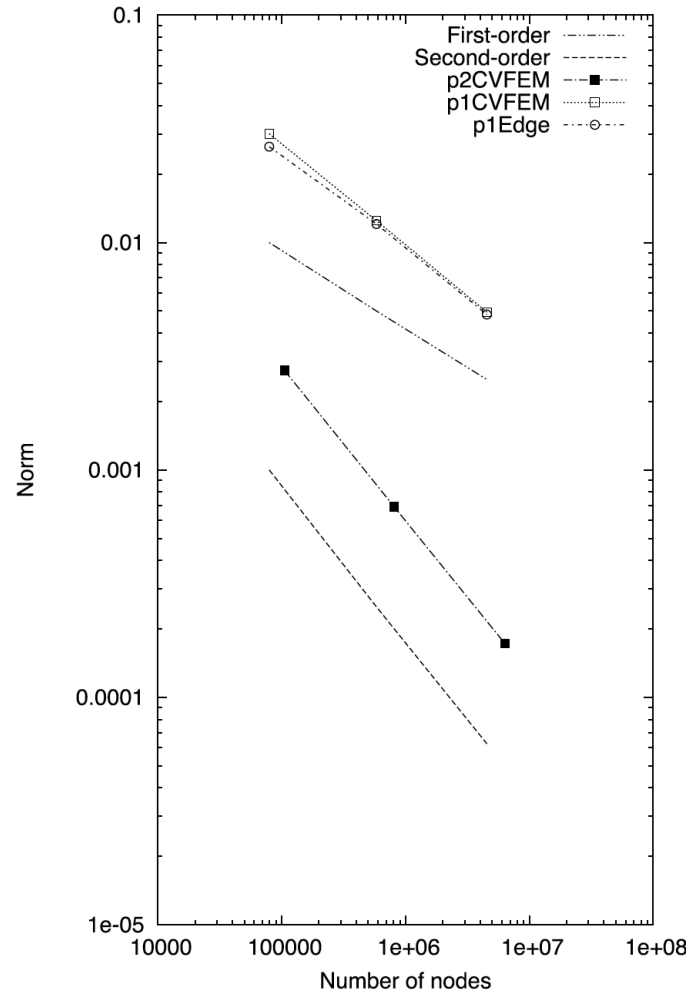
# Non-Conformal Laplace Verification



S.P. Domino / Journal of Computational Physics 359 (2018) 331–351



(a) Temperature error norms.

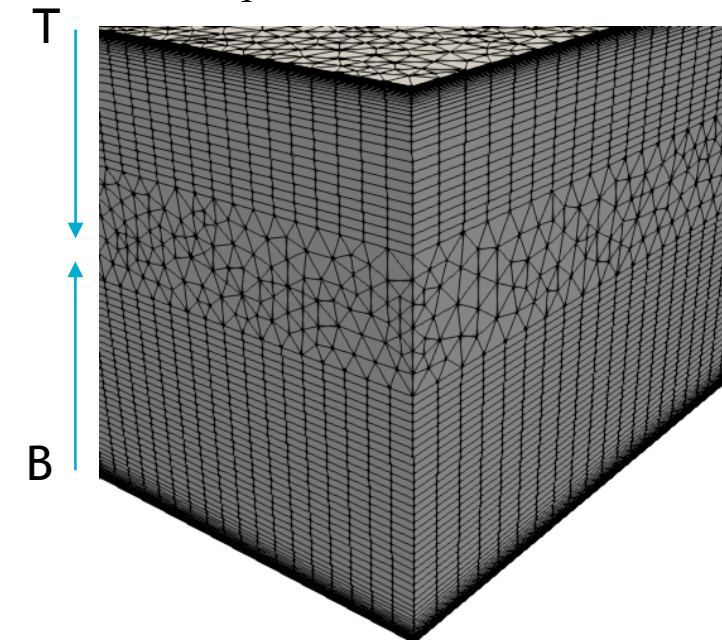
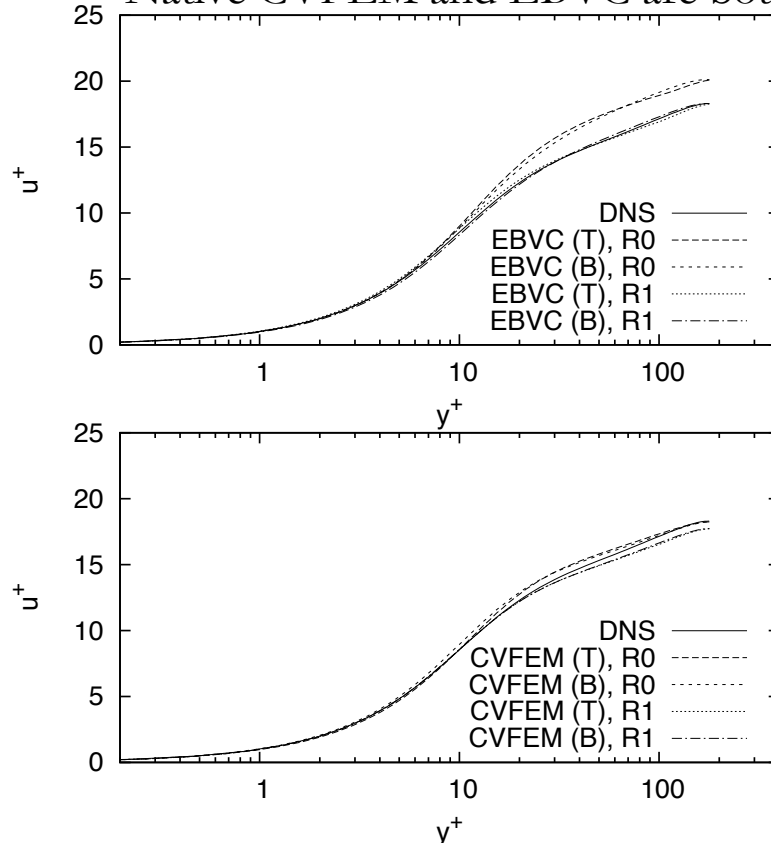


(b) Projected nodal gradient error norms.

## Hybrid Meshes, Even for LES!



- Hybrid mesh study based on Ham and Iaccarino, *CTR Annual Brief*, 2006, found that simulations were extremely sensitive to mesh topology
  - Non-symmetric time mean flow found for cell-centered; better for the CTR node-centered formulation
  - Native CVFEM and EBVC are both symmetric in mean quantities

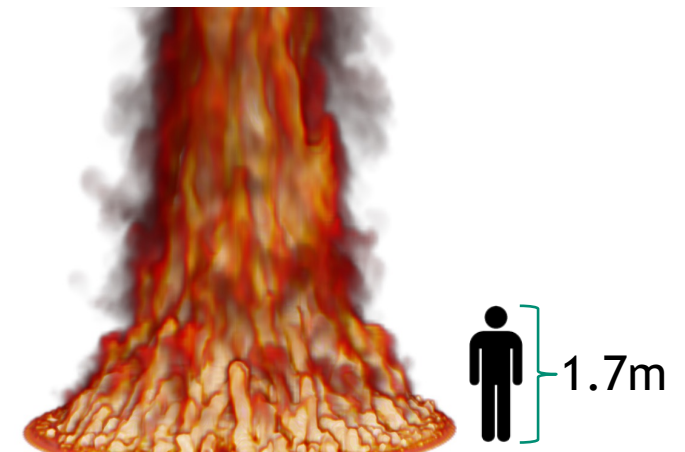
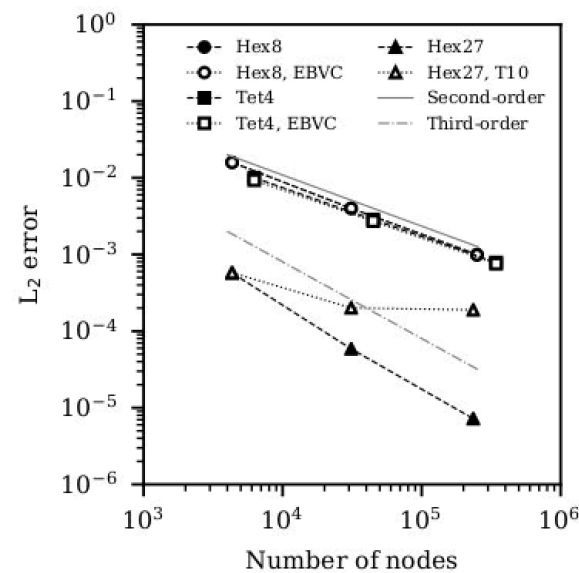
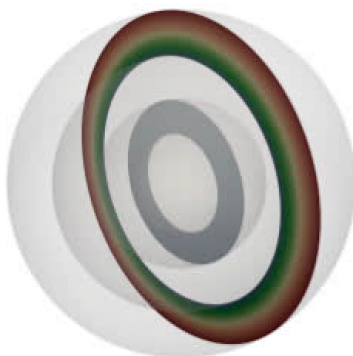


Domino, et. al, “The suitability of hybrid meshes for low-Mach large-eddy simulation” Stanford CTR Summer Program, 2018

## 5m JP-8 Pool Fire Validation



- Novel participating media radiation solver verification (Tet4, Hex8, Hex27): EBVC and CVFEM, however, based on Streamwise Upwind Petrov Galerkin (SUPG), Burns, 1997



$$s_j^k \frac{\partial I^k}{\partial x_j} + (\mu_a + \mu_s) I^k = \frac{\mu_a \sigma T^4}{\pi} + \frac{\mu_s G}{4\pi}$$

$$\int \tilde{w} \left( s_j^k \frac{\partial I^k}{\partial x_j} + (\mu_a + \mu_s) I^k - \left( \frac{\mu_a \sigma T^4}{\pi} + \frac{\mu_s G}{4\pi} \right) \right) dV = 0$$

$$\tilde{w} = w + \tau \left( s_j \frac{\partial}{\partial x_j} w + \alpha \mu_a w \right)$$

$$\int s_j^k I^k n_j dS + \int ((\mu_a + \mu_s) I^k - S) dV = \int \tau s_j^k R^k n_j dS$$

Domino et al. "Predicting large-scale pool fire dynamics using an unsteady flamelet- and large-eddy simulation-based model suite", Physics of Fluids, 2021 (Editor's pick: August 4, 2021).